Journal of CO2 Utilization 69 (2023) 102412

Contents lists available at ScienceDirect

Journal of CO2 Utilization

journal homepage: www.elsevier.com/locate/jcou

Review article

Electrocatalytic CO_2 conversion on metal-organic frameworks derivative electrocatalysts

Kayode Adesina Adegoke *, Nobanathi Wendy Maxakato *

Department of Chemical Sciences, University of Johannesburg, Doornfontein 2028, South Africa

ARTICLE INFO

Keywords:
MOF-derived electrocatalyst
CO_2 electroreduction
Electrocatalytic CO_2RR mechanism
Value-added chemical/fuels
Modification strategies/industrial applications

ABSTRACT

Metal-organic frameworks (MOFs)-derived nanomaterials offer several competencies as viable electrocatalysts for converting notorious CO_2 to value-added products with realistic electrochemical activity and stability without additional CO_2 emission. This study discussed recent advancements in MOF-derivative nanomaterials for CO_2 reduction reaction (CO_2RR) to value-added chemicals/fuels. The corresponding active sites, activities, and selectivity for each MOF-derivative electrocatalysts for CO_2RR were discussed. The synthetic techniques of MOF-derivatives with their corresponding regulations of compositions, structures, performance and modification strategies, and mechanistic aspects of CO_2-electroreduction were discussed. Confinement engineering of MOF-derived nanomaterials and discussion on controlling the electrocatalytic performances via confinement engineering were discussed. Insight into the structure-activity relationships of MOF-derived electrocatalysts for CO_2RR was explained. Detailed electrocatalytic performance towards forming different products on MOF-derived isolated (single) metal atoms, MOF-derived heteroatom-doped carbon, MOF-derived transition metal nanoparticles, MOF-derived transition metal oxide, and MOF-derived transition metal phosphide electrocatalysts were discussed. Distinct from the earlier reports, this study also discusses the key factors towards optimizing the efficiency of CO_2RR electrocatalysts for promising performance. Various industrial prospects of CO_2R on MOF-electrocatalysts were unveiled to bridge the research gaps. Despite some remarkable progress, the subject is in its infancy; several obstacles and shortfalls for future study still exist to advance this field into full-fledged commercial applications.

1. Introduction

Energy consumption worldwide has been projected to rise from 575 quads in 2015–736 quadrillion Btu (quads) in 2040, an increase of 28%. Currently, the atmospheric CO_2 concentration worldwide has risen from ~330 ppm in 1981 to ~ 418.94 ppm in June 2021, as shown in Fig. 1a is expected to increase with a similar trend [1,2]. A steady increase in yearly CO_2 emissions may ultimately lead to a synchronized rise in global-mean air surface temperatures on both the earth and sea levels between 1990 and 2100 [3–5]. Several systematic proofs of the continuous rising CO_2 levels have been associated with urbanization and industrialization [6,7], which correspondingly pose adverse consequences on the alarming increase in the average temperature and sea level (Fig. 1b) [8].

Developing an innovative process for recycling captured CO_2 is becoming an attractive prospect owing to its ability to allow CO_2 valorization. In this way, CO_2 is converted to valuable or useful products, including fuels and other hydrocarbons. Effective chemical conversion of CO_2 to some liquid fuels is of high importance to allow its recycling and the re-use of essential fuels. This approach is believed to offer a feasible solution to the increasing environmental problem of atmospheric CO_2 and its associated global warming, while at the same time, it renders renewable fuels environmentally carbon-neutral [9–14]. Such an approach would be considered as a potential candidate having the ability to offer solutions to the environmental crisis resulting from increasing atmospheric CO_2 and associated global warming.

Currently, renewable energy sources have been touted as a rapidly expanding source of electricity. An electrochemical oxidation-reduction process happens at the electrode interface when renewable energy [15,16] is combined with it for a sustainable alternative energy cycle (Fig. 2). Unlike chemical processes, the electrochemical system is recognized for having a simple reaction rate controllability by adjusting the applied bias and a more straightforward manner of isolating the products from the half-reactions. Electrochemical reactions are

* Corresponding authors.
E-mail addresses: kwharyourday@gmail.com (K.A. Adegoke), nmaxakato@uj.ac.za (N.W. Maxakato).

https://doi.org/10.1016/j.jcou.2023.102412
Received 29 June 2022; Received in revised form 27 December 2022; Accepted 14 January 2023
Available online 11 February 2023

characterized by interactions between electrolyte, electrode, and dissolved products or reactants by a series of conductive diffusion reactions [12,17–22]. However, the high activation energy barrier between the intermediates and dissolved reactants resulted in low efficiency and high overpotential for electrochemical reactions, thereby necessitating a high demand for ionic and electric conductivity and a large surface area to ensure phase interactions [23]. To satisfy the practical/industrial expectations of the area, research into electrocatalyst development that lowers the activating energy barrier and activates intermediates with lower energy is presently a research hotspot.

The electrocatalysts used and the voltage applied is critical for CO_2R selectivity and efficiency. Nevertheless, for a given set overpotential, electrodes often create a wide range of products rather than a single product, resulting in poor product selectivity. Furthermore, in a conventional batch reactor, the pace of reaction is always faced with the reduced solubility of CO_2 in the reaction system, particularly at high overpotential, resulting in low current density (*j*) or deterioration of electrocatalytic activity [24–26]. The state-of-the-art technology is currently unable to meet/address the criteria for large-scale industrial applications due to the low stability and selectivity of existing electrocatalysts. Therefore, new innovations and the simplicity of the existing technology are required to design efficient materials for CO_2RR.

Metal organic frameworks (MOFs)-derived electrocatalysts are organic-inorganic porous materials made of organic ligands and metal centers with appealing crystalline morphologies [27–30]. They exhibit following benefits: (i) higher porosity, tunable pore size, and larger specific surface area, that facilitates molecule adsorption around the reaction substrates, material transports, and active center activation [31,32]. (ii) Organic linkers and metal nodes in MOF can catalyze difficult reactions by transferring charge to active centers via coordination or π–π forces, hence enhancing the chemical microenvironment of pore structures [33–37]. (iii) When compared to typical carbon-based electrocatalysts, the MOF shells efficiently enclose the active centers and prevent metal sites from agglomeration or leaching, thereby resulting in high electrocatalytic process stability [38,39]. (iv) Transition metal units in MOF materials are frequently employed as electrocatalytic active sites. MOF electrocatalysts' active sites could be equally distributed due to their periodic arrangements [40]. These associated benefits among others have endowed MOF-derived electrocatalyst materials to selectively confine metals of various size simply adjusting the synthetic technique. As a result of optimizing synthesis methodologies, numerous researchers apply MOF-derived materials in diverse electrocatalytic activities [41–49].

Several techniques such as photoelectrochemical, thermochemical, photochemical, and electrochemical [12,50–62] have been developed for CO_2R to fuels. The uniqueness of the electrochemical conversion method, including its operation at ambient pressure and room temperature [23], as essential working conditions, thus increasing the practicality of reducing atmospheric CO_2 to valuable products of interest. Furthermore, the electrochemical CO_2 conversion is recognized to have a highly controlled feature as well as the potential for extremely high conversion efficiencies. In addition, the electrochemical methodology has various benefits over other technologies due to its industrial prospects and practicability. For example, photochemical conversion produces only a few products, including carbon monoxide [63–66], formate [67], formic acid [68], and methanol [68,69] whereas, electrochemical produces a wide range of conversion products, including carbon monoxide [70,71], formic acid esters [72], methane [73–75], methanol [76–81], formic acid [25,82–85], dimethylcarbonate [86,87], aliphatic polycarbonates[72], carbamic acid esters [72], alkylene carbonates [88], lactones [72], formamides [88].

Till date, there is absence of comprehensive or combine information on the recent advancement on MOF-derived nanomaterials for CO_2RR to value-added products, and also information on the confinement and structure-activity relationships of MOF-derivative nanomaterials for CO_2 conversion is scarce. Thus, this study presents recent advances in using MOF-derived nanomaterials for electrocatalytic CO_2RR to value-added chemicals/fuels. It discussed the corresponding electrocatalytic performance of MOF-derived electrode materials for CO_2RR. This work began by firstly exhibiting the extraordinary capabilities of MOF materials over other electrocatalysts as well as the superiority of MOF-derivative materials to their pure counterparts. This was followed by synthetic techniques of MOF derivatives with the corresponding regulations of compositions, structures, performances, modification strategies, and mechanistic aspects of electrocatalytic CO_2RR. Confinement engineering of MOF-derived nanomaterials and discussion on controlling the electrocatalytic performances via confinement engineering were discussed. In addition, the insight into the structure-activity relationships of MOF-derived electrocatalysts for CO_2RR was explained. A detailed discussion on the advancement in the electrocatalytic performance of MOF-derived electrocatalysts for CO_2RR towards the formation of various products was provided. The categories of MOF materials discussed include the MOF-derived isolated (single) metal atom materials, MOF-derived heteroatom-doped carbon, MOFs-derived transition metal nanoparticles, MOF-derived transition metal oxide electrocatalysts, and MOF-derived transition metal phosphide electrocatalysts covering the previous decade. Unlike earlier studies, the important parameters for enhancing the efficiency of CO_2RR electrocatalysts for promising performance (activity, stability, and selectivity) were also explored. In addition, various industrial potential of CO_2RR on MOF electrocatalysts were discussed in order to fill the knowledge gaps in the field. Conclusively, despite some amazing success in MOF-derived

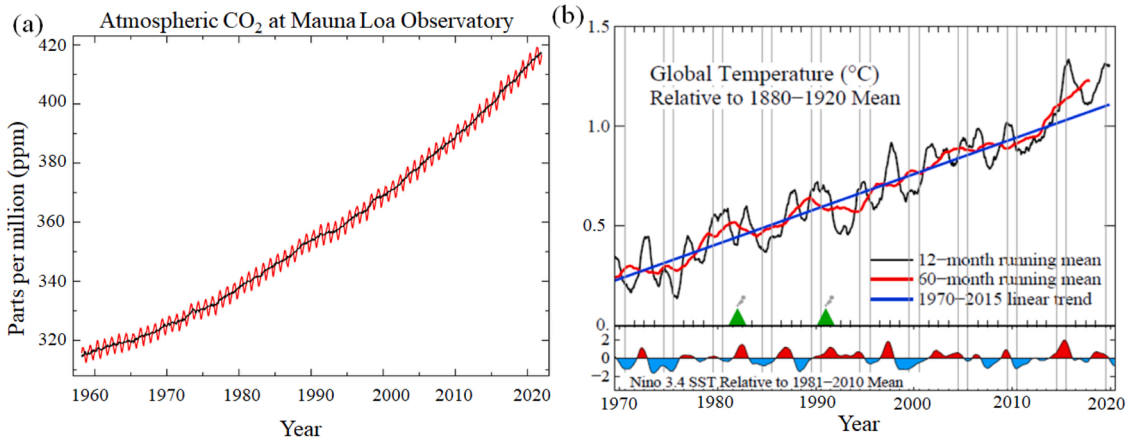

Fig. 1. (a) Global temperature and Niño3.4 Index through November 2020 (Source: www.CO_2now.org. (b) CO_2 concentration over the years (source: https://gml.noaa.gov/ccgg/trends/index.html).

materials for CO_2RR, the subject is still very much in infant, and there remain obstacles and shortfalls for future studies which are discussed in the concluding remarks to stimulate more or better progression in the area toward full-fledged practical implementations.

2. What is unique about MOFs electrocatalysts

MOFs have been regarded as promising emerging and smart materials due to their exceptional catalytic properties, attractive crystallinity, and self-assembly organic-inorganic hybrid units with metal nodes or polynuclear secondary building units (SBUs) that form porous with periodic frameworks [46,89–92]. Remarkable properties of MOFs as multipurpose catalysts include the feasibility of tuning their structures, diversified constituents (pores, linkers, and nodes), adjustable and well-defined frameworks for a thorough understanding of the catalytic mechanisms, abundant active sites, and uniform porosity; and tunable environment, transport, and recognition of the substrates and products, structural-functional relationships at the molecular level, and rigorous electrocatalytic performance. Additionally, these materials as catalysts have an appropriate band gap, valence and conduction bands, an optimal structural architecture for charge transport, and a stronger corrosion resistance towards light [89,93].

In recent decades, various techniques for synthesizing MOFs have been intensively researched, including self-assembly approaches using hydro- or solvothermal procedures with conventional or microwave-induced heating, mechanochemical syntheses, ultrasonic methods, and electrochemical techniques. Additionally, the precursors used and synthetic processes may be tailored to control the resultant nanostructures, including crystallite size, morphologies, surface areas, and pores, which are critical for applying MOFs in energy conversion technologies [94]. Unfortunately, since MOFs continue to exhibit instability, particularly in organic reactions involving extreme temperatures in organic/water solvents and an acidic and basic environment, high electrocatalytic activities and recyclability are usually difficult to accomplish. The production of MOF-derived carbon-based nanomaterials and metal/metal oxides is currently gaining attention due to its structural tunability [95]. These electrocatalyst materials usually display a higher tolerance for difficult process conditions, so they are almost guaranteed reusability.

Generally, the composition and structure of MOF-derived materials are determined mostly by incorporating the additional materials and the pyrolysis processes (e.g., annealing temperature, atmosphere, heating rate, and retention time). Direct pyrolysis of MOF precursors remains the simple technique of derivatization. To produce metal-free carbon-based electrocatalysts, high-temperature carbonization in an inert environment (e.g., Ar, N_2) results in the framework disintegration, from which metal entities may be eliminated in-situ or through the following acidic etching. After metals are removed, the pore volume and surface area may be enhanced. Metal species from Zn-based MOFs (e.g., MOF-5 and ZIF-8) and Co-based MOFs, in particular, may be readily evaporated (>700 °C) or etched by acid treatment [95–99]. MOFs are widely used as precursors to build porous carbon nanostructures [47,100]. For heteroatom-doped (e.g., N, S, or P) carbon electrocatalysts, the functionality associated with organic linkers such as UiO-66-NH_2 or N-containing additive are often involved [96,101]. ZIFs, a subtype of MOFs with a zeolite-like structure, is composed of tetrahedral metal ions coupled to imidazolate moiety. Due to the abundance of N species within ZIFs offers excellent templates for derivatizing N-doped carbon materials.

In complement to the single components, the hybrid structure of C-supported metal/metal oxide electrocatalysts may be synthesized from MOFs using a direct carbonization process in an inert environment at a temperature suitable for metallic species preservation. Frequently used ZIFs for the preparation of various M@N-doped C electrocatalysts are Co- and Zn-based ZIF-67 and ZIF-8 [97,102]. MOF-derived heteroatoms, metals, and metal oxides are incorporated within the pore of C-based nanomaterials. Alternatively, the calcining MOF in air or O_2 may eliminate the C to yield porous metal/metal oxide compounds [103]. Additionally, careful selection as well as mixing of MOF precursor considerably increases the diversity; for example, synthesizing MOFs using a mixed-metal approach might result in bimetallic electrocatalysts after annealing [104,105].

Considering the necessity for variable compositional properties in a variety of electrocatalytic processes, modifications of MOFs before the pyrolysis may include encapsulating the guest species, combined with another substrate to form composites and solution impregnation. For instance, in-situ encapsulation and MOF pyrolysis have been employed to produce Au-NPs encapsulated in N-doped porous C [106]. This method for electrocatalyst production increases the metal loading active site numbers and ensures that the guest species are distributed uniformly inside the MOF-derived supports. Similarly, by using the mixed-linker method, it is possible to concurrently incorporate a variety of species or heteroatoms into the MOF-derived materials [90–92].

Due to the preorganized structural properties of MOFs, which are usually conserved in the MOF-derived materials, their structures have the benefit of providing the platform for electroactive species with higher metal loadings and good diffusion. A well MOF structure promotes atom dispersal of metallic species and inhibits annealing agglomeration. Such parameters are critical for increasing electrocatalytic performance since microscopic particles provide higher specific surface areas for electrocatalytic processes. Due to higher porosity and larger surface area, improved mass transfer facilitates both adsorption and dispersion of reactants [93,107,108]. Additionally, research of non-noble metal-based electrocatalyst including Cu, Co, Ni, and Fe generated from ZIF-67, MIL-88B, and a Ni-bdc-based MOF is of great interest, as their intrinsic magnetic characteristics might enable recycling processes and extend the life of heterogeneous catalysis [102, 109,110].

The qualities and advantages outlined above offer MOF-derived

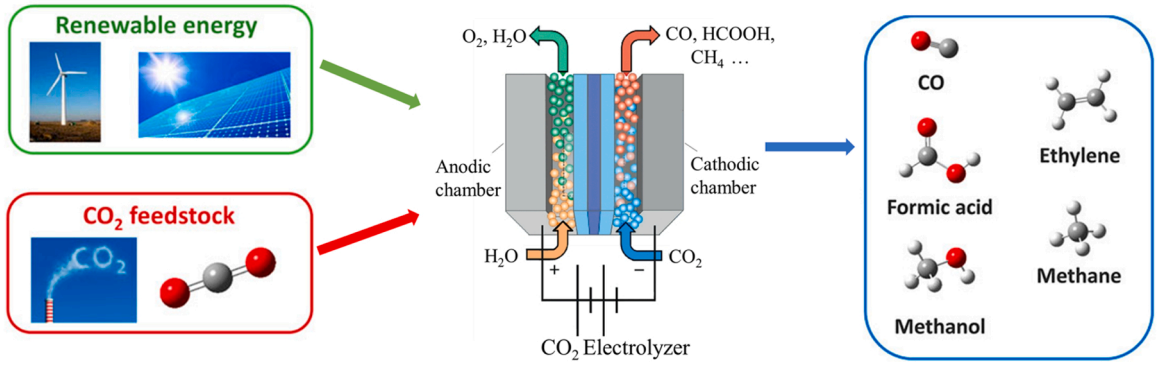

Fig. 2. Schematic illustration of the carbon cycle in electrochemical CO_2R.

nanostructures very appealing as effective electrocatalysts for CO_2RR. Nevertheless, adequate knowledge about how the MOF-derived nanostructures are formed during high-temperature annealing remains unclear. Therefore, the basic knowledge of these process steps is necessary to develop an effective and target-oriented electrocatalytic system(s). By using these optimized electrocatalysts, an approach for employing MOF-derived nanomaterials with high efficiency for the electrocatalytic system for the organic transformation associated with the synthesis of value-added chemicals from CO_2R is a hotspot research area.

3. Why MOFs derivative electrocatalysts?

The increasing variety of MOFs with different structural properties has offered numerous opportunities to develop innovative materials with improved functionalities and numerous electroactive sites for CO_2RR. Pristine MOFs have been employed in a variety of significant electrocatalytic reactions, including energy conversion technologies such as HER, OER, CO_2RR, and ORR [111,112]. However, pristine MOFs usually show lower activity than conventional, heterogeneous inorganic electrode materials based on the following issues: (i) low intrinsic conductivity, and (ii) low electrochemical and structural stability/durability. Notably, addressing these difficulties requires using MOFs as a sacrificial template to construct various conductive carbon-based materials such as N-doped graphitic porous carbon, metal/metal-oxide doped carbon, and heteroatom doped carbon materials [113,114].

Nonetheless, several studies have shown that MOF-derived nanomaterials are offered with several competencies for use as efficient electrocatalysts for CO_2RR to value-added products with realistic electrochemical activity and stability. In particular, the concept of using MOFs as templates to build complex porous nanostructure is crucial, which has resulted in several impressive advancements in MOF-derived electrode materials in the last decade [115]. The transformation of MOFs to alternative classes of materials that are easy to tune and convert to other related materials in controllable manners provides well-dispersed active sites which are absent in the original MOFs. In this way, the new material called MOF-derived nanostructures is formed, thereby offering the materials a higher surface area for enhancing the electrocatalytic performance and stability for CO_2R to fuels. These MOF-derivative materials have hierarchical porous architectures, tunable morphologies, heteroatom doping, chemical/structural strengths, improved electronic and ionic conductivities, and easy surface modification (functionalization) compared to pristine MOF materials [115–118].

The development of MOF-derived materials with high electrocatalytic performance has been predicated on improving desirable attributes such as conductivity, the number of active sites, and stability. In-situ MOF assemblies on a conductive substrate, such as graphene, carbon nanotubes, carbon paper, and Al_2O_3 nanorods, are often used [119–125]. This method allows for a greater connection between the substrates and the MOFs, which helps to expose the active sites and facilitate the charge transfer from the electrodes to the electrocatalysts. As a result, the composite shows greater CO_2R electrocatalytic activity and current densities. Pyrolysis of MOFs and MOF-based composites has been proposed as another method for producing MOF-derived electrocatalysts [121,126–130]. This method produces a uniform distribution of metal nanoparticles and atoms on the framework, resulting in carbon matrix defects that aid interaction between active sites and dissolved CO_2 [103,126,129,131–133].

MOFs as precursors to generate MOF derivatives have been proposed to overcome the drawbacks of weak conductivity and stability of different MOFs during electrocatalytic CO_2R. Tables 1 and 2 show an overview of CO_2R electrocatalysis on several manufactured MOF derivatives. MOFs-Transition metal Nanoparticles [128,134–136], MOFs-Transition metal phosphide [137,138], and MOFs Transition metal oxide electrocatalysts [139,140] are some of the other MOF-derived metal-based electrocatalysts that are currently available.

Table 1
MOF-derived isolated (single) for electrocatalytic CO_2RR to different products.

Electrocatalysts	MOF precursors	Metal configurations	j (mA/cm^2)	Products	FE (%)	Potential (V)	TOF	Refs.
Bi SAs/NC	Bi-MOF	Bi–N_4	–	CO	> 97	–	5535 h^{-1}	[317]
C-AFC©ZIF-8	AFC©ZIF-8	Fe–N_x	–	CO	93	− 0.43	–	[326]
C–Fe30–N30/30	Fe-ZIF-7	Fe–N	17.8	CO	–	–	–	[327]
C-FePc$(CN)_8$/ZIF	FePc/ZIF-8	Fe–N_4	5	CO	94	− 0.46	0.13 s^{-1}	[328]
Co@NC	ZIF-67	Co–N_x	18.1	CO	94	–	18 200 h^{-1}	[175]
Co_1–N_4	Co-ZIF-8	Co–N_4	15.8	CO	82	− 1.0	1455 h^{-1}	[329]
Co–HNC	Co–ZnO@ZIF	Co–C_2N_2	–	CO	35	− 0.8	–	[330]
CoPc©FeNC	Fe-CoPc	Fe–N	275.6 ± 27.0	CO	> 90	− 0.84	–	[331]
CuN_4C/1100	Cu–Zn-MOF	Cu–N_4	–	CO	98	− 0.9	1012 h^{-1}	[332]
CuNC-900	Cu$(BTC)(H_2O)_3$MOF	Cu–N_x	14.8	CH_4	38.6	− 1.6	–	[333]
CuSAs/TCNFs	Cu/ZIF-8	Cu–N_4	93	CH_3OH/CO	44/56	− 0.9	–	[334]
CZn_xNi_y ZIF-8	Ni-ZIF-8	Ni–N_4	71.5 ± 2.9	CO	92–98	− 1.03	10 087 ± 216 h^{-1}	[335]
Fe^{3+}NC	Fe-ZIF-8	Fe^{3+}–N_4	20	CO	> 80	− 0.47	–	[336]
FeNC	Fe-ZIF-8	Fe–N_4	25	CO	> 90	− 0.8	–	[337]
Fe-NCS	Fe-ZIF-8-S	Fe–N_4	4	CO	93	− 0.4	–	[338]
InNC	In-ZIF-8	In–N_4	–	HCOOH	–	− 0.99	–	[339]
$In^{\delta+}$–N_4	In/ZIF-8	In–N_4	8.87	HCOOH	96	− 0.65	–	[318]
Mn_{SA}/SNC	Mn/Zn-MOF	MnN_3S_1	–	CO	70	− 0.45	–	[340]
MOF-NS-Co	Co-MOF-NS	Co–N_4	–	CO	98.7	− 0.6	–	[341]
Ni SAs/NC	Ni-ZIF-8	Ni–N_3C_1	10.48	CO	71.9	-	5273 h^{-1}	[294]
Ni SAs/NCNTs	ZIF-8/DCD/Ni^{2+}	Ni–N_4	41.5	CO	97	− 0.9	1176 h^{-1}	[342]
Ni/FeNC	Ni/Fe-ZIF-8	Ni/Fe-NC	7.4	CO	98	− 0.7	–	[278]
Ni/N @ CNTs	Ni_2(NDISA)	Ni–N_x	–	CO	> 96	− 0.67	–	[343]
Ni/NCTs	ZnO@ZIF-NiZn	Ni-NC	34.3	CO	98	− 1.0	9366 h^{-1}	[344]
Ni_1NC	Ni-MTV-MOF	Ni–N_4	27	CO	96.8	− 0.8	11 315 h^{-1}	[345]
Ni–N_3C	Ni-ZIF-8	Ni–N_3C	6.64	CO	95.6	− 0.65	1425 h^{-1}	[114]
Ni–N_4/C–NH_2	Ni-ZIF-8	Ni–N_4	76.7	CO	96.2	1.0	–	[346]
Ni–N_4–O/C	Ni–Mn-MOFs	Ni–N_4–O	23	CO	99.2	− 0.9	11 187 h^{-1}	[347]
Ni-NG	NH_2–Ni-MOF	Ni–N_4	27.2	CO	97	0.79	–	[348]
NiNPIC	Ni-ZIF-8	Ni–N	10.2	CO	95.1	-	1886 h^{-1}	[295]
Ni_{SA}–N_2–C	MgNi-MOF-74	Ni–N_2–C_2	–	CO	98	− 0.8	1622 h^{-1}	[349]
SE-Ni SAs@PNC	Ni NPs@NC	Ni–N_x	18.3	CO	88	− 1.0	47 805 h^{-1}	[350]
ZIF-A-LD	ZIF-8	Zn–N_4	–	CO	90.57	− 1.1	–	[281]

Table 2
Electrocatalytic CO_2R on other MOF derivatives.

MOF electrocatalysts	Synthetic/preparation methods	Electrolytes	Products	FE (%) and potential (RHE)	Ref
AFC@ZIF-8	Pyrolyzed in Argon	$KHCO_3$ (1 M)	CO	93 at − 0.43 V	[326]
Ag/Co-MOFs	Air pyrolysis	$KHCO_3$ (0.1 M)	CO	55.6 at −1.8 V vs. SCE	[351]
BEN-Cu-BTC	Pyrolyzed in Argon	$KHCO_3$ (0.1 M)	C_2H_5OH and C_2H_4	18.4 and 11.2 at −1.01 V	[128]
Bi(btb)	Cathodization	$KHCO_3$ (0.5 M)	formate	95 at −0.97 V	[134]
Bi-MOF	Pyrolyzed in Argon	$NaHCO_3$(0.1 M)	CO	97 at −0.5 V	[317]
Co/Zn-ZIF	High temperature decomposition in Nitrogen	$KHCO_3$ (0.1 M)	CO	82 at −0.8 V	[175]
Co/Zn-ZIF	High temperature decomposition in Argon	$KHCO_3$ (0.5 M)	CO	94 at −0.63 V	[175]
Co-doped ZIF-8		$KHCO_3$ (0.1 M)	CO	45 at −0.58 V	[296]
$Cu(BTC)(H_2O)_3$	High temperature decomposition in Argon	$KHCO_3$ (0.1 M)	C_2H_4	24.8 at −1.4 V	[333]
Cu^{III}/ade-MOFs	Cathodization	$KHCO_3$ (0.1 M)	CH_4, and C_2H_4	15, and 45 at −1.4 V	[135]
Cu-MOF	High temperature decomposition in Nitrogen	$KHCO_3$ (0.5 M)	CO	43.8 at −0.76 V	[352]
Fe doped ZIF-8	High temperature decomposition in Argon	$KHCO_3$ (0.1 M)	CO	93 V	[296]
Fe, Ni-doped ZIF-8	High temperature decomposition in Argon	$KHCO_3$ (0.5 M)	CO	98 at –0. 7 V	[278]
Fe-doped ZIF-8	High temperature decomposition in Nitrogen	$KHCO_3$ (0.5 M)	CO	80 at −0.2 V	[336]
Fe-ZIF@SiO_2	High temperature decomposition in Nitrogen	$KHCO_3$ (1 M)	CO	98.8 at −0.58 V	[353]
Fe-ZIF-8	Pyrolyzed in Argon along with post-impregation	KOH (0.5 M)	CO	> 90 at –0.13 to −0.87 V	[322]
HKUST-1	Phosphorization in Argon	$KHCO_3$ (0.1 M)	CO	47 at −0.3 V	[137]
HKUST-1	Pyrolysis in Argon	$KHCO_3$ (0.1 M)	C_2H_5OH and CH_3OH	24 and 24 at −0.1 V vs. R.H.E	[136]
InCu-MOF	Air pyrolysis	$KHCO_3$ (0.5 M)	CO	92.1 at −0.8 V	[139]
MoO_3, In-MOF	Phosphorization in Hydrogen/Argon	[Bmim]PF_6 /MeCN/H_2O (30/65/5 wt %)	formate	96.5 at −2.2 V vs. Ag/Ag+	[138]
Ni^{2+}@ZIF-8	High temperature decomposition in Argon	$KHCO_3$ (0.5 M)	CO	71.9 at −0.9 V	[294]
Ni-doped ZIF-8	High temperature decomposition in Argon	$KHCO_3$ (0.5 M)	CO	95.1 at −0.65 V	[295]
PPy@MgNi-MOF-74	High temperature decomposition in Nitrogen	$KHCO_3$ (0.5 M)	CO	98 at −0.8 V	[204]
ZIF-8	High temperature decomposition in Argon	$NaHCO_3$ (0.1 M)	CO	100 at − 0.86 V	[287]
ZIF-8	High temperature decomposition in Argon	[Bmin]PF_6/DMAC (0.15 M)	CH_3OH	at −2 V vs. Ag/Ag+	[354]
ZIF-8	Pyrolyzed in Nitrogen	$KHCO_3$ (0.1 M)	CO	78 at − 0.93 V	[286]
ZIF-8	Pyrolysis in Argon	$KHCO_3$ (0.5 M)	CO	95.4 at − 0.5 V	[127]
ZIF-Fe30	High temperature decomposition in NH_3 and Argon	$KHCO_3$ (1 M)	CO	85 at −0.43 V	[327]
ZnFe-ZIFs	High temperature decomposition in Argon	$KHCO_3$ (0.5 M)	CO	86.9 at −0.47 V	[120]

3.1. Comparison of MOF-derived nanomaterials with state-of-art materials

The recent years has witnessed extensive utilizations of MOF-derived electrocatalyst materials for diverse electrocatalytic energy conversion reactions. Currently, the state-of-the-art electrocatalysts rely heavily on noble metals such as Pt, Pd, and Ru. However, the increased cost and instability issues associated with noble/precious metals have hampered their wider implementation. These disadvantages have prompted the development of transition metal-based MOFs (e.g., Co-MOFs, Fe-MOFs, Ni-MOFs, Zr-MOFs, etc.), which are commonly used in the preparation of metal-based, carbon-based, and their hybrid materials for improving catalytic performance [102,141–147].

Modulation of the physical and chemical characteristics of inorganic functional material has been regarded as a useful microstructure strategy. The design and composition of the material structures may be altered by the fabrication strategy of the MOF-materials-derived nanomaterials, thereby improving the electrochemical performance [46, 142]. For example, the electrocatalytic activity of the MOF-derived nanomaterials may be modulated and enhanced by the incorporation of various constituents and tunable chemical compositions. The greater active surface, mass transfer, facile charging, and effective strain accommodation during the electrocatalytic process can be achieved by a large surface area and higher porosity of these nanomaterials [148–150]. Therefore, comparing MOF-derived nanomaterials to materials fabricated by conventional methods, the compositional and structural properties provide MOF-derived nanomaterials a favorable possibility for electrochemically CO_2RR application.

The first study on MOF-derived nanomaterials has described the thermal transition of MOF precursor to produce pristine carbons [151]. Since then, employing MOFs as a starting material has witnessed utilization of different metal categories such as oxides, chalcogenides, phosphides, carbides, and nanoparticles for producing efficient electrocatalysts [152,153]. Earlier research also showed that MOF tends to collapse and lose its original morphology when subjected to the severe and elevated pyrolysis conditions [151,154], thereby resulting in a bulk material with featureless morphology. It has been recently observed that selection of appropriate MOF precursors and application of controlled strategy has enabled the pyrolysis process possible to rationally create MOF-derived nanomaterials with a variety of morphologies. There are other several benefits of using MOF as a precursor to create electrocatalysts, few of them include: (a) The variety of organic ligands and metal nodes that can produce MOFs, because by judiciously selecting the organic ligands and metal nodes of a MOF precursor, the composition and structure of the resulting MOF-derived nanomaterials could be adjusted. (b) The atomically homogeneity distribution of the organic ligand and metal node in a MOF precursor could result in high dispersed electroactive sites in the MOF-derived nanomaterials. Controlling the MOF precursor and conversion process can enable the production of clusters, single-atom sites, and nanoparticles, that are consistently dispersed across MOF-derived nanomaterials [46,155]. The applications of such as generated MOF-derived nanomaterials are currently hotspot research areas in catalysis, gas storage and purification, sensing, and energy conversion and storage [49,156–158]. These research areas are mostly motivated by the realization of the significance of shape in improving the performances of the MOF-derived materials in certain applications [159,160].

Summarily, the main strengths of MOF-derived electrocatalyst materials are as follows: (a) Compared with original MOF catalysts, the pyrolysis of MOFs generates carbon-based catalysts with hydrophobicity, structural flexibility and enhanced conductivity that allow electron transfer throughout the electrocatalytic processes. (b) The resultant materials have higher porosities and inherited larger surface areas which are favourable to the distribution and availability of high-density

active sites. (c) compared to the MOF precursor, the prospect of improving the stability of the generated porous materials in resulting in an exceptional recyclability. Owing to these benefits, MOF-derived nanomaterials are interesting materials for a variety of electrochemical energy conversion technologies especially in CO_2RR.

Despite the benefits of MOF-derived electrocatalyst materials outlined above, an effective technique to precisely regulate and optimize their structural-compositional properties for is still unavailable. This difficulty results from inadequate knowledge about the relationship between the structure and composition performances of the MOF-derived electrocatalyst materials from atomic scale to device scale. Also, insufficient control of the intricate processing methods (especially thermal treatments). Numerous studies have been conducted to consolidate reported activities in this field, and much effort has been put into investigating effective methods to precisely tailor the structure and composition of MOF-derived nanomaterials for energy electrocatalysis [47,142,148,155,161–166]. The design and manufacturing of MOF-derived electrocatalysts based on the structural-compositional performance relationships from the multi-scaling viewpoint need an in-depth investigation.

4. Synthetic techniques of MOF derivatives and the corresponding regulations of compositions, structures, and performances

In general, the synthetic method for MOF-derived materials is divided into two stages: the design and manufacture of MOF-based precursor(s) and the application of purposeful post-treatments to those precursors. The MOF-based precursors used in this study include both pristine (pure) MOFs and MOF composites [167,168]. The former is primarily designed using a solvothermal method by selecting the appropriate solvent, organic ligand, and metal source [169,170]. In contrast, the latter are prepared through various methodologies such as blending assembly, impregnating guest species, electrodeposition, surface coating/growth, mechanical mixing, and electrospinning [166, 171]. Instead, the post-treatment technique and conditions of the

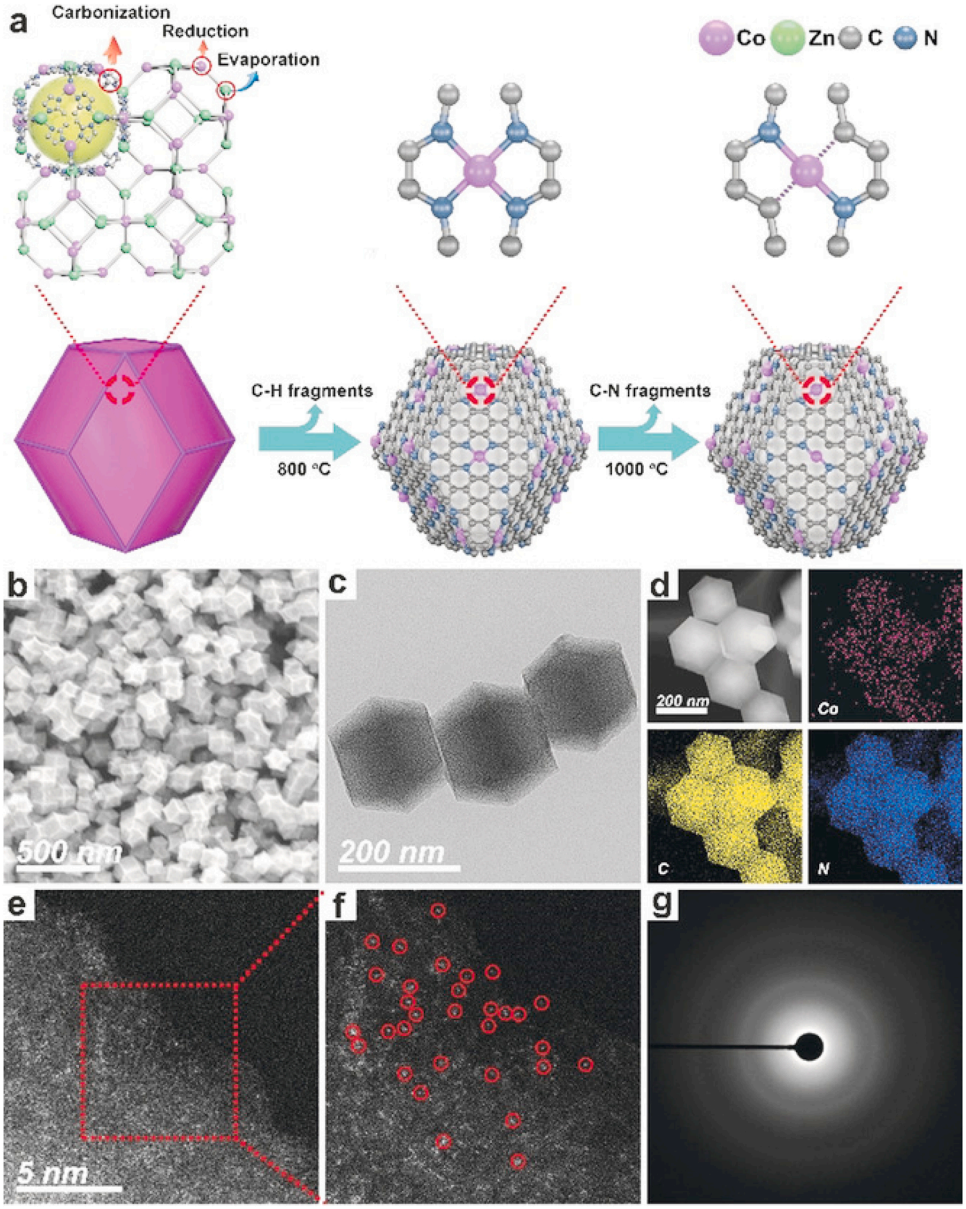

Fig. 3. (a) The formation process of Co-N_4 and Co-N_2. (b) SEM and (c) TEM images of Co-N_2. (d) Examination of the corresponding EDS mapping reveals the homogeneous distribution of Co and N on the carbon support. (e,f) Magnified HAADF-STEM images of Co-N_2 shows the atomic dispersion of Co atoms. (g) Corresponding SAED pattern of Co-N_2 [175].

MOF-based precursor(s) nearly entirely dictate the resultant structure, composition and morphology of the derivatives, and this eventually affects the electrochemical properties [14,166,172,173]. Based on this, numerous efforts have been dedicated to investigating and developing novel conversion techniques. For instance, Zhao et al. created porous carbon with atomically dispersed Ni sites through simple pyrolysis of Zn-based MOF with Ni ions adsorbed within the pores for electrocatalytic CO_2RR [174]. The electrocatalysis of the resulting single Ni catalyst may reach a high CO current density of 7.37 mA/cm^2 and TOF of 5273 h^{-1} at an overpotential of 0.89 V, as well as a high Faradaic efficiency for CO generation. The advantageous CO_2RR performance was related to the abundance of exposed active single Ni active sites, enhanced electrical conductivity, and decreased CO adsorption energy on single Ni sites. In other situation by Wang et al., porous carbon materials were generated from MOFs and doped with atomically scattered Co or Fe sites (Fig. 3) were created for CO_2RR to CO, achieving 94% FE [175].

Considering the MOFs' chemical and thermal fragility, two widely used post-process methods include wet chemical reaction and pyrolysis at high temperatures. These strategies could be classified into four categories depending on the various conversion mechanisms that occur during the postprocessing: (i) gas-phase chemical reaction [176,177], (ii) self-pyrolysis under inert atmosphere [178,179], (iii) chemical reaction combined with heat treatment [180,181], and (iv) liquid-phase chemical reaction [173,182,183]. Different dimensional MOFs ranging from 0D to 3D can be obtained by carefully controlling the sizes, morphological characteristics, structural configuration, and compositions of the MOF precursors, as well as manipulation of the conversion processes, diverse compositions (carbons, metal compounds, metal/-carbons, and metal compounds/carbons) as well as various structures (porous, hollow, hierarchical, yolk-shell, frame, etc.) can be achieved in the MOF derivatives,

To meet the specific requirements of some electrochemical systems, other wide range of approaches, including surface/interfacial modulations, such as support interactions [178], defects/doping [14,167,181, 184], heterostructure [167,168,179], surface modifications [185], etc, have been established to stimulate novel physicochemical characteristics and stronger synergistic influences to improve the electrochemical behavior significantly. The chemical and structural characteristics of these MOF-derived functional materials are fascinating, and they have considerable potential for use in various electrochemical systems. As shown in Fig. 4, a high-level overview of the synthetic technique, compositions, structures, and enhanced performances can be obtained using these approaches for MOF-derived functional materials for electrochemical CO_2R applications.

5. MOF modification strategies and confinement engineering

Based on the sequential perspective of MOF crystallization and functionalization, the strategies for modifying MOF-nanomaterials can be divided into post-synthetic and in-situ modification approaches. The latter technique entails introducing molecules, polymers, or ions into the pores of a MOF during crystallization. The interconnections, including covalent, coordination, and electrostatic forces between the skeletal and functional, confer high durability (stability) on produced MOF-derived/hybrid nanomaterials. On the other hand, post-synthetic (Fig. 5) refers to functional alterations made during the fabrication of MOFs [186, 187]. This strategy uses the hybrid characters of MOFs by applying orientated modifications to the organic ligands, metal ions, or clusters and micro-environment cavities, integrating crystal-to-crystal structural alterations. This may result in the formation of new MOF materials, which may be challenged with a larger energy barrier through the direct growth nucleation method [188,189].

To improve the energy conversion performances of MOFs, modification techniques should focus on constructing a system that narrows confinement action spaces in cages, intensifies adsorption affinities, and

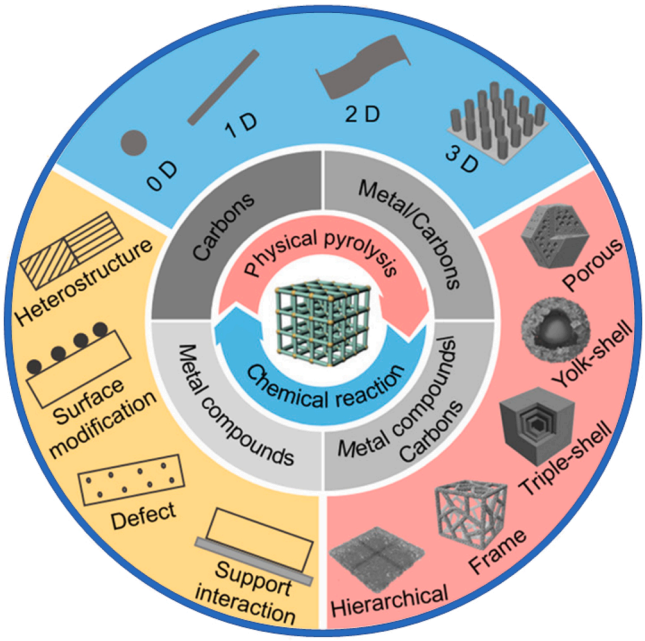

Fig. 4. Synthetic technique of MOF derivatives and the corresponding regulations of composition, structure, and performance [168].

removes non-selective intercrystallite defects [190,191]. A detailed advancement in different post-synthetic modifications (such as chemical function decoration, component replacement, defect sealing with flexible coating, and in-situ modifications (such as in-situ hybridization and encapsulation in the cages) have been reported previously [190,192].

5.1. Confinement engineering of MOF-derived nanomaterials

As a general rule, confinement engineering of MOF-derived nanomaterials is focused on synthesis and electrocatalysis. For synthesis, confinement engineering plays a crucial role in controlling the size of metal species. In addition to the various electrocatalytic properties of metal species of different sizes (e.g., nanoclusters, NPs, and single atoms), the metal–support contacts and metal–reactant interaction can substantially impact the electrocatalytic performances of metal electrocatalysts. Therefore, various metals can be fabricated by using the right synthesis approach [193,194]. Due to their effective techniques, MOF-derived materials offer special confinement effects when used in diverse electrocatalytic processes. The two primary subtypes of this confinement phenomenon are spatial confinement effects and coordination of the chemical environment. In addition to improving the electrical structures of the active centers and stabilizing the active metal center, they can also enhance the electrocatalyst performances.

In terms of confinement engineering on the synthesis strategies, the interaction between multi-scale metal active centers (clusters, NPs and single atoms) and reactant/support affects the activity and stability of an electrocatalyst: (i) during the sintering process, metals of various sizes can undergo varying Ostwald ripening speeds, resulting in varied migration and agglomeration. [195–197], (ii) The size of the metal affects the transport of electrons between supports and metals [198]. (iii) Therefore, it is essential to note that when metals are employed as electrocatalysts, their sizes impact how they interact with their reactants and their electrical and geometric structures [199]. (iv) More active sites may be found in the supports with a smaller metal cluster because they are more equally distributed [199]. For instance, MOF-derived-based materials that support metal species of varied sizes may be created by varying the ratio of metal precursors in the MOF precursors. The effectively synthesized MOF-derived-based materials, including clusters, NPs, and single atoms by controlling the Zn/Co ratio, have been

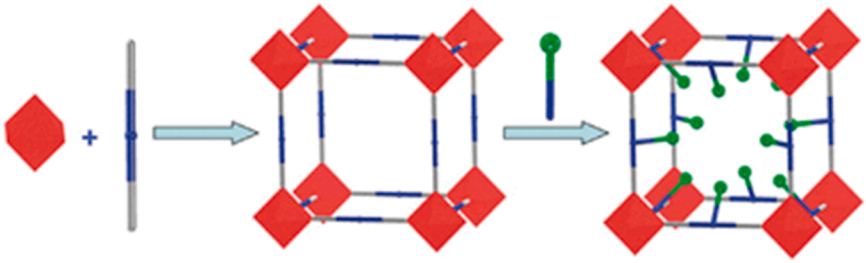

Fig. 5. General schematic representation of the concept of the post-synthetic modification of MOFs [186].

reported. This synthesis method enables the investigation of the electrochemical behavior of single atoms and NPs [200]. In addition, a novel method for stabilizing Co single atoms by predesigning the Zn/Co ratio has been reported, demonstrating the possibility of decreasing Zn using the carbonization process or selectively vaporizing Zn over 800 °C during the pyrolysis processes. Although a rise in the ratio of Zn/Co did not result in the accumulation of Co atom under identical pyrolysis conditions, the ratio of Zn/Co decreasing to 0.75:1 is insufficient and led to the Co-NPs formation [201]. The detail explanation about the confinement effect of MOF-derived materials on electrocatalyzing CO_2RR has been reviewed extensively by another authors [194], therefore, this section will only focused on the fundamental principle.

5.2. Controlling the electrocatalytic performances via confinement engineering

MOF-derived carbon-based materials have a strong confinement effect when employed as electrocatalysts because of their ordered pore size, higher surface area, higher porosity, and highly customizable chemical compositions: To improve the electronic structures of the active sites and increase the electrocatalytic activity and stability, different metallic nodes, as well as changeable organic linkages, may work together. Secondly, the crystal structure and distributions of organic ligand and metallic nodes are positioned for further investigation of prospective electrocatalysts and their processes. MOF channel/cavity confines the active sites (cluster, NPs, and single atom) to increase electrocatalytic stability by preventing them from aggregating. In order to fine-tune electrocatalytic selectivity through reaction kinetics, MOF pores may selectively enrich distinct compounds. As a result, the active sites of the MOF-derived nanomaterials are more stable because of the confinement effects. Improved adsorption and desorption rates of reaction intermediates, reduced energy barriers in the electrocatalytic process, faster reaction time, and increased activity may be achieved by altering the electronic structures and stabilities of the active sites [194, 202].

To modulate the electrocatalytic performance modulation via chemical coordination confinement, the MOF precursor can be contained in the abundance of ligands and metallic nodes, which are electrochemically conducive to the single metallic atom confinements. Target metal atoms may be included in MOFs by replacing some original metal nodes. Beneficially, the interactions between the ligands and the confined metallic atom(s) on the MOF precursors can stabilize the active sites of the confined metals [203]. In addition, the MOF precursors have several additional coordination atoms (N, O, etc.) that may be employed to stabilize metallic atoms. Other coordination structures can be employed to confine the metallic atoms in the MOFs. For instance, the recent year has recorded the Ni@N_xC_y coordination environment in the CO_2RR. By pyrolyzing MgNiMOF-74, Gong et al. created Ni_{SA}-N_x-C (x = 2–4) which demonstrated h FE of 98% for CO formation on Ni_{SA}-N_2-C electrocatalysts. Though, the tuning of the N-coordination number could be achieved from 2 to 4, the structure of Ni_{SA}-N_1-C electrocatalysts is still not cleared. Additionally, the MgNiMOF-74 electrocatalysts is expensive and the loss of Mg^{2+} during pyrolysis prevent their large scale applications [204].

Recently, Yang et al. [205] used a inexpensive carbon substrate to prepare atomically dispersed Ni-based MOF electrocatalysts with different N/C coordination numbers denoted as Ni@N_xC_y (Fig. 6). Increased pyrolysis temperature from 800° to 1100°C, reduced the N coordination number in Ni@N_xC_y electrocatalyst from 4 to 1, evidencing from EXAFS fitting analysis, but the C coordination number exhibited the reverse trend. At − 0.7 V vs RHE, the Ni@N_xC_y-1000 electrocatalyst with the optimal coordination numbers of two N and two C atoms produced the greatest FE= 98.7% for CO formation (Fig. 6). According to the DFT calculation, Ni-N_2C_2 active site was advantageous for producing more unoccupied Ni 3d orbitals, which would lower the rate-determining step of the free energy (to +0.80 eV) and significantly boost CO_2RR electrocatalytic performance (Fig. 6) [205].

6. Mechanistic aspects of CO_2 electroreduction

Despite the fact that electrochemical paths are thermodynamically preferred, the overall energy barrier referred to as overpotential affects actual selectivity between the products. Higher current intensity and selectivity as well as robust and steady and extended operating period, are requisites for considering electrocatalysts for industrial practicability [206]. The mechanistic investigations of CO_2 conversion can be separated into two steps, namely intermediate formation and final product generations, which varies depending on the products. The C_1 products such as formic acid (HCCOH) and carbon monoxide (CO) normally come after the important initial process, in which CO_2 is stimulated that is *CO_2, through the adsorption of an electron on an electrocatalyst's surface [12, 207–210]. The proton-coupled-electron transfer (PCET) mechanism is then initiated by reacting the atomic carbon with (*CO_2), resulting in the formation of a crucial intermediate (*COOH). By using a second-step PCET process, the *COOH intermediate may be transformed into the end (final) product CO. The interaction of oxygen with the *CO_2 and the protonated oxygen atoms produces intermediate *OCHO, that can be transformed to $HCOO^-$/HCOOH through PCET [211]. According to the experimental and theoretical investigations, the first-step intermediary in the CO_2RR to CH_4, CH_3OH and HCHO is *CO [207,212]. The hydrogenation of *CO results in the formation of intermediate *HCO, *H_2CO, and *H_3CO, followed by their transformation into CH_4, HCHO, and CH_3OH. Nevertheless, there are two opposing justifications for converting *CO to CH_4. One suggested strategy is to convert *CO into *C through a *COH intermediate, which could then be extended to include the reduction of *CH, *CH_2, and *CH_3 to *C and eventually produce CH_4 [213,214]. The other route, which is the most widely recognized pathway, as determined by experimental and theoretical calculations [215], involves:

$$*CO \rightarrow *CHO \rightarrow *CH*CH_2 \rightarrow *CH_3 \rightarrow * + CH_3$$

Furthermore, for the generation of C_2 + product(s), the *CO intermediate route is often used, and the *CO reduction determines the ultimate product(s) along with experimental condition(s) [216,217]. Typically, ethane is generated by a proton-coupled electron transfer process after protonating *CH to *CH_3. The *CH_3 dimerization results in

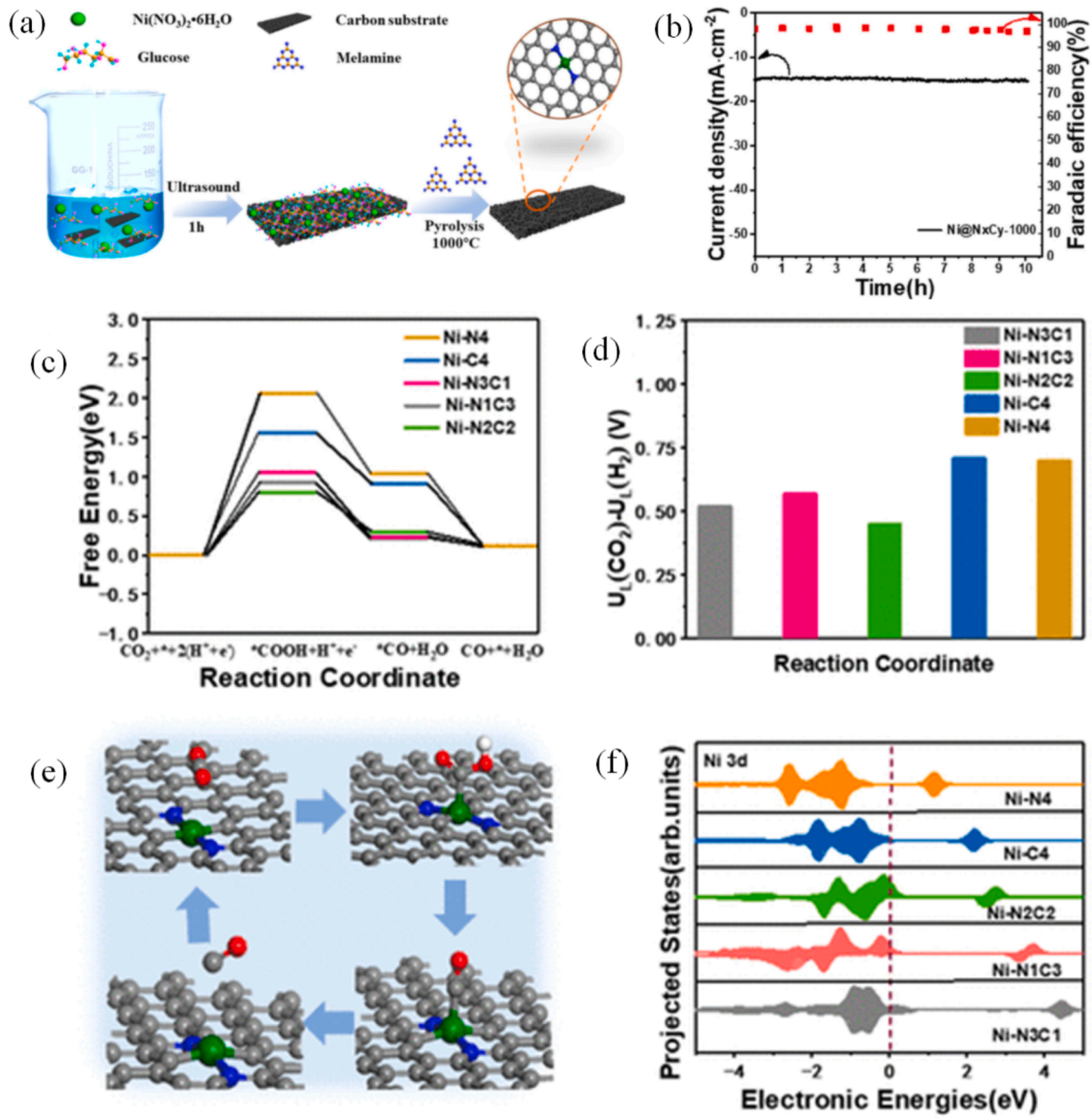

Fig. 6. Synthesis strategy of Ni single atoms were loaded on N-doped C substrate pyrolyzed at 1000 °C to prepare the Ni@N_xC_y-1000 electrocatalyst. (b) Stability test of CO_2RR over the Ni@N_xC_y-1000 catalyst at − 0.7 V vs RHE. The solid line and dots show the FE_{CO} and corresponding current density of different samples, respectively DFT calculations of CO_2RR over different electrocatalysts. (c) Free energy diagram for CO_2RR to CO over Ni sites in Ni–N_4, Ni–N_3C_1, Ni–N_2C_2, Ni–N_1C_3, and Ni–C_4 active sites. (d) Potential differences in the limiting steps of CO_2RR ($U_L(CO_2)$) and HER ($U_L(H_2)$) on Ni sites in the Ni–N_4, Ni–N_3C_1, Ni–N_2C_2, Ni–N_1C_3, and Ni–C_4 active sites. (e) Schematics of CO_2RR on Ni sites in the Ni–N_2C_2 active sites. (C, gray; N, blue; O, red; H, white; Ni, green). (f) Projected density of states (PDOS) of Ni single atoms in different electrocatalysts [205].

C_2H_6. The addition of CO to *CH_2 resulted in the formation of $OOCCH_3$. The dimer of *CO-CO generated the intermediate *CH_2CHO by a sequence of electron/protonation transfer processes, which served as the selectivity's deciding steps in the generation of C_2H_5OH and C_2H_4 [216, 218].

Some experimental studies on the bulk metal surfaces for CO_2RR, in addition to the theoretical patterns, have been reported [219–227], and metal electrodes have been divided into four types: (i) carbon monoxide producing metals (e.g. silver, palladium, gold, gallium, and zinc); (ii) formic acid creating metals, such as thallium, tin, cadmium, indium, mercury, bismuth, lead, and so on; (iii) H_2-generating metals, such as nickel, titanium, iron, and platinum; (iv) copper is commonly considered as for the manufacturing of various hydrocarbon products [228–230].

Along with the classified metal active sites, H- bond is important, because competing HER reactions may limit the efficiency and selectivities of the end products. Therefore, Faradaic efficiency (FE) is regarded as a critical issue in assessing CO_2R activities. Research has shown that structure modification or manipulation of a natural active site generate variations in the products, selectivity, and FE. For instance, Zn and Cu exhibit identical 3d electronic structures but distinct electrocatalytic performances, i.e., Zn electrode shows two electron CO_2 reduction to produce CO, whereas Cu yields numerous hydrocarbons [231,232]. However, a Zn doped onto Cu (denoted as Cu/Zn) selectively produces alcohol product [233,234]. Additionally, a physical mixture of ZnO and CuO (0.5:1 wt%) yielded CH_3OH with a FE = 25.2% [235].

On the other hand, the S-doping in Cu has been observed not to provide superior performance and was ascribed to the comparatively stronger attachment of the intermediate (*CO) and the Cu-surfaces [236, 237]. As a result, the retention time of intermediate on the electrocatalyst surfaces is regarded a vital descriptor for controlling the product selectivities during CO_2RR. Therefore, the construction of electrocatalysts with extended interactions with intermediates can result in the formation of multicarbon (C_2) products [238–243]. Benefitting from

this, Song et al. showed the switching of adsorption states of CO_2 intermediate and improved the selectivity of formate formation during CO_2RR using an S-doping onto Cu-electrocatalysts [243]. The in-situ Raman spectroscopy findings indicated the CO_2R mechanisms includes changing the adsorption states of CO_2 intermediates from coexisting OC*O* or O*CO to the dominant OC*O* . The density functional theory (DFT) indicated lower intermediates were binding energy on the S-doped Cu(111) surfaces than that of the undoped electrocatalyst. This electrocatalyst achieved 76.5% FE and a maximal partial $j = \sim 21.1$ mA/cm^2.

Physicochemical characteristics of electrocatalysts have recently been considered to modify the reaction kinetics/mechanism toward product selectivity, and porous electrocatalyst materials are currently receiving remarkable attention. This is due to their attractive properties, including an improved surface-to-volume ratio, active site, tunable pore structures for mass transfer of reactant/product, and controllable local pH [240,244].

The employment of self-assembly involving two polymers to construct hierarchical macroporous-mesoporous (20 and 320 nm) Cu/Zn alloy, and the findings indicated that Cu_5Zn_8 had the best performances for CO_2RR to C_2H_5OH with FE = ~47% at 0.8 V) with high stabilities up to 11 h [71,223]. The study noted that decreasing the porosity with the sizes ranging from 300 nm to 30 nm led to concerted production of ethylene as a major product, thereby increasing the FE from 8% to 38%.

Furthermore, electrocatalyst nanostructuring has been observed as a major influence on CO_2RR performance. For instance, SnO_2 and Au, which share identical morphologies, demonstrated comparable effects during CO_2RR [242,245]. Yang et al. [246] hypothesized morphology-dependent reaction kinetics for CO_2RR to C_2 product on the Cu-based mesoporous electrocatalyst by carefully regulating the size and morphology. This demonstrated that morphology might be used to accelerate C-C coupled and lengthen retention time by regulating the flow field and pH [246]. Currently, MOFs are especially appealing as

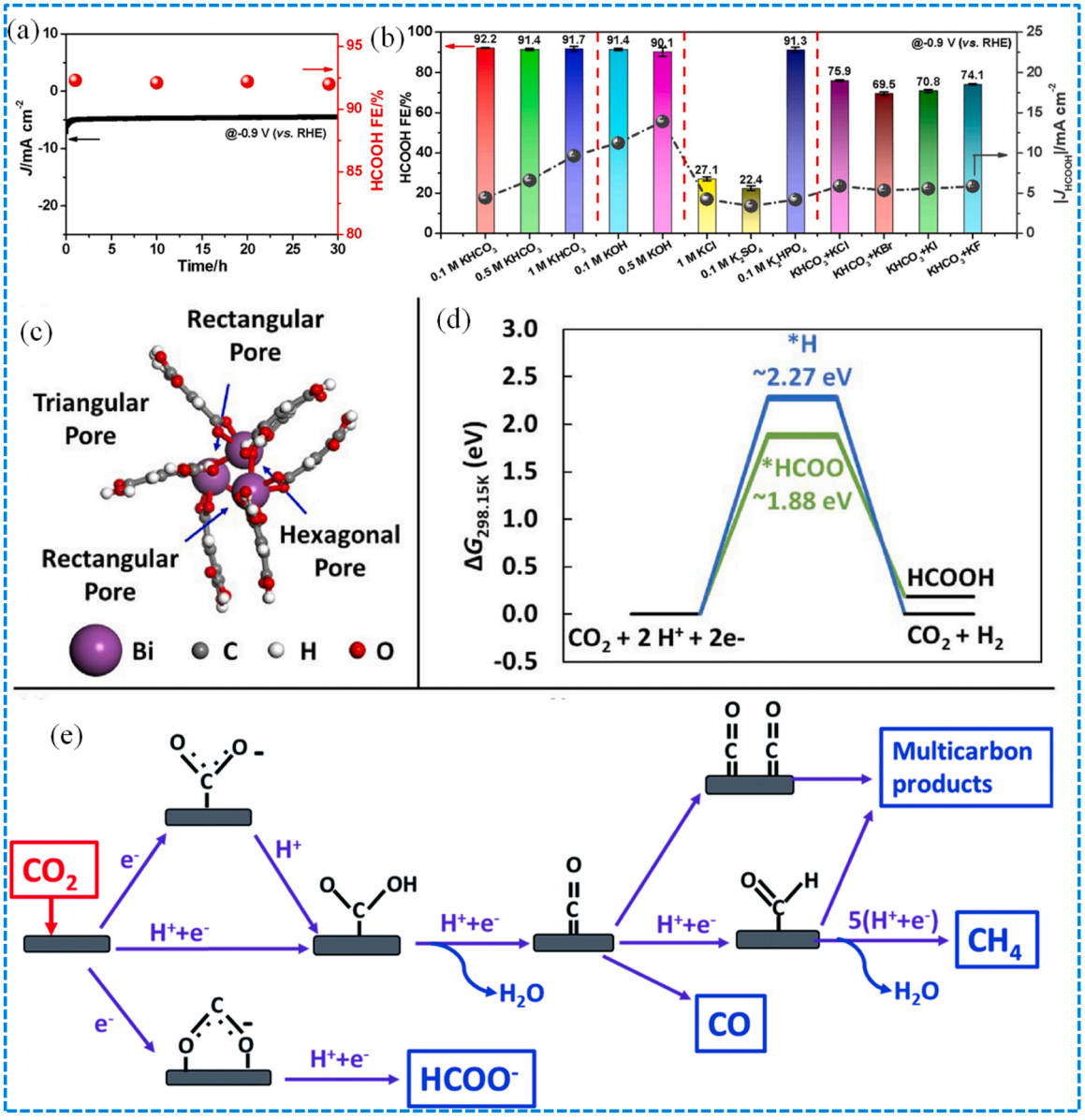

Fig. 7. (a) Current density and HCOOH FE of Bi-MOF during long-time electrolysis at ~ −0.9 V. (b) HCOOH *FEs* (column) and HCOOH partial current densities (grey ball) of Bi-MOF in various electrolytes with different concentrations (c) Simulated cluster representing Bi-MOF catalytic sites. Blue arrows show the binding sites of adsorbates. (d) Free energy diagram of HER and formic acid formation. The ~energy value indicates the average energy of the three binding sites. (e) Suggested reaction pathway. Each arrow indicates a reaction with an addition of an electron. [247,248].

catalysts for CO_2R due to of their highly variable surface area and porosity with a sequence of nanostructures. Typically, a 2D Bi-based MOF with abundant porosities that outperformed the reversible hydrogen electrode (RHE) has been reported for CO_2RR. This produced HCOOH with 92.2% at 0.9 V and 30-hour durability (Fig. 7a-b). The specific mass of formic acid (HCOOH) with partial *j* reached 41.0 mA/mg, four folds higher than the industrial Bi or Bi_2O_3 sheet at 1.1 V. (vs RHE) [247]. The DFT studies demonstrated that an abundant Bi active site with a crystallographic channel in the MOF structures favoured the *HCOO formation and suppressed the side reaction, e.g., HER, thereby resulting in higher selectivity toward HCOOH (Fig. 7c-e).

Previous research has shown that advanced instrumental approaches play an important role in discovering electrocatalytically active sites and facilitating the identification of detailed mechanistic information for CO_2RR. Due to the significant complexity of electrochemical CO_2RR processes, a single in-situ/operando characterization approach is generally insufficient for understanding and resolving all the chemical intermediates and routes involved in product generation. Therefore, combining in-situ/operando approaches is extremely desired for gaining detailed quantitative insights into the electrocatalytic CO_2RR mechanism. Currently, the available progress in this direction in past years is insufficient.

Electrochemical shell-isolated nanoparticle enhanced Raman spectroscopy and tip-enhanced Raman spectroscopy have been shown to be strong methods for revealing activity and structural relationship under catalytic environments with nanoscale spatial precision, however, their applicability in the electrochemical CO_2RR domain remains limited [249]. Additionally, the application of spectroscopic methods for in-situ product identification is beneficial since it reduces sample contamination, which may easily result in false positive results. Control studies using $^{13}CO_2$ are strongly recommended for validating the carbon source in the liquid products, particularly when the amount is minimal. Isotope tests can also give information on the mechanisms involved in the synthesis of C_2 and C_3 products [250,251]. Till date most of the available instrumental analytical methods have primarily been used qualitatively, which means that essential information on the lifespan of CO_2R intermediates is still quite limited. Because several of these approaches allow access to extremely high time resolution, for example, time resolved XAS provides picoseconds to microseconds time resolution [249,252,253], therefore, future quantitative kinetic investigations should be investigated.

The retention period of intermediates on the electrocatalyst surface is also regarded as a crucial descriptor for controlling product selectivity in CO_2RR, and it is suggested that designed electrocatalysts with longer contact with intermediates may result in multicarbon products [240, 243,246,254]. Furthermore, many more complicated electrocatalytic processes need not just high activity but also careful control of product selectivity. (4) The more complex and possibly more controllable ligand environments surrounding the metal centers in MOFs (such as periodicity, coordination numbers, topology, and open sites) may provide more possibilities to rationally construct the efficient electrocatalytic center to control product selectivity by adhering to the design principles such as established in the molecular homogeneous catalysts. Such catalytic processes, although while presumably more complicated than those simpler electrocatalytic reactions typically investigated, might highlight, and increase the benefits of MOF materials in electrocatalysis and the overall outlooks can be employed as a strong starting point for constructing of efficient electrocatalysts.

7. DFT calculations

Electrocatalysts with distinct atomic-level electrocatalytic sites could be studied using the DFT-based theoretical calculation technique to obtain new and detailed perspective in the examination of the electronic configuration of the MOF-derived electrocatalysts. Adsorption energy and reaction mechanism on transition metal surfaces have been regularly calculated using DFT calculations [255–257], which are nowadays irreplaceable in exploring electrode materials. This provides an opportunity to understand the effects of certain important structural factors such as charge distributions, adsorption energy, electronic structures, and defect states on electrocatalytic performances [258–260]. Appropriate insights from the DFT calculations could aid an improved understanding of the link between surface structure modifications and electrocatalytic activity and selectivity. In this regard, DFT approaches can supplement experimental data for the electrodes, thereby developing comprehensive structural–activity relations. For instance, the DFT technique has been used on core-shell Pt alloy NPs on a FeNC substrate with an atomic dispersed single Fe atom. The study revealed that electrocatalytic performances, electronic structures, and adsorption-desorption processes could be significantly enhanced by the exceptional structures of the electrocatalysts as well as the interactions between the neighboring atom and isolated metal atom [261]. On the other hand, designing and building metal sites that can be easily adjustable in their coordination modes and definitively linked to their electrocatalytic characteristics is still a major hurdle for an unsaturated coordinated metal site.

Wu et al. [262] first show that the crystal plane of Sn(101) is energetically more advantageous for CO_2RR using DFT calculations (Fig. 8a-c). Thereafter, by using Sn-MOF ($Sn_3O(1,4\text{-}BDC)_2$) as a carbon source, they developed a variety of $Sn/SnO_2/C$ composite electrocatalysts with exposed facets Sn(101) via carbonization at various temperatures in an argon environment. $Sn(101)/SnO_2/C$-500 (carbonization of Sn-MOF at 500 °C) electrocatalyst accomplished a higher selectivity of CO_2 electroreduction to formate when compared with others. The XRD analysis and electrochemical studies (Fig. 8d-e) confirmed that the intensity of the Sn(101) diffraction peak is significantly important to the electrocatalytic activity and selectivity, which could be further improved by optimizing the acid etching and carbonization time [262].

The mechanistic aspect of MOF derived bimetallic CuBi has been reported for electroreduction of CO_2 to formate (Fig. 8f-g) [263]. Here, the CuBi-MOF precursor was carbonized and oxidized to a create the rod-shaped CuBi bimetallic electrocatalyst. The activity and selectivity of the bimetallic CuBi electrocatalyst was significantly improved due to the synthesis of Bi_2CuO_4 at the electrocatalytic interface, displaying an alluring higher FE of 100% for formate production at − 0.77 V vs. RHE, an extremely broad potential window of 900 mV, and good durability in H-cell. The HCOO* route was evidently dominating based on the results of the in-situ FTIR and DFT calculations. The activity and formate selectivity of Bi_2CuO_4 for CO_2RR are improved by its ability to increase the adsorption capacity of the CO_2 molecules and improve the capacity for charge transport. This research provides suggestions for enhancing the CO_2RR electrocatalytic performance of bimetallic materials.

8. Structure-activity relationships

MOF-derived electrocatalysts have shown promising results for the CO_2RR, as demonstrated in this study. However, the structure-activity relationship is still a mystery. Therefore, additional research into the effect of structural characteristics such as metal type, coordination environments, and linker electrical properties is required. Several studies on active sites of MOFs (*H, *COOH, *CO, and *CHO) could preferably be complemented with computational methods/simulations to determine the binding energy of the intermediates that function as a descriptor for predicting the activity and selectivity of the electrocatalytic process [115,264–266]. The combination of theoretical with experimental has demonstrated that the MNC electrocatalyst selectivity has been proven to be depending on the type of metals included in the carbon matrices due to the differential in binding energies between the reaction intermediates and active metals [267–272]. Analogous to metal electrocatalysts, the binding energy of *COOH could be employed to describe CO_2RR onset potential, while the greater strength of H

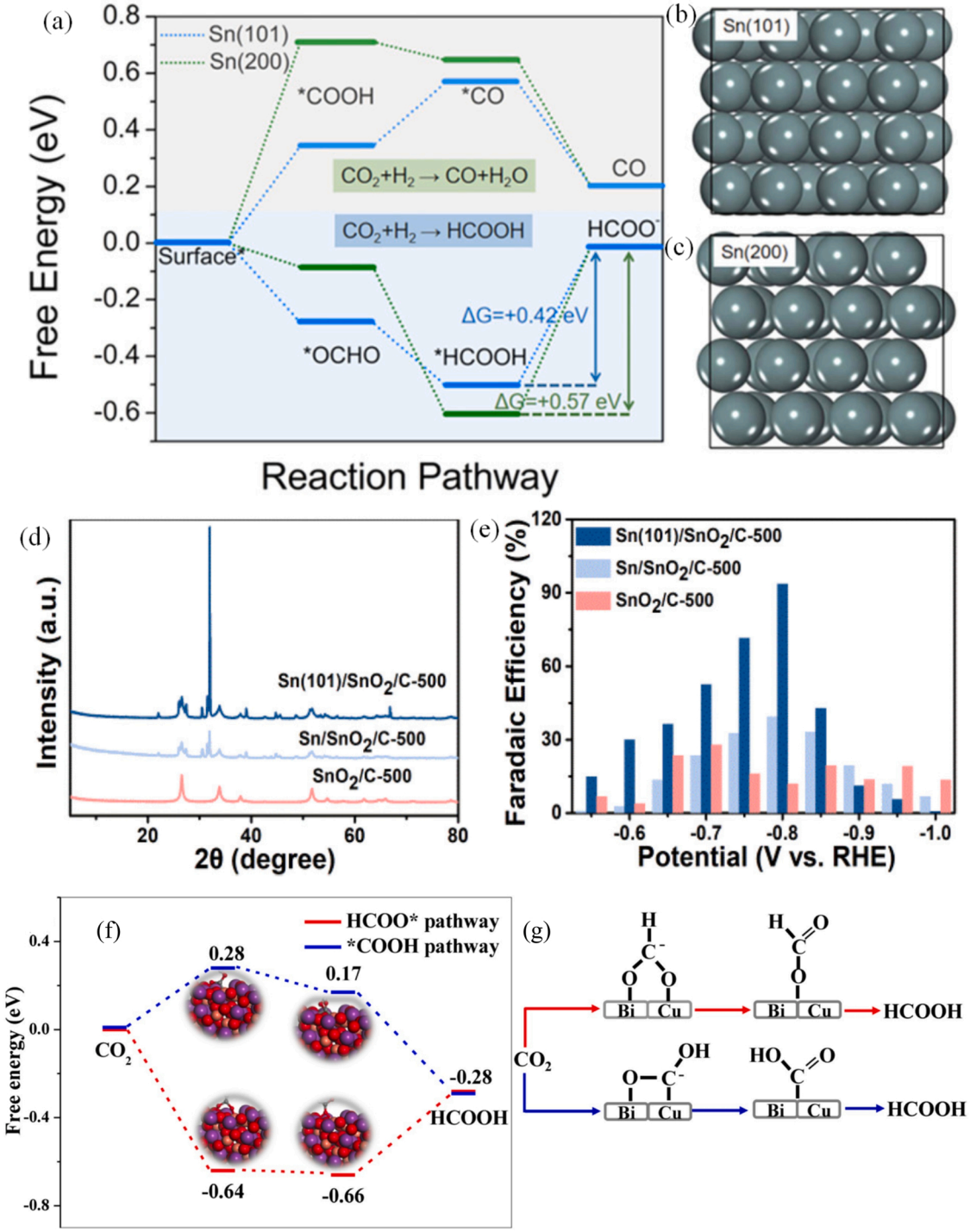

Fig. 8. DFT simulation of the CO_2RR process on Sn(101) and Sn(200) planes. (a) Calculated free-energy diagrams for HCOO–, CO formation; optimized geometric structure of (b) Sn(101) and (c) Sn(200). Sn-MOF was carbonized at 500 °C with different hydrochloric acid concentrations for etching (d) XRD and (e) FE of formate [262]. (f) Free energy diagrams of different pathway of CO_2 to formate on CuBi75 (211) plane, (g) Proposed mechanism of CO_2 reduction on the CuBi75 electrode [263].

adsorption led to increased H-induced HER activity and decreased CO selectivity [272].

To date, the combined experimental and theoretical investigations to understand the roles of the metal centers in MOF electrocatalysts are currently limited. Notably, the application of DFT calculation to describe the discrepancy in electrocatalytic activity between Ni and Co 2D MOFs consisting of metal-phthalocyanine (MPc) linker and Cu node has been reported [273]. Low activation energy for carboxyl intermediates (*CHOO) production in CoPc-based MOFs is consistent with both the high CO activity and selectivity. Many groups have also employed computational screening to predict the activities of various MOF electrocatalysts for CO_2RR. The activities and selectivity of the products of electrocatalysts could be determined using the binding energies of the intermediates and the computed Gibbs energy of every stage in the reaction pathway. According to Xing et al., the 2D metal hexahydroxybenzene frameworks ($M_3(HHB)_2$ (M = Rh, Ru, Cr, and Mo)) have shown to be promising for CO_2RR electrocatalysis by using the binding energies between reaction intermediates and the metal centers

to establish the rate-determining step [272]. Based on their predictions, the predominant product depended on the metal centers, and CH_4 was identified as the major product case of Mo and Cr, whereas CH_3OH in the case of Rh and Ru. Another study looked at the electrocatalytic activities of the 2D conducting MOFs (($M_3(HITP)_2$, M = Co, Fe, Ni, Pd, Rh, and Ru) [274]. Each electrocatalyst determined the adsorption energy of *CO intermediate using the predicted value and then estimated the free energy profiles for reduction mechanisms. Their findings showed that MOFs with M = Co, Fe, or Rh catalyzed the CO_2R and produced CH_3OH as a product, while only $Ru_3(HITP)_2$ was projected to exhibit a preference for CH_4 generation.

The employment of the D-band center as a descriptor for intermediate has been demonstrated [275], and they examined another series of materials involving the $M_3(HITP)_2$ MOF series, M is from Ti to Cu. It was shown that FeN_4 demonstrated the highest active site for selective electroreduction of CO_2 into CH_4. [276]. Theories predict that highly desirable reduced products such as CH_3OH and CH_4 could be formed from CO_{2R}on MOF electrocatalysts. However, just a few empirically proven MOFs could practically achieve this. There are also inconsistencies in some of the predicted reaction product and selectivity between the two experiments on $M_3(HITP)_2$ MOFs that have been described previously; therefore, it is imperative that researchers test these predictions and gain more insight into what structural characteristics are responsible for CO_2R selectivity.

Additionally, the importance of metals allows the employment of multi-metal MOFs to improve their electrocatalytic performances. Incorporating two different active sites could form tandem electrocatalysts, where the earliest reaction phases occur on one site and completion of the reaction occur on the other. After converting CO_2 to hydrocarbon on a Cu nanoparticle, Choukroun et al. used this method for an effective CO_2R to CO on a Ni single site [272]. In addition, it is also possible that the two metals are working together to speed up the electrocatalytic reactions. For instance, Zhong et al. employed the bimetallic MOFs with a Cu–phthalocyanine ligand (CuN_4) and Zn complex (ZnO_4), which acted as a linkage. It was hypothesized that a synergistic electrocatalytic mechanism where the ZnO_4 node operated as a CO_2RR electrocatalytic site while the CuN_4 center enhanced the CO_2RR [277].

Intriguingly, the two metals may be participating in the same active sites and modulatory influence its electrical structure. With this technique, the adsorption of the reaction intermediate can be optimized to promote the target reaction rate. Heterometallic active site MOFs have exhibited promising performance in various electrocatalytic processes [13–15], but they are currently not tested for CO_2RR. A dual isolated metal site on MNC material has been proven as a highly effective electrocatalyst for CO_2RR [278]. In addition, the development of new electrocatalysts for the formation of multi carbon compounds presents an opportunity for developing multi-metal sites since a neighboring active site for binding the *CO intermediate is required to facilitate their production.

Although several researchers have concentrated on the significance of the metal centers in determining the activities of single atom electrocatalytic systems, their coordination environments are critical. The CO electrocatalytic activity of CO_2RR has been shown to be greater on graphene-containing carbon–nitride-coordinated metal sites than on phosphorus and sulfur-coordinated metal sites [279]. Similarly, the intrinsic activities of metals in MOFs can be controlled by the nature of linkers, which affects the density of electronic charges on the metal sites [280]. The doping of Zn-ZIF-8 MOFs with the more electron-donating species such as 1,10-phenanthroline led to an increase FE towards CO production. [281]. Another possibility for ligand involvement in the electrocatalytic processes has been reported to involve a series of Zn-ZIF electrocatalysts with similar topologies but distinct organic linkers (imidazoles) [282]. It was discovered that the electrocatalysts' selectivity might be improved by using a different linker. Since the sp^2 C atom in the imidazolate ligand operated as the electrocatalyst active site, this finding and subsequent DFT calculations revealed the system's complexity as multiple active sites could be present. For this reason, it is necessary to engage in a holistic perspective to figure out how MOF electrocatalytic performances are affected by various factors.

In order to boost the capacity of MOF-545-Co to transfer electrons, Xin et al. introduced the electron-conductive polypyrrole (PPy) molecule into the MOF channels using in-situ polymerization of pyrrole in the pore (Fig. 9) [283]. The resulting hybrid materials exhibit outstanding electrocatalytic CO_2RR performance (Fig. 9), translating to high FE of 98% for CO formation on a PPy@MOF-545-Co that was about two times greater than that of bare MOF-545-Co at − 0.8 V. Incorporating PPy acted as electric cables in the MOF channels to assist electron transport during the CO_2RR, thereby responsible for its excellent performance. This initiative offers unique perspectives enhancing the MOFs' electrocatalytic efficiency for CO_2RR.

Recently, 2D MOF clearly have been reported to outperform 3D bulk MOFs in terms of their chemical and structural characteristics. Particularly, the enormous porosity and ultrathin structure of the 2D materials have been noticed to contribute to unusual characteristics like improved electrical conductivity and quick mass transfer during electrocatalytic CO_2RR [284].

9. Electrocatalytic CO_2RR on MOF-derivative nanomaterials

9.1. MOF-derived heteroatom-doped carbon materials for CO_2RR

The usage of heteroatom to dope virgin carbon helps to distribute the carbon atom charge next to the heteroatom or generates active areas to include structural flaws for electrocatalytic CO_2R. N-doping is the most prevalent kind of MOF-derived carbon-heteroatom doping [127, 285–287]. For example, the use of N-rich organic linker and ZIF-8 as critical sacrificial templates has been reported, resulting in a synthesized N-doped carbon catalyst where the quaternary-N and pyridinic-N species unambiguously demonstrated essential roles in the selective production of both CO and H_2 by-products. Furthermore, calcination effects and the CO_2R mechanism were given a lot of attention [127]. The N-doped carbon catalyst's remarkable electrocatalytic performance was reportedly better (Fig. 10) at higher temperatures, with the highest CO production with FE reaching 95.4% and an overpotential of about −0.5 V vs. RHE (Fig. 10a-e). However, an increase in pyrolysis temperature reduced the pyridinic N content. The DFT calculation demonstrated that the N4 (fourfold pyridinic N), showed less activity when compared with that of N3 (triple pyridinic N), N2 (twofold pyridinic N), and N1 (single pyridinic N) as presented in Fig. 10 f [127].

Additionally, thermal synthesis of MWCNTs (multi-walled carbon nanotubes) aided ZIF-8 in the preparation of ZIF-CNT-FA-p (hybrid N-doped porous carbon), which is selective in the catalytic reduction process of CO_2 to CO in an aqueous solution. The current density was determined to be 7.7 mA/cm^2 with an estimated overpotential of 740 mV. This feat was attributed to the efficient flow of CO_2 molecules in MWCNTs' mesoporous structure, which facilitated the electron transport on the MWCNTs network [287].

Since the main problems with MOF electrocatalytic materials are poor conductivity and sluggish electron transport. One viable technique for addressing this issue is controlling interfacial gas adsorption - a process where carbon defects can induce a reversible carbon-carbon (C-C) interface with the CO_2 gas molecule, thereby facilitating further strengthening under applied bias [288]. In such process a hierarchical porous carbon electrocatalysts with defects (DHPC) by carbon thermal reaction can be formed thereby providing good CO_2RR selectivity and stability [288]. Metal-free electrocatalyst can be more effective if carbon-based material interfacial gas adsorption features can be controlled. For instance, DHPC have been synthesized via a carbonized thermal process (Fig. 11a-d) and observed to demonstrate excellent CO_2RR selectivity with long-term durability [288]. A defective carbon was noted to be an electroactive center for effective CO_2RR since it

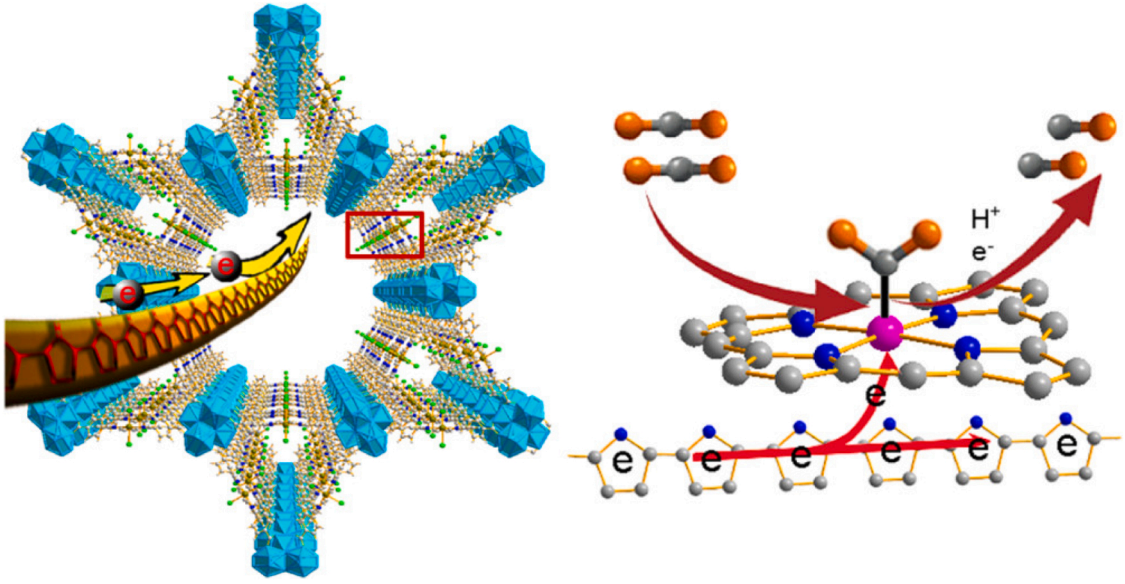

Fig. 9. Representative benefits of PPy in the MOF-545-Co channel for electrocatalytic CO_2RR [283].

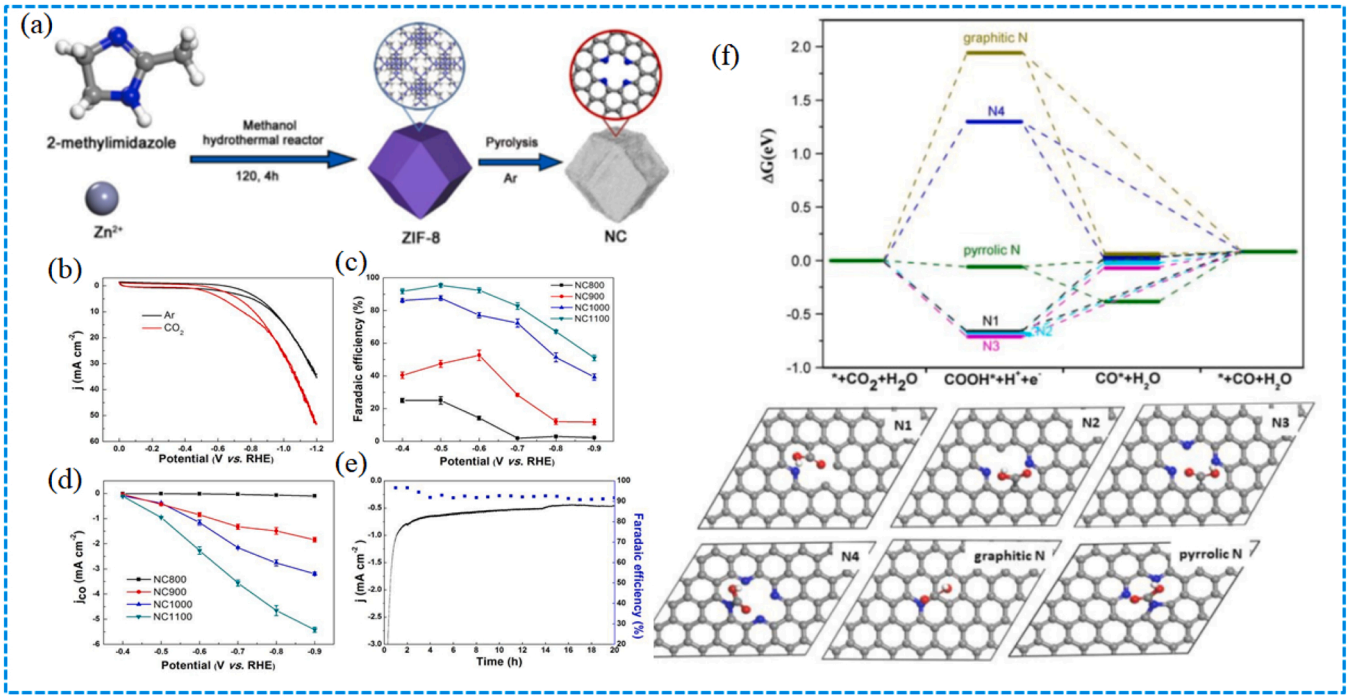

Fig. 10. (a) Schematic illustration of the synthesis of NC samples. Electrocatalytic performance of NC samples for electroreduction of CO_2 to CO. (b) CV curves of NC1100 in Ar and CO_2 saturated 0.5 M $KHCO_3$ electrolytes, 5 mV s-1. (c) Dependence of FE toward CO on the applied potential for NC samples. (d) The partial current density of CO on the applied potential for NC samples. (e) Stability of performance of NC1100 for CO_2R operated at − 0.5 V vs. R.H.E. for 20 h. (f) Gibbs free energy diagram of electrochemical reduction of CO_2 to CO on NC samples. The most stable structures of COOH adsorbed on NC samples are also displayed. [127].

served as a Lewis-base center, thereby providing suitable CO_2-chemisorption energies. The Lewis base sites on DHPC might result in a C-CO_2 interface that is advantageous for the CO_2R reaction [288]. However, the performance of the CO_2RR is usually greatly influenced by the competitive relationship between the characteristics of proton adsorption and CO_2 adsorption on the electrocatalyst surfaces [289]. In addition, according to the X-ray absorption spectroscopy (XAS), carbon defects have been shown to generate C-C- interfaces with gaseous CO_2 molecules that are further enhanced under the influence of applied bias. The higher performance of DHPC was further explained through its inherent defective sites, as demonstrated by the $^{13}CO_2$ isotope labeling experiments and DFT calculations. In addition, the desorption studies of the electroreduction reaction *CO intermediate on DHPC electrocatalyst were exothermic in nature (Fig. 11e-f). This study indicates an electrocatalytic mechanism based on carbon defects and opens up new development avenues for electrocatalytic CO_2RR.

Another study involving heating the porous carbon materials to a temperature exceeding 750 degrees Celsius with annealing in an NH_3 environment for removing pyridinic-N and pyrrolic-N has been reported for effective introduction of topological defects into the carbon materials (Fig. 11 g) [290]. It was found that when sintering temperature increased, pyrrolic-N and pyridinic-N contents decreased in the carbon

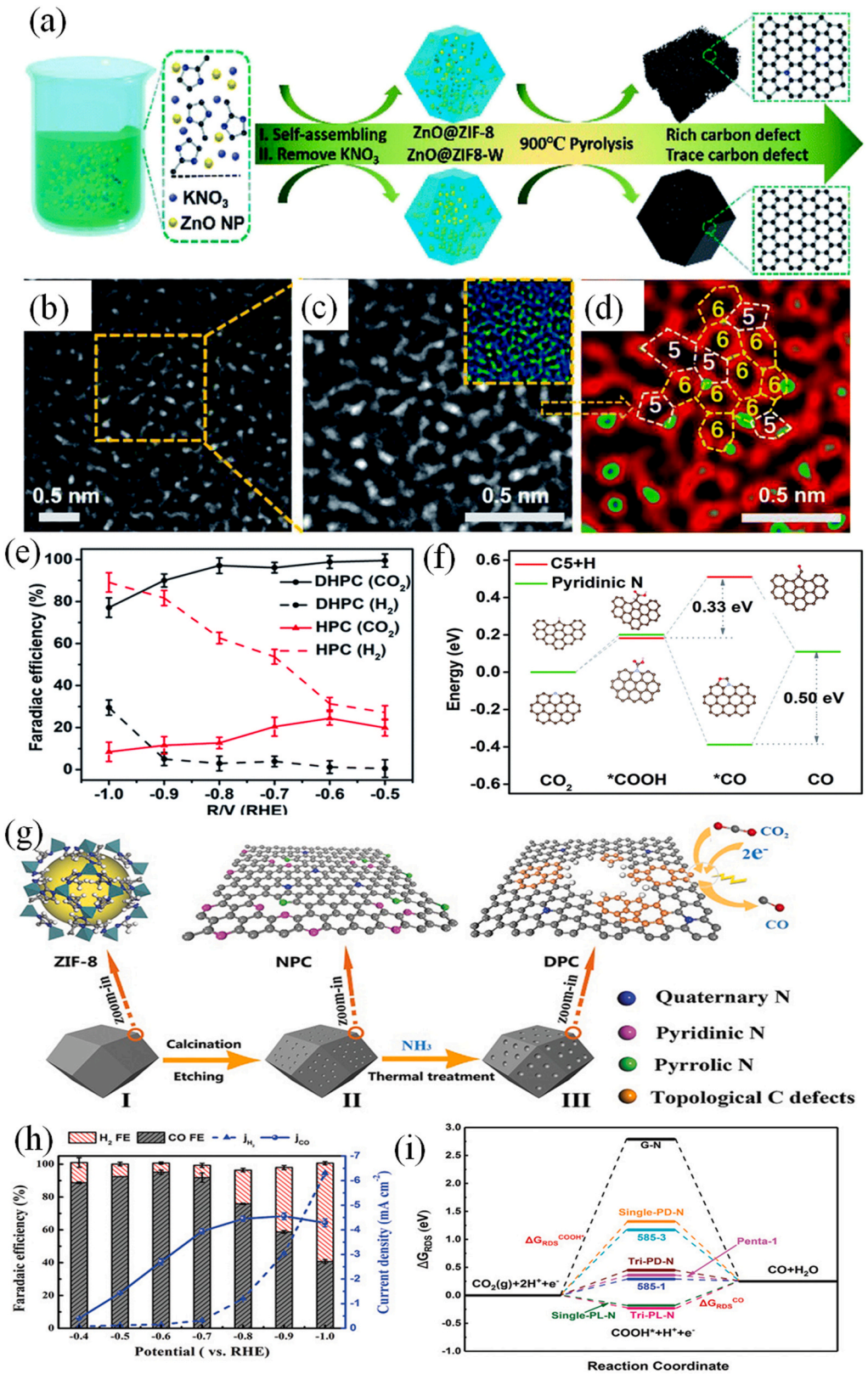

Fig. 11. (a) Synthetic process of DHPC and HPC, (b) High Resolution Transmission Electron Microscopy (HRTEM) of DHPC. (c) Magnification of one segment of the HRTEM image. The inset image is the HRTEM image of DHPC after fast Fourier transformation (FFT) filtering. The bright green spots are carbon atoms. (d) Magnification of one segment of the HRTEM after fast Fourier transformation (FFT) filtering. (e) FEs of DHPC and HPC in 0.5 M $KHCO_3$ at various potentials. (f) Free energy diagram for CO_2 reduction to CO over C5 + H defect site and pyridinic N site [288]. (g) Schematic illustration of the synthetic route and the corresponding models of: (I) ZIF-8 precursor, (II) 3D N-enriched porous carbon particles, and (III) 3D topologically defected porous carbon particles. (h) FEs of CO (gray) and H_2 (red) and the partial current of CO on DPC-NH_3-950 under a range of applied potentials. (i) The calculated free-energy diagram for CO_2RR at N-doped sites, Penta-hole, and 585–1(3) sites. G-N, single/tri-PD-N, and single/tri-PL-N refer to graphite-N, and single or triple pyridinic-N and pyrrolic-N, respectively [290].

skeletons. NEXAFS studies showed that the topological density defect increased steadily, improving the electrocatalytic performance (Fig. 11h-i). According to DFT calculations, the defective carbon materials possessed appropriate free energy for absorbing and desorbing the chemical intermediate(s).

Several more recent research based on conductive MOFs has been conducted to address conductivity concerns and increase the electrocatalytic performance of these materials for CO_2RR [291–293].

In order to create superior CO_2RR electrocatalysts, many techniques such as doping various elements, developing multidimensional structures, and constructing hierarchical pores have been frequently used. The production of heteroatom-doped MOF-derived electrode materials often have the benefits of moderate reaction conditions, an easy operating procedure, and low cost. In addition, the obtained electrode materials have hierarchical pore's structure, ultrahigh specific surface area, high-density active sites with a good dispersion, which will provide fast mass and proton transfers as well as the improved electrocatalytic activity. This is made possible by the distinctive and adaptable structure of MOF precursors. The main method for producing non-metal heteroatom-doped carbon electrocatalysts from MOFs involves either adding guest molecules or directly carbonating the heteroatom-containing MOF precursors. However, they could have some metal residues, which would lead to unclear electrocatalytic mechanism for metal-free carbon-based electrocatalysts. It has been shown that adding more carbon to host MOFs' carbonation process not only helps to completely remove any remaining metals or their compounds, but also increases the degree to which final carbon-based materials graphitize. However, this process is still in its early stages. To address the problem of metal residues and investigate the electrocatalytic mechanism of pure metal-free carbon MOF-derived electrocatalysts, further research efforts for non-metal heteroatom-doped carbon electrocatalysts should be encouraged.

9.2. MOF-derivative isolated (single) metal-atom materials for CO_2RR

The isolated metal systems are single-atom-level coordinative unsaturated transition metal-nitrogen sites enclosed in a carbon matrix (M-N-C) derived from MOFs. They have unique electronic structures and a unique coordination environment, which significantly impacts the selectivity and activity of electrocatalytic CO_2R [204,294–296]. Fig. 12 presents the historical insight into the development of MOF-derived single-atom electrocatalysts for CO_2RR, while different electrocatalytic performances of recent MOF-derivative isolated electrocatalysts are presented in Table 1. They offer certain impressive advantages such as (a) maximum atom usages, exceptional electronic features and unsaturated coordinated environments, (b) a straightforward coordination atmosphere, distinctive in-situ synthesis mechanism, and adjustable topological structures that allow possible adjustable the type and quantity of metal and ligand (c) chemically stable characteristics and a clear porous structures that can tremendously enhance the mass transport and electrocatalytic efficiency [46,297–301].

Based on the exceptional higher surface energy of the isolated metal atom can stimulate the aggregation onto the NPs or clusters even during the synthetic or electrocatalytic process. Currently, one of the leading research hotspots lies in the isolated metal atom electrocatalysts is the development of stable, appropriate single (isolated) atom materials to inhibit the agglomeration of active metal atoms. To date, three important sample ways including metal node, coordination capture, and space restriction strategies have been discussed recently by Zhou et al. as veritable additional useful strategies for synthesizing MOF-derived isolated atoms with homogenous and stable atom sites as indicated in Fig. 13 [302–313].

For the electrocatalytic CO_2R, one example is the creation of M-N-C (M = Co or Fe) electrocatalysts using Fe- or Co-doped ZIF-8 [296]. When compared to Co in the M–N_4 coordination for an electrocatalytic CO_2RR, it was hypothesized that Fe is naturally more active. Similarly, the dispersed Fe-Nx active sites in a system of bimetallic ZnFe-ZIFs for the electrocatalytic reduction of CO_2 to CO (Fig. 14) exhibited significant electrocatalytic performance and selectivity towards the reduction of CO_2 to CO with 86.9% FE for CO at −0.47 V vs. RHE (Fig. 14) [120]. Changing the pyrolytic temperature produced atomic dispersion of Co

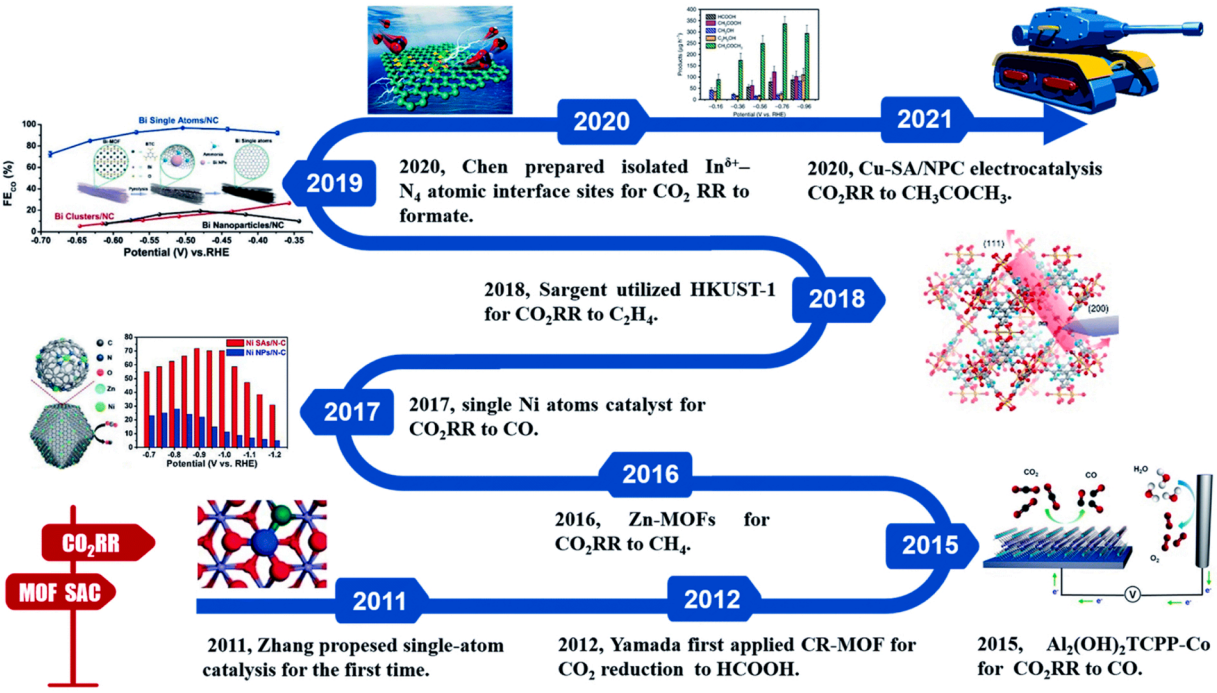

Fig. 12. A brief history of the development and the latest progress of MOF and MOF-derived carbon-based single-atom catalysts for the electroreduction of CO_2 [302]. Until 2021, the booming MOF and MOF-derived carbon-based single-atom catalysts have been vigorously developed for CO_2RR, and the catalytic performance including Faraday efficiency and stability have been greatly improved. 2011, Pt_1FeO_x [314]. 2012, CR-MOF [315]. 2015, $Al_2(OH)_2$TCPP-Co[122]; 2016, Zn MOFs [123]; 2017, Ni SAs/N–C [294]; 2018, HKUST-1 [316]; 2019, Bi–N_4 [317]; 2020, In$^{\delta+}$–N_4 [318]; 2021, Cu-SA/NPC [319].

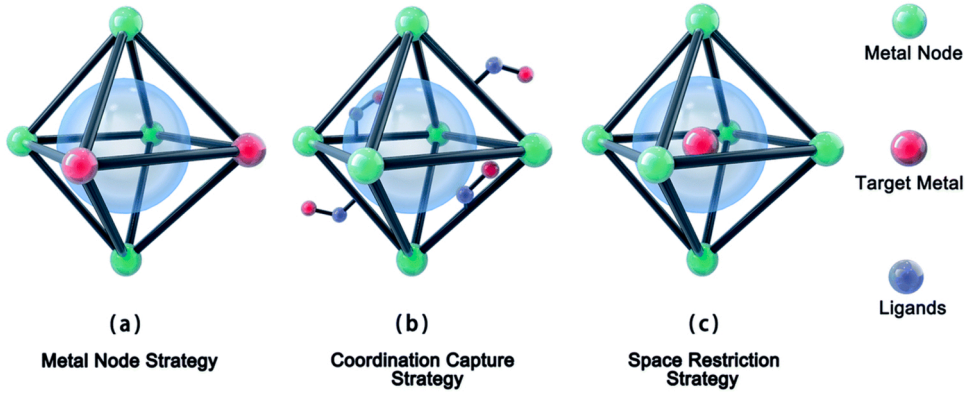

Fig. 13. Schematic illustration of three main synthesis strategies of MOF-derived single-atom catalysts, including (a) metal node, (b) coordination capture and (c) space restriction strategies[302].

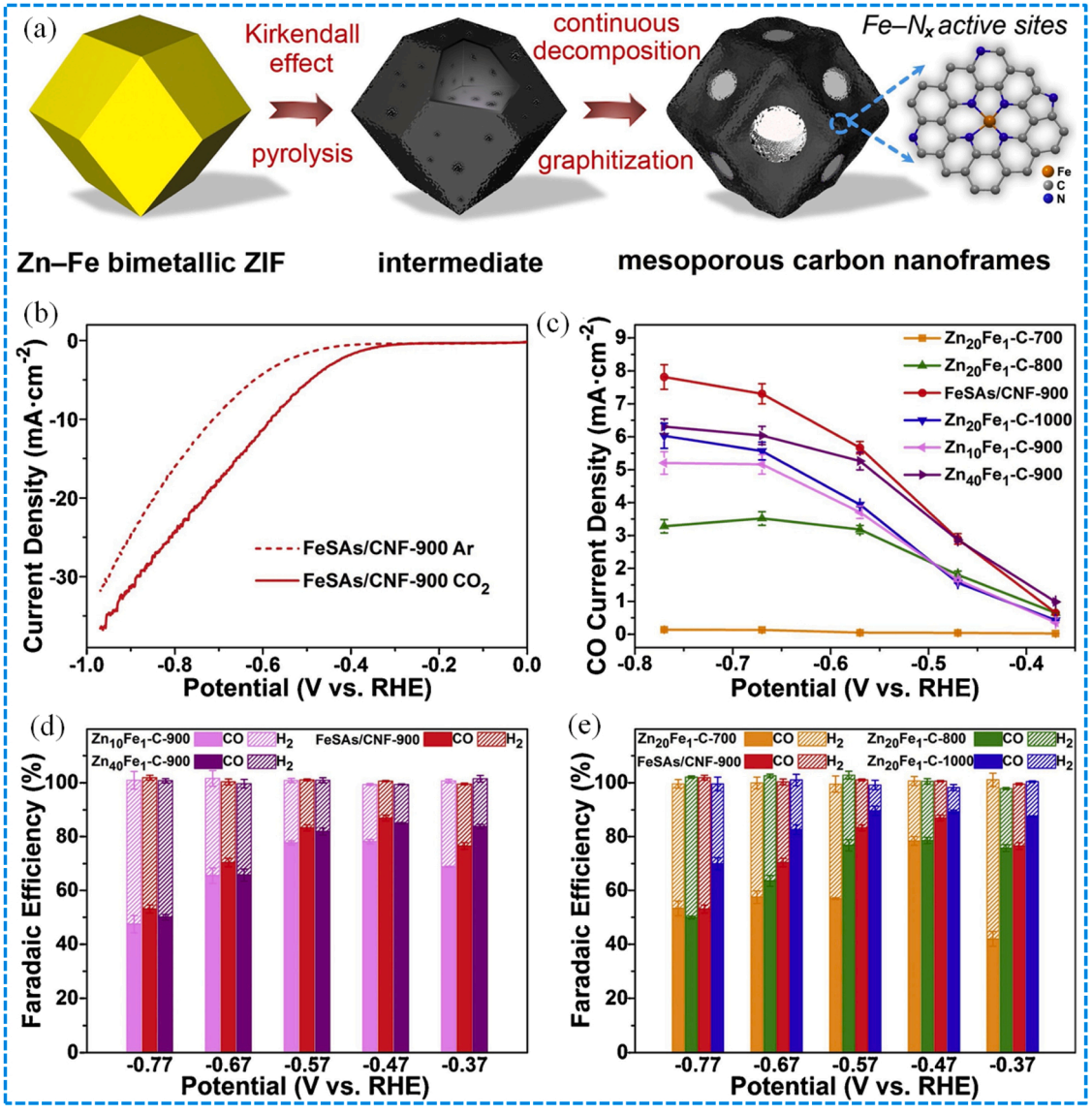

Fig. 14. (a) Schematic illustration of the formation of FeSAs/CNF-900. Evaluation of CO_2R electrocatalytic performance for the catalysts. (b) LSV curves of FeSAs/CNF-900 in Ar- and CO_2-saturated 0.5 M $KHCO_3$ aqueous solution at the sweep rate of 10 mV/s. (c) Partial current densities of CO for the ZnxFey-C-T catalysts at different potentials. Potential-dependent Faradaic efficiencies for CO and H_2 productions over the (d) ZnxFey-C-900 and (e) Zn_20Fe1-C-T catalysts [120] .

electrocatalyst on bimetallic Co/Zn ZIF with varied nitrogen coordination numbers. The study demonstrated an improved electrocatalytic CO_2R on Co–N_2 sites, with 94% FE for CO at 18.1 mA/cm^2 at −0.63 V vs. RHE. According to the results, this was much higher than the almost inert electrocatalyst mostly covering Co–N4 sites (Wang et al., 2018b).

In general, ZIF MOF-derived electrocatalysts have been reported to exhibit strong selectivity for CO_2RR toward CO production when compared to other electrode materials. Recently, an electrocatalyst created from ZIF-8 MOF and anchored on a CNT substrate was observed to offer a conductive channel for electroactive sites of Fe-N incorporated in a ZIF-8 MOF with an N-doped carbon-derived from ZIF-8. This was created using a two-step modification procedure that included chemical treatment subsequent to a pyrolytic process (Fig. 15a). This translated to an exception CO_2 electroreduction performance with about 100% efficiency for CO generation (Fig. 15b-c) [287]. Also, a MOF-derived aerogel has been constructed by Albo and co-workers for CO_2RR to C_2H_5OH and CH_3OH with a lesser efficiency of around 10% [320]. However, the formation of low C_2H_5OH yields on ZIF-8 NPs placed on Ti/TiO nanotubes was observed when the NPs were deposited on the nanotubes [321].

In order to stabilize Ni single-atom active site for selective a CO production, N-doped carbon from ZIF-8 has been investigated [294]. This resulted in a greater turnover rate, outstanding electroactivity, and good stability (Fig. 15d-g). The reaction route revealed that the MOF-derived electrocatalysts exhibited a large number of a low coordinated surface site with a stronger binding to CO_2•–, which enabled a good CO_2RR performance on the electrocatalyst (Fig. 15 h). Similarly, ZIF-67 was reportedly used to improve the stability and electrocatalytic performance of single Co-atom electrocatalysts for selective conversion of CO_2 to CO [175].

A distribution of Ni atoms in an N-doped porous C (Ni SAs/N-C) for the CO_2R through an ionic exchange process between adsorbed Ni ions and Zn nodes located in the ZIF-8 cavities has been reported [294]. Fig. 15g-j depicts the outstanding electrocatalytic capabilities of this electrocatalyst. Compared to Ni NPs and Ni foam, the Ni SAs/N-C showed a 71.9% FE for CO generation and a current density (j) of 10.48 mA/cm^2 at a − 0.9 V vs. RHE (Fig. 15d-g) and stability up to 60 h (Fig. 15 g). A greater CO_2• bonding accounted for the effective CO_2R

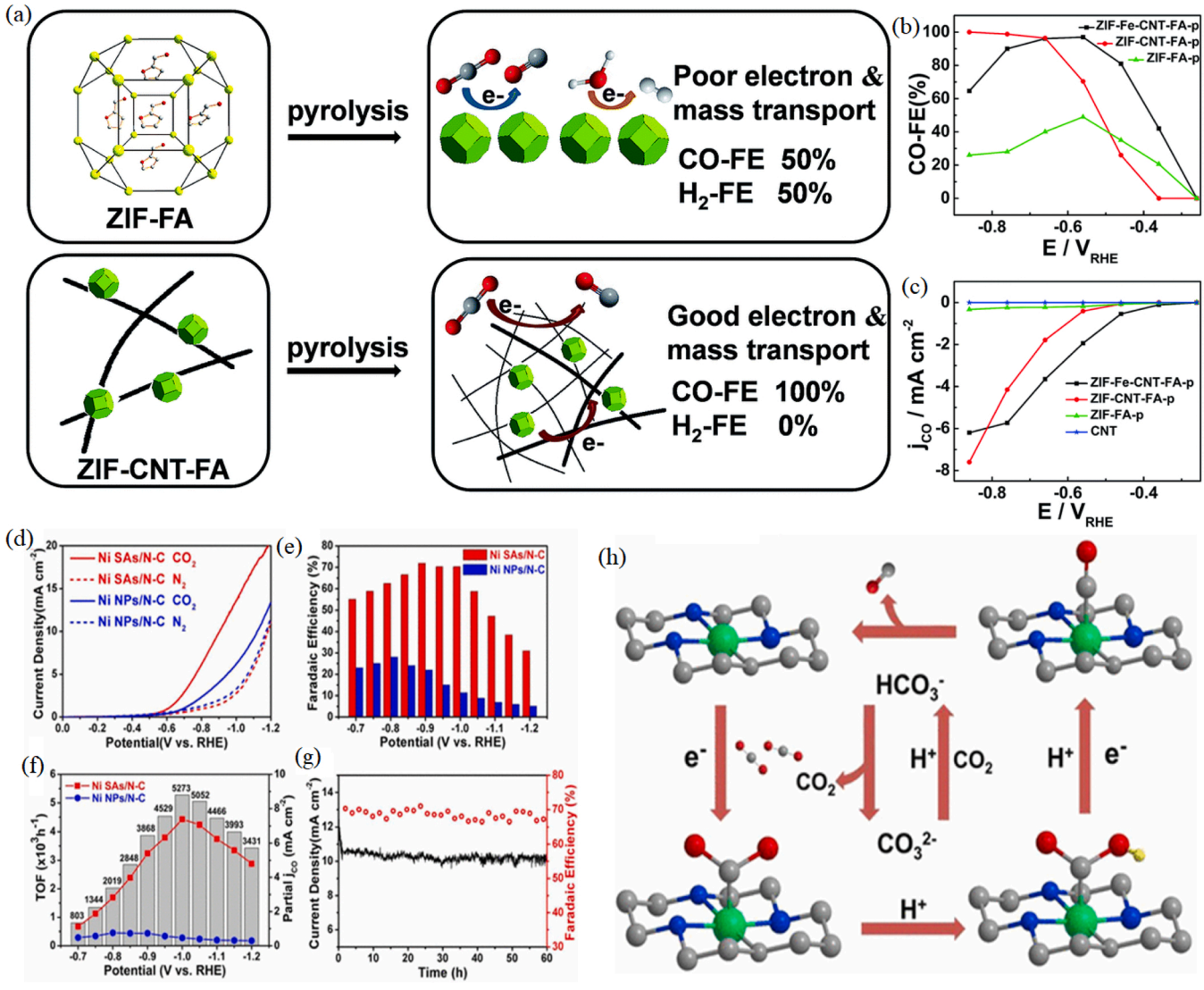

Fig. 15. (a) Illustration depicting how the MWCNT support improves the interparticle conductivity and mass transfer of pyrolyzed ZIFs for CO_2RR. (b) different Faradaic efficiencies for CO, plotted against the electrolysis potential for various electrocatalysts (c) partial current densities for CO_2RR to CO, plotted against the electrolysis potential [287]. (d) LSV plots under the N_2-saturated (dotted line) and CO_2-saturated (solid line) in 0.5 M $KHCO_3$ electrolyte (scan rate =10 mV/s). (e) FEs of CO, (f) the partial current density of CO (based on geometric surface area), and the TOFs of Ni SAs/N-C and Ni NPs/N-C at various potentials. (g) 60 h stability for Ni SAs/N-C,at a potential of 1.0 V (vs. RHE). (h) Proposed pathway for CO_2RR on Ni SAs/N-C [294].

with lower coordinated Ni SAs/N-C abundant surface sites (Fig. 15 h) [294]. However, a cooperative protective host-guest approach managed the coordination environments of single-atom Ni electrocatalysts [204]. This resulted in the NiSA-Nx-C system having Ni–N coordinating number varying from 2 to 4 [204]. When compared to other equivalents, the NiSA-Nx-C had the best CO activity and selectivity at 98% FE and −0.8 V vs. RHE for CO_2R to CO.

Despite significant progress in single atom MNC electrocatalysts, owing to the straightforwardness of the single atomic core, problems such as poor kinetics in the initial PCET resulting in higher overpotential persist. Isolated diatom MNC electrocatalyst systems have been established to overcome this hurdle. The isolation of diatomic Ni-Fe sites attached to nitrogenated carbon (Ni/Fe-NC) has allegedly shown a strong selectivity for CO of 98% FE at −0.7 V vs. RHE [278]. DFT calculations indicated the structural evolution system into a CO-adsorbed moiety based on CO_2 adsorption and a reduction in the reaction barrier to synthesize *COOH coupled with CO desorption [278]. A synergetic electrocatalyst has been described by affixing FeN site with a Co-phthalocyanine (CoPcFe-NC). The projected gap of FE for CO is now 0.71 V on a CoPcFe-NC, although the starting potential of the electrocatalysts were 0.13 V vs. RHE [322].

Summarily, although single-atom electrocatalysts show remarkable benefits for electrocatalytic CO_2RR and attract numerous research interests, certain significant constraints make their practical implementation challenging. For instance, their preparation typically necessitates a complex synthetic method which is challenging to implement to commercial operations at the mass-production level. In addition, many superior single-atom electrocatalysts are premised on precious metal atoms, which restricts their potential for future extensive commercial applications [323]. Despite several relevant studies regarding highly mass-loaded single-atom electrocatalyst materials, their synthesis with higher metal loading in supports remains a significant difficulty [324]. Additionally, single-atom electrocatalyst support materials have a significant impact on their electrocatalytic activity, stability and selectivity. Single metal atoms could be tightly contained on the surfaces of the supports because of the stronger bond that exists between them and the surfaces of the support materials. For the development of advanced single-atom electrocatalyst, adequate support materials with the requisite characteristics are also essential. To stabilize, trap, and protect more single metal atoms, ideal supports should

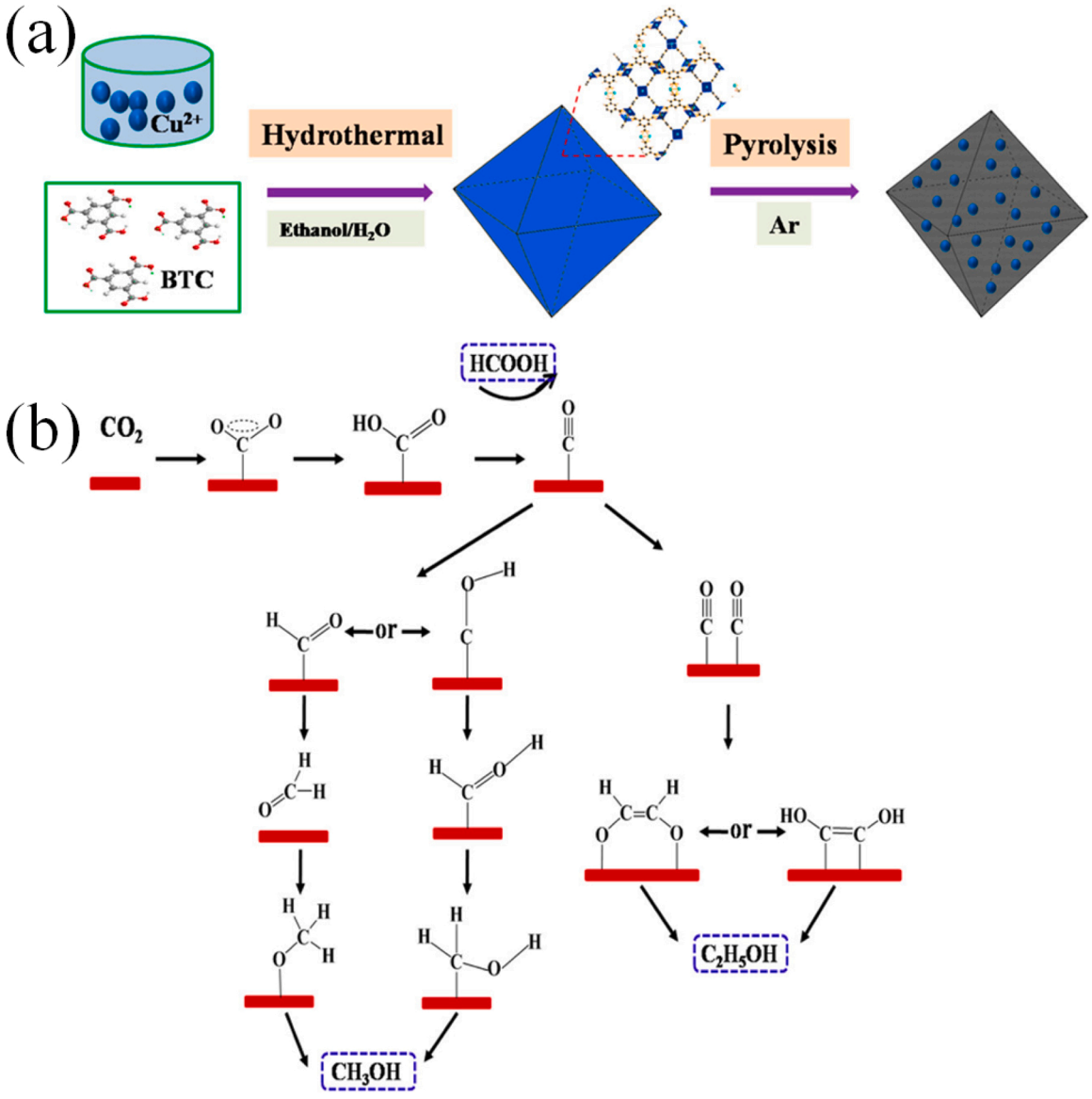

Fig. 16. (a) Synthetic route of oxide-derived Cu/C MOF electrocatalysts (b) Proposed reaction pathways for CO_2R on OD Cu/C-1000, for formation of HCOOH, CH_3OH, and C_2H_5OH [136].

typically have larger surface areas and porous structures with numerous anchoring sites. In addition, the support materials may offer extra active sites for electrocatalytic CO_2RR processes and may affect the conductivity of single-atom electrocatalysts [325].

9.3. MOFs-derived transition metal nanoparticles

To obtain higher electrocatalytic activity and selectivity for CO_2RR, the active transition metal NPs such as Cu, may be generated from MOFs. For example, the fabrication of an oxide-derived Cu/C (OD Cu/C) electrocatalyst through the facile carbonized HKUST-1 has been reported (Fig. 16a). The as-obtained electrocatalyst demonstrated electroactivity for CO_2R to CH_3OH and C_2H_5OH leading to a combined FE of approximately 45.2–71.2% at −0.1 V to −0.7 V vs. RHE [136]. The electrochemical performance was explained by a synergistic interaction amongst the high distributed Cu and porous carbon matrices. An in-situ IR spectroscopy and theoretical calculation suggested that the adsorption of *CO intermediates onto the OD Cu/C surfaces and the porous C support promoted the coupling of C-C coupling, which is necessary for the generation of C2 species (Fig. 16b). Similarly, other interesting finding were reported including Nam et al. for CO_2 to C_2H_4 on HKUST-1 (MOF)-regulated Cu cluster [316].

Similarly, the synergistic impact among Cu and N-doped carbon for CO_2R on a MOF-derivative Cu@N-doped C(Cu/NC) has been reported. The as-synthesized electrocatalyst was generated by a calcination process involving the modified Cu-BTC MOFs with N-containing benzimidazole at various temperatures (Fig. 17) [128]. A high concentration of pyrrolic-N and Cu–N species on the surface of the copper was observed to promote the formation of ethanol and ethylene, whereas a high concentration of N-graphitic and N-oxidized on the copper surfaces caused higher ratio of hydrogen evolutions and a quickly reduced the electroactivity for CO_2R. Aside from higher-pyrolytic temperature, the rebuilding of cathodized MOFs may also result in the formation of electroactive Cu NPs.

Another authors have reported the cathodization of Cu^{II}/adeninato/carboxylate meal-biomolecular framework (Cu^{II}/ade-MOFs) nanosheet for CO_2R into methane and ethylene [135]. Rebuilding of cathodic Cu^{II}/ade-MOF electrocatalyst produced Cu NPs modified with the N-comprising ligand capable of producing ethylene with a FE = 45% at −1.4 V vs. RHE and CH_4 (with FE= 50%) at −1.6 V vs. RHE. The fabrication of Bi(1,3,5-tris(4-carboxyphenyl)benzene, abbreviated Bi (btb) that operated as a precatalyst, has been reported. It underwent structural rearrangements at a reducing potential to generate highly active and selective Bi-based NPs distributed in the porous organic matrices. This electrocatalyst exhibited an impressive higher selectivity for formate formation (FE= 95(3) % and a huge current density of about 261(13) Ag^{-1}, thereby outperforming most other Bi nanostructural materials [134].

Although typical electrochemical characterization techniques such as cyclic voltammetry and electrochemical impedance spectroscopy may be used to understand electrode behaviour, detecting the intrinsic properties of the electrode materials during cycling is challenging. Therefore, sophisticated in situ/ operando characterization methods including as in-situ/ operando XRD, SEM, TEM, XPS and EIS, have been used to investigate structural evolution, morphological and component modifications during cycling. Although in-situ characterization approaches can provide more reliable and important information, the design of detection equipment is complex, the measuring environment is too stringent, and there is currently no standard for correlating the information with material attributes and performance. Recently, simulations based on DFT, and others have been investigated to better understand the relationship between composition/nanostructure and electrocatalytic behaviors.

In conclusion, while MOFs-derived transition metal nanoparticle materials with complex structure and diverse composition have received increasing interest, their commercialization and industrialization are still not realized.

9.4. MOF-derived transition metal oxide electrocatalysts

Due to their exception higher stability and relatively lower cost, transition metal oxides have been frequently employed for various electrocatalytic processes. For example, MOF-derived metal oxides have been demonstrated to inherit porous architectures of MOF, which could also enhance the number of accessible electroactive sites, thereby promoting mass transfer. Recently, a simple MOF-derived approach has been reported for creating the porous In-Cu bimetallic oxide electrocatalyst (InCuO) with varying Cu/In ratios and employed for CO_2RR into CO (Fig. 18a-g) [139]. Regulating the ratio of In/Cu in the MOF precursor translated to a remarkable FE of 92.1% for CO formation and a j=11.2 mA/cm^2 at −0.8 V vs. RHE. This was ascribed to a stronger CO_2 uptake, large electroactive surface areas, and lower charged transfer resistance (Fig. 18a-g). Moreover, electrocatalytically reduction of CO_2 to acetated and formate on a cathodized Cu (II) paddle wheel cluster-based porphyrinic MOF (Cu-MOF) has been reported (Fig. 18h-i). It was discovered that the nodes of Cu (II) carboxylate might have been converted to Cu_4O_3, Cu_2O, and CuO, which noticeably electrocatalyzed CO_2 to acetated and $HCOO^-$ with synergistic improvement from the Cu (II)-porphyrin complexes [140].

Currently, different strategies have resulted in diverse structures and morphologies of MOF-derived transition metal oxide electrocatalysts using annealing, microwave-assisted procedures, and solvothermal techniques, ultimately resolving the issue of energy conversion. Despite significant advancements in the study of MOF-derived transition metal oxide electrocatalysts, several problems still prevent the widespread utilization of these materials, including the following: (a) The cost of some organic linkers is too high, and the synthetic processes are difficult. As a result, it is essential to develop quick, cheap, and environmentally friendly synthesis techniques. (b) Due to the lower quality yields, mass manufacturing of target materials starting with MOF precursors is challenging.

However, due to their benefits of controlled structure, composition, and morphology, MOF-derived metal oxides continue to maintain the position of significant potential templates in the electrocatalytic energy conversion. Advanced instrumentation techniques should be employed to gain deeper understanding of their working mechanisms.

9.5. MOF-derived transition metal phosphide electrocatalysts

Currently, the most common electrocatalyst for CO_2RR are transition metal phosphides. Han et al. described the use of MoP NPs supported by In-doped porous carbon (MoP@In-PC) electrocatalyst CO_2RR (Fig. 19a-b) [138]. As a carbon precursor, In-MOF (MIL-68) was chosen, and vaporized MoO_3 was collected by porous an In-MOF-derivative In-PC forming a Mo-based type. The as-obtained MoP@In-PC was reported to possess a higher FE of 96.5% for formic acid production with a current density of = 43.8 mA/cm^2 at 2.2 V vs. Ag/Ag+ . In addition, the performance in an ionic liquid 1-butyl-3-methylimidazolium hexafluorophosphate as electrolyte support was due to the extensively distributed MoP active NPs, thereby promoting the effective CO_2 uptake and electrolyte dispersion, and also the synergy impact of In-PC and MoP. In addition, the construction of Cu_3P/C nanocomposite using a one-step phosphating HKUST-1 and the Cu_3P/C has been reported for its effective electrocatalytic CO_2RR. This resulted in the generation of CO with FE of 47% at −0.3 V vs. RHE [137]. Similarly, as presented in Fig. 19c-e, with an asymmetrically electrolyte, the Zn-CO_2 battery with the Cu_3P/C electrocatalyst demonstrated moderate electrochemical performance achieving a power density= 2.6 mW/cm^2 at 10 mA/cm^2, and an open-circuit voltage of 1.5 V.

In summary, it has not yet been possible to create ultrafine MOF-derived transition metal phosphide nanocrystals with a size of less than 2.0 nm. Since ultrafine nanocrystals smaller than 2.0 nm contain a

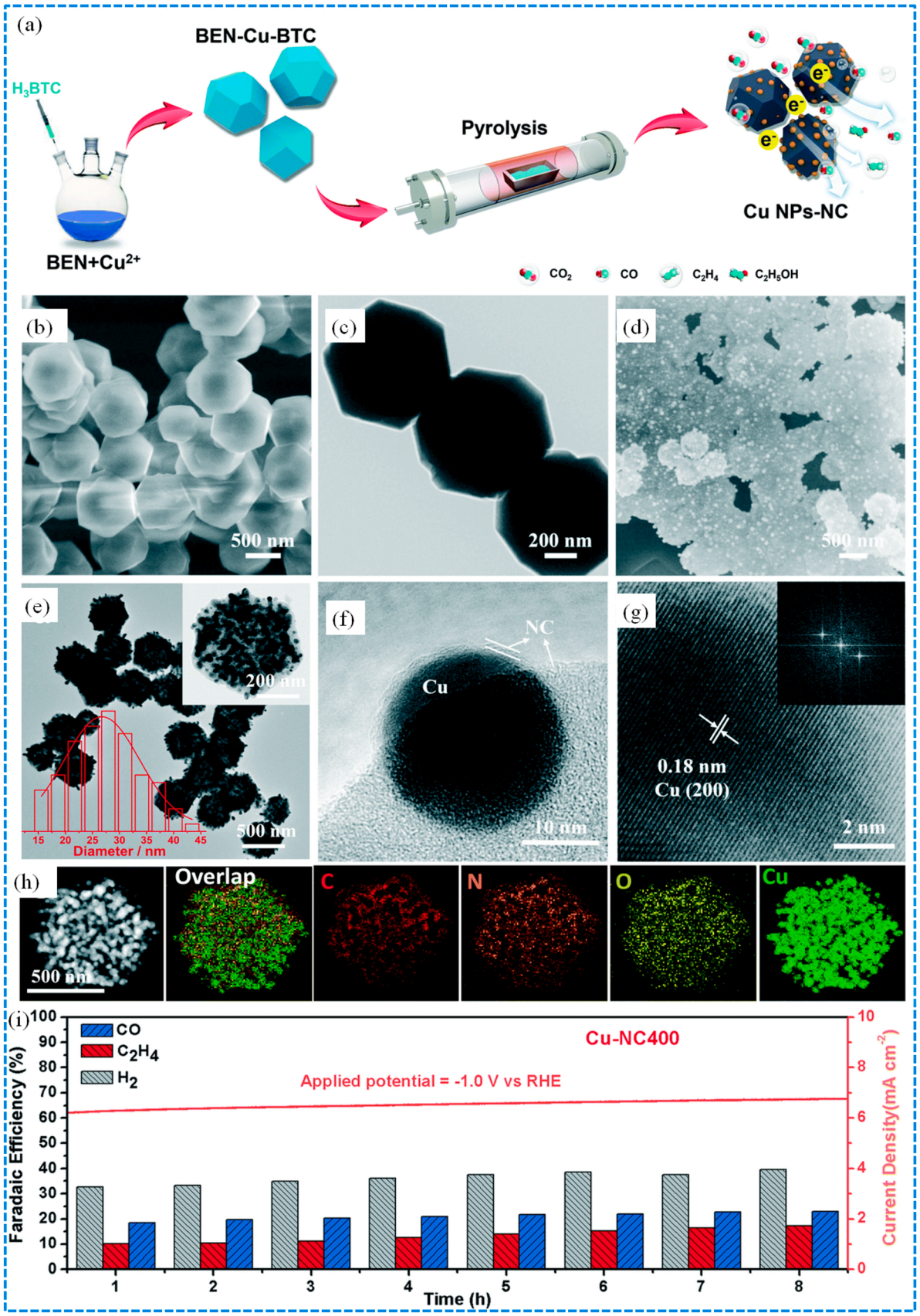

Fig. 17. (a) Schematic fabrication process for the Cu NPs-NC composite. (b and c) the SEM and TEM images of BEN-Cu-BTC; (d) SEM image, (e) TEM image, (f and g) HRTEM images, (h) HAADF-STEM and corresponding EDS elemental mapping images of Cu–NC400 (the inset in (e) and (g) are high-magnification TEM images, particle size distribution of Cu NPs and FFT images of Cu–NC400). (i) h) chronoamperometry result at − 1.0 V vs. RHE with the corresponding FEs for gas products of Cu–NC400 [128].

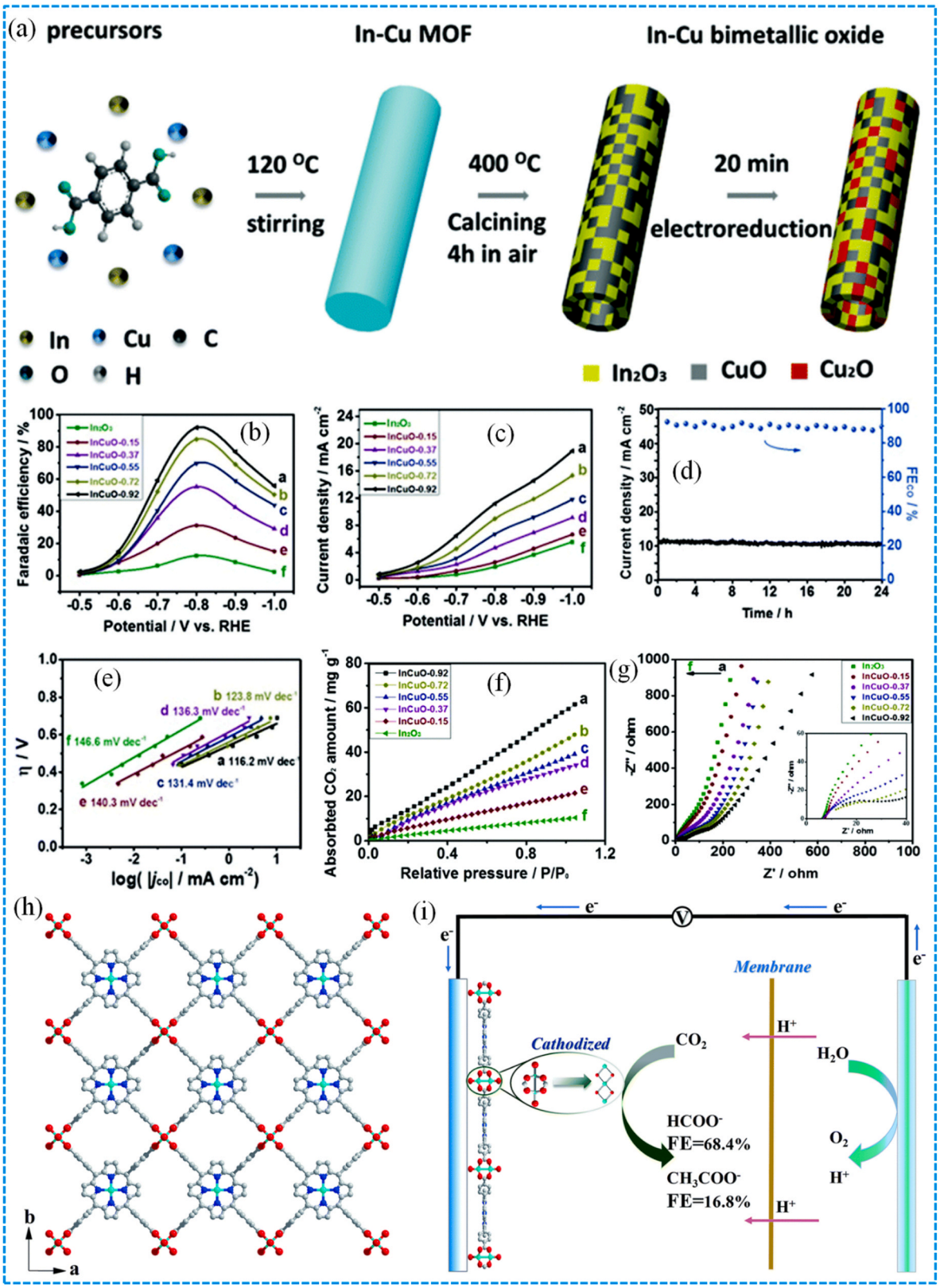

Fig. 18. (a) Schematic illustration of the preparation process of InCuO. Electrolysis results in CO_2-saturated 0.5 M $KHCO_3$ aqueous solution (pH = 7.2). (b) FE of CO for different electrocatalysts at the applied potentials. (c) Total current density for different catalysts at the applied potentials. (d) The long-term stability of InCuO-0.92 at − 0.8 V vs. RHE during 24 h electrolysis. (e) Tafel plot for CO production over different catalysts. These data were obtained at ambient temperature and pressure with a CO_2 stream of 2 sccm. (f) CO_2 adsorption isotherms on different catalysts at 25 °C. (g) Nyquist plots for different catalysts in CO_2-saturated 0.5 M $KHCO_3$ [139]. (h) Crystal structure of Cu_2(CuTCPP) nanosheets along the *c* axis. Red is O, blue is N, grey is C and cyan is Cu; (i) CO_2 electrochemical reduction system with Cu_2(CuTCPP) nanosheets as the catalyst [140].

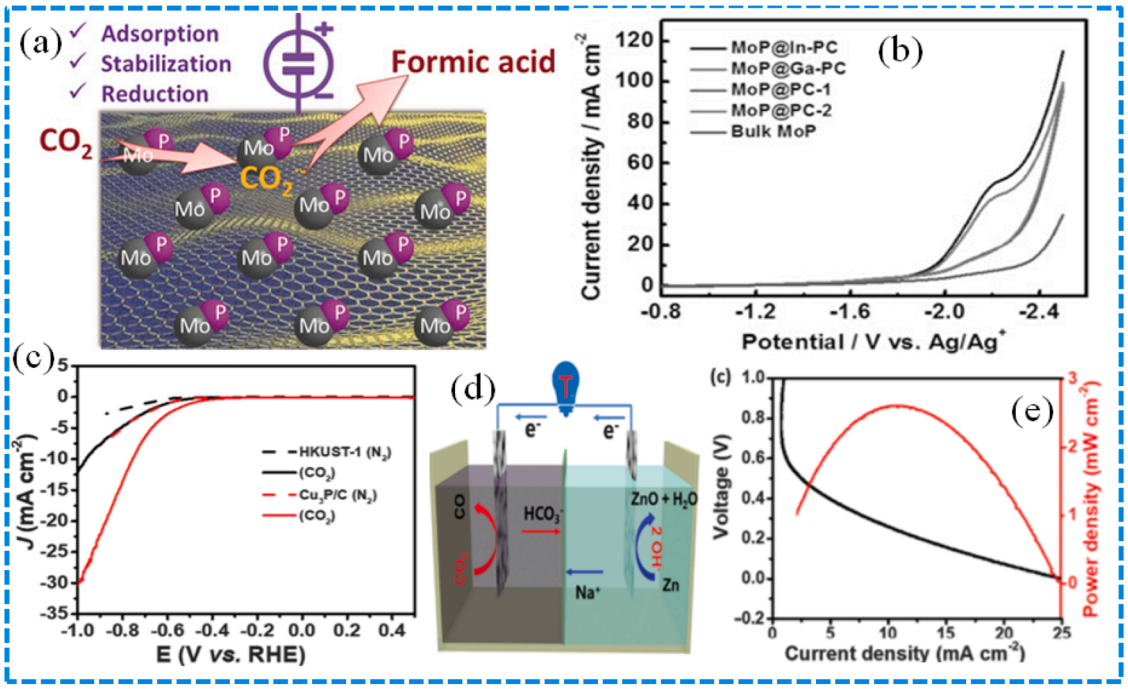

Fig. 19. (a) MoP and In-doped carbon support synergistic effect for promoting CO_2RR. (b) LSV curves for CO_2RR in CO_2-saturated [Bmim]PF_6 (30 wt%)/MeCN/H_2O (5 wt%) electrolyte [138]. (c) LSV curves of HKUST-1 and Cu_3P/C in N_2- or CO_2 -saturated solution with a scan rate of 50 mV/s (a) Schematic diagram of Zn–CO_2 battery with Cu_3P/C cathode (c) polarization and power density curves of the as-proposed Zn–CO_2 battery with Cu_3P/C cathode [137].

higher concentration of exposed electrocatalytically active sites, therefore, they often have outstanding electrocatalytic performance. At the moment, transition metal phosphide nanocrystals are often bigger than 5.0 nm in size, hence, developing ultrafine yet stable metal phosphide nanocrystals at the cluster level remains a significant difficulty. In addition, the absence of highly active transition metal phosphide electrocatalysts promote total hydrolysis at higher current densities. The employment of lower overpotentials to generate high current density is a fundamental need for the commercialization of electrocatalysts. Lastly, the precise electrocatalytic mechanism and active sites of MOF-derived transition metal phosphide electrocatalysts for CO_2RR should be established.

10. Key factors towards optimizing the efficiency of CO_2RR electrocatalysts

The three important parameters for an effective electrode material are (a) higher electrical conductivity, (b) favorable electrocatalytic activities, and (c) extended durability or stability at extremely high temperatures or over a wider pH range. The first factor is essential for decreasing Ohmic loss and enhancing electrochemical efficiency. To prevent a decline (deterioration) in overall performance, the electrocatalysts' relatively high conductivity must not inhibit electron transport while increasing the active surface area. The distinctive qualities of electrocatalysts for effective performance and stability under electrochemical circumstances have been ascribed to the rapid and effective charge transfer produced by the carbon matrix's conductivity and the micropores for accessing the active surface area. In an aqueous environment, e.g., a family of transition metals (Co, Fe, and Ni) N-doped porous carbon electrocatalyst for CO_2 conversion systems exhibited an improved activity and selectivity [355].

Tripkovic et al. [356] offered a hypothesis indicating the influence of the metal-core. The author showed that a incorporating porphyrin-like metal hybridized with graphene might be active in the CO_2RR process, thereby permitting the transformation of intermediates to more important products. Several electrocatalysts with several metal centres have proposed the unique functionalities of metal centers [239,355, 357–366].

Boosting intrinsic activity and increasing the number of accessible active sites in MOF-derivatives, for example, by enhancing electrocatalyst loadings and modifying the electrocatalyst nanostructure, are other important approaches for improving electrochemical performance. It is vital to determine the practical limitation of electrocatalyst loadings without interfering with other crucial parameters (mass/charge transportation). It should be noted that the performance increases only when the mass loading approaches the monodisperse surfaces. If the electrocatalyst mass loading(s) surpassed this amount, agglomeration and sintering become inevitable, thereby serving as potential harm to the MOF-derivative electrocatalyst distribution and performances. The influence of material percentages on electrochemical performances has established previously [367–369], demonstrating that material contents and architectures are important in developing an effective electrocatalytic CO_2RR.

To increase electrocatalyst efficiency of MOF-derivatives, process parameters (such as pH and temperature) must be investigated [367, 370–375]. Heat treatment (temperature) should really be evaluated for its effect on the structural characteristics (properties) of the electrocatalyst activity and selectivity towards CO_2 conversion. pH and local pH have significant effects on the FE and product selectivity [216,376, 377]. Electrochemical reactions at different pH values may influence the pH on the selectivity for CO_2RR, thereby revealing the importance of proton concentrations [378].

Furthermore, the effect of metal precursors on CO_2 uptakes into the active centres on the overall electrochemical performances should not be underestimated. This is due to the fact that the increased metal-carrier interactions (contacts) amongst a well-distributed metal monoatomic and carbon substrate may change the geometric configuration and electronic structures of the electrocatalytically active sites, as well as inhibit metal atom aggregations/associations [379–383]. It should be noted that a multitude of characteristics impacts electrocatalyst performance for CO_2RR; nonetheless, electrocatalyst designs, compositions, and process conditions remain common concerns.

Due to expanding worldwide demand and sufficient electrocatalysts delivering the affordable and sustainable energy, electrocatalysts for CO_2RR are rapidly emerging research issues. The production of electrocatalysts and their use in CO_2RR has surged in recent decades. Many electrocatalysts have been observed to be long-lasting, selective, and efficient, necessitating the attention of businesses, expecting to benefit from the expanding renewable energy marketplaces. Consequently, the current study recommends that pushing the boundaries of electrocatalyst materials for CO_2RR capabilities is the greatest way to achieve a significant breakthrough on the horizon in the industry.

To incorporate electrochemical CO_2RR setups for homogeneous and heterogeneous processes, viable intelligent/smart adaptations of convectional analysis and spectroscopic approaches are required. These are expected to give a thorough and clear grasp of the chemical properties of the process intermediates. The oprando study may be utilized to investigate the mechanistic aspects that might be leveraged to allow major customizable fabrication changes/design. Although it is acknowledged that such a technique might take some time for its full-fledge, it has a higher chance of success than the usual random trials and errors. Therefore, despite great achievement in CO_2RR electrocatalysts over the years, the route ahead requires invention or creation of such a unique interrogation- and interception-based technology.

Microscopic kinds of MOF electrode materials are often ignored in order to produce accurate and effective CO_2RR applications on an industrial scale. Several academic investigations on these electrocatalysts have mostly focused on powdered forms, which are seldom suitable for commercial usage. This is due to the dustiness of dynamic fluid operations and the unavoidable pressure drops. Based on this, palletization is likely one of the finest and most straightforward techniques. However, additional pressure is necessary during the palletization procedures, which may deteriorate or change the electrocatalyst porosity. Therefore, choosing an appropriate mechanical condition and binder are crucial for an effective CO_2 conversion technology. Madden et al. [384] proposed using a monolithic shape for CO_2 separation. In contrast to higher-pressure palletization requirements, the self-shaping technique may lower the expense and danger of MOF collapse. As a result, monolithic MOFs were shown to have better CO_2 adsorption capability than packed powdered materials while preserving identical reaction kinetics [384].

11. Industrial prospects of MOF electrocatalysts

The science of MOF materials is presently transitioning from a scientific to a commercial phase. MOF materials have sparked widespread interest owing to excellent material designability and extensive applications in energy conversion and storage, separation, gas storage, water harvesting, water purification, and so on [385,386]. Currently, there are 24 start-ups linked to MOF materials that were established internationally [387].

From an industrial standpoint, manufacturing costs continue to be critical factor. The entire estimate of industrial-scale MOF manufacturing is now associated with the development of the economical greener and ton-scale fabrication of a prototype MOF MIL-160(Al) [386]. This involves a thorough financial study that takes into account the investments in the manufacturing plants. It has been stated that the scale of production has a significant impact on the production cost, which falls as the manufacturing scale increases. Yao et al. revealed that MOFs might perhaps achieve acceptable competitive pricing, indicating their potential to join the market for a relatively large application [385, 386].

In addition, when it comes to industrial scaling-up, using a green synthesis technique is critical. The synthesis technique for MOFs often involves non-negligible health and environmental concerns. The solvothermal technique, for example, is the most often used synthetic technique for MOFs, and it frequently entails the use of non-renewable and hazardous solvents. As a result, greater emphasis is required to develop green and sustainable synthetic standard operating procedures that are safe and industrially acceptable. Typically, such a procedure should employ sustainable metal ions, safer reaction media or solvent (e.g., water), biocompatible organic linkers, and reduce environmentally harmful by-products [385,388–390]. Consequently, a better knowledge of the greener synthetic process involved in MOF manufacturing might increase electrocatalytic CO_2RR.

12. Concluding remarks/research gaps

The study of MOF-derived electrocatalysts as the platform for the application of sustainable energy is clearly one of the most active topics in the material science community. In recent years, significant advancements have been recorded in the production of MOF-derived materials for solar CO_2RR to value-added products. However, this has been followed by both opportunities and obstacles in terms of putting them into practice:

Preliminary research findings corroborate the notion that MOFs exhibit the same ion diffusion-limited electron transport, evidencing from other nanoconfined systems. For instance, ion diffusion problem has been established as the primary causes of low conductivity in Zr-based MOFs [391,392]. Even though, increasing the pore sizes MOFs of enhances ion movement and overall apparent conductivities, but it poses a detrimental effect on electron transport. Therefore, future research should concentrate on the precise pore engineering and counterion sizes and shapes, or by incorporating functional groups within the pores to assist ion transport, create MOF cavities that would allow ion transport while still retaining high electron hopping rates. Additionally, understanding the solvent characteristics within the MOF pores could help towards attaining better conductivities. The future research would undoubtedly benefit redox-hopping MOF devices.

The MOFs' aptitude in CO_2 conversion is influenced by their changeable compositions, porous architectures, and tunable crystalline nature. The unrestricted integration of functional elements such as metal/metal oxide NPs, graphene, and carbons in MOFs provides a foundation of confinement and the synergistic impact that boosts MOF electrochemical activities in CO_2 conversion technology. Despite this, the low structural stability of most MOFs has limited their use in long-term and dreadful environments such as high temperature, alkalinity, and acidity. Similarly, poor electron transfer rates and reaction kinetics in electrochemical processes have been linked to a majority of MOFs' low electrical conductivity. As a result, MOF conductivity and stability should be improved.

By comparison, MOF-derived materials prepared via high-temperature pyrolysis have a large number of exposed and active centers, as well as tremendous structural durability and electrical conductivity, and have thus been widely employed as electrocatalysts or electrocatalyst supports for high performance in a variety of electrocatalysis processes. However, the high cost of the MOF precursor and the complicated synthesis process limit the economic viability of MOF-derived materials. It worth mentioning that there are certain obstacles in the synthesis and uses of MOF-derived carbons which require investigating further in the future. For example yield is low (about 13–21% depending on carbonization temperature), therefore, this challenge should be resolved to ensure large-scale manufacturing of MOF-derived carbons.

Furthermore, when MOF-derived materials are created via high-temperature pyrolysis, accurate control of their microstructures is challenging. Nonetheless, precise microstructure control in MOF-derived materials such as metal-cluster, single-atom, and di-atom catalysts has progressed significantly. Although carbonization of MOFs as well as other sources might significantly increase carbon production, the presence of other sources would influence the microstructures and active sites of these carbons. As a result, further optimization in these areas has opened the possibility of developing MOFs that solve or circumvent the aforementioned challenges.

Future research in this subject should focus on reducing the drawbacks of already produced MOFs and their derivatives and generating novel materials based on MOFs that are free of existing flaws. Furthermore, sophisticated instrumentation methods are anticipated to give a comprehensive knowledge of the processes involved in creating MOF-derivatives. It is believed that the present study serves as a wake-up call to the research community for designing/developing MOF-derived materials for better CO_2R performances for the benefit of global economic growth, reduction of CO_2 emissions, and energy security.

Despite some understanding of the electrocatalytic mechanism of conventional electrocatalyst behavior, this mechanism is yet to be found in MOFs, thereby restricting searching for efficient MOFs in CO_2RR. Therefore, in order to overcome this constraint, more studies involving accurate tests and computational calculations must be designed and performed. Although the confinement effects have been recognized to study the mechanistic aspects due to its ability to improve not only the electrocatalytic performance of the MOF electrocatalyst materials but also facilitate exhibition of multifunctional electrocatalytic effects, however, it is still unclear how this confinement effect impacts the reaction intermediates in order to effectively enhance the performance of a specific electrocatalytic reaction. This could be mostly due to the complicated electrocatalytic mechanism and several competing reaction routes, particularly the complex CO_2RR pathway. Thus, certain routinely used characterization methods including HAADF-STEM, XAFS, and IR spectroscopy are not able to meet the expected demands. Therefore, in-situ characterization methods such as Raman spectroscopy, X-ray absorption spectroscopy, Fourier transform infrared spectroelectrochemical, and transmission electron microscopy are extremely effective for capturing the reaction intermediates, transition states, and electrocatalyst reconstructions. Even the steadily evolved operando technology, such as cutting-edge operando Synchrotron radiation-based Fourier transform infrared (SR-FTIR), opens up the black box of the limited catalytic process. These advanced characterization techniques combined with theoretical simulation studies should therefore provide clear mechanistic information and pathways of confined electrocatalytic reactions. This in turn establishes a corresponding electrocatalytic reaction descriptor, provide guiding design procedure, fabricating and optimizing MOF-derived electrocatalytic materials for early commercial operation of these electrocatalysts.

CRediT authorship contribution statement

K.A. Adegoke: Conceptualization, Investigation, Methodology, Validation, Visualization, Writing – original draft preparation, and Writing – review, and editing. **N.W. Maxakato:** Validation and supervision. All authors read and approved the manuscript".

Declaration of Competing Interest

The authors declare that they have no known competing financial interests or personal relationships that could have appeared to influence the work reported in this paper.

Data availability

No data was used for the research described in the article.

Acknowledgments

K. A. Adegoke acknowledges the Global Excellence Stature (GES) 4.0 Postdoctoral Fellowships Fourth Industrial Revolution and the University of Johannesburg, South Africa. N. W. Maxakato acknowledges the support received from the National Research Foundation of South Africa: Grant Number 118148, National Research Foundation of South Africa: Grant Number 138083, and Centre for Nanomaterials Science Research-University of Johannesburg, and University of Johannesburg, South Africa.

References

[1] K.W. Energy, Key world energy statistics 2009, Statistics (2009) 82, https://doi.org/10.1787/9789264039537-en.
[2] B.P. Energy, BP Energy Outlook 2019 edition, 2019. ⟨https://www.bp.com/content/dam/bp/business-sites/en/global/corporate/pdfs/energy-economics/energy-outlook/bp-energy-outlook-2019.pdf⟩.
[3] X. Li, J. Yu, M. Jaroniec, X. Chen, Cocatalysts for selective photoreduction of CO_2 into solar fuels, Chem. Rev. 119 (2019) 3962–4179, https://doi.org/10.1021/acs.chemrev.8b00400.
[4] M. Meinshausen, N. Meinshausen, W. Hare, S.C.B. Raper, K. Frieler, R. Knutti, D. J. Frame, M.R. Allen, Greenhouse-gas emission targets for limiting global warming to 2°C, Nature 458 (2009) 1158–1162, https://doi.org/10.1038/nature08017.
[5] M. Vermeer, S. Rahmstorf, Global sea level linked to global temperature, Proc. Natl. Acad. Sci. U. S. A 106 (2009) 21527–21532, https://doi.org/10.1073/pnas.0907765106.
[6] S. Solomon, G.K. Plattner, R. Knutti, P. Friedlingstein, Irreversible climate change due to carbon dioxide emissions, Proc. Natl. Acad. Sci. U. S. A 106 (2009) 1704–1709, https://doi.org/10.1073/pnas.0812721106.
[7] K.A. Adegoke, N.W. Maxakato, Porous metal oxide electrocatalytic nanomaterials for energy conversion: Oxygen defects and selection techniques, Coord. Chem. Rev. 457 (2022), 214389, https://doi.org/10.1016/j.ccr.2021.214389.
[8] D.L. Hartmann, A.M.G. Klein Tank, M. Rusticucci, L.V. Alexander, S. Brönnimann, Y.A.R. Charabi, F.J. Dentener, E.J. Dlugokencky, D.R. Easterling, A. Kaplan, B. J. Soden, P.W. Thorne, M. Wild, P. Zhai, Observations: atmosphere and surface, : Clim. Chang. 2013 Phys. Sci. Basis Work. Gr. I Contrib. Fifth Assess. Rep. Intergov. Panel Clim. Chang. (2013) 159–254, https://doi.org/10.1017/CBO9781107415324.008.
[9] G.A. Olah, A. Goeppert, G.K.S. Prakash, Chemical recycling of carbon dioxide to methanol and dimethyl ether: from greenhouse gas to renewable, environmentally carbon neutral fuels and synthetic hydrocarbons, J. Org. Chem. 74 (2009) 487–498, https://doi.org/10.1021/jo801260f.
[10] G.A. Olah, G.K.S. Prakash, Recycling of Carbon Dioxide Into Methyl Alcohol and Related Oxygenates for Hydrocarbons, Across Conventional Lines (2003) 1235–1242, https://doi.org/10.1142/9789812791405_0239.
[11] A.A. Olajire, CO_2 capture and separation technologies for end-of-pipe applications - A review, Energy 35 (2010) 2610–2628, https://doi.org/10.1016/j.energy.2010.02.030.
[12] K.A. Adegoke, R.O. Adegoke, A.O. Ibrahim, S.A. Adegoke, O.S. Bello, Electrocatalytic conversion of CO_2 to hydrocarbon and alcohol products: realities and prospects of Cu-based materials, Sustain. Mater. Technol. 25 (2020), e00200, https://doi.org/10.1016/j.susmat.2020.e00200.
[13] K.A. Adegoke, N.W. Maxakato, Efficient strategies for boosting the performance of 2D graphitic carbon nitride nanomaterials during photoreduction of carbon dioxide to energy-rich chemicals, Mater. Today Chem. 23 (2022), 100605, https://doi.org/10.1016/j.mtchem.2021.100605.
[14] K.A. Adegoke, N.W. Maxakato, Electrochemical CO_2 conversion to fuels on metal-free N-doped carbon-based materials: functionalities, mechanistic, and technoeconomic aspects, Mater. Today Chem. 24 (2022), 100838, https://doi.org/10.1016/j.mtchem.2022.100838.
[15] X. Li, Q.L. Zhu, MOF-based materials for photo- and electrocatalytic CO_2 reduction, EnergyChem 2 (2020), 100033, https://doi.org/10.1016/j.enchem.2020.100033.
[16] C.A.R. Pappijn, M. Ruitenbeek, M.F. Reyniers, K.M. Van Geem, Challenges and opportunities of carbon capture and utilization: electrochemical conversion of CO_2 to ethylene, Front. Earth Sci. 8 (2020), https://doi.org/10.3389/fenrg.2020.557466.
[17] V. Charles, A.O. Anumah, K.A. Adegoke, M.O. Adesina, I.P. Ebuka, N.A. Gaya, S. Ogwuche, M.O. Yakubu, Progress and challenges pertaining to the earthly-abundant electrocatalytic materials for oxygen evolution reaction, Sustain. Mater. Technol. 28 (2021), e00252, https://doi.org/10.1016/j.susmat.2021.e00252.
[18] N.L. Panwar, S.C. Kaushik, S. Kothari, Role of renewable energy sources in environmental protection: a review, Renew. Sustain. Energy Rev. 15 (2011) 1513–1524, https://doi.org/10.1016/j.rser.2010.11.037.
[19] J. Kibsgaard, Z. Chen, B.N. Reinecke, T.F. Jaramillo, Engineering the surface structure of MoS_2 to Â preferentially expose active edge sites forÂ electrocatalysis, Nat. Mater. 11 (2012) 963–969, https://doi.org/10.1038/nmat3439.
[20] I.E.L. Stephens, A.S. Bondarenko, U. Grønbjerg, J. Rossmeisl, I. Chorkendorff, Understanding the electrocatalysis of oxygen reduction on platinum and its alloys, Energy Environ. Sci. 5 (2012) 6744–6762, https://doi.org/10.1039/c2ee03590a.
[21] K.F. Babu, M.A. Kulandainathan, I. Katsounaros, L. Rassaei, A.D. Burrows, P. R. Raithby, F. Marken, Electrocatalytic activity of BasoliteTM F300 metal-organic-framework structures, Electrochem. Commun. 12 (2010) 632–635, https://doi.org/10.1016/j.elecom.2010.02.017.
[22] M.S. Faber, S. Jin, Earth-abundant inorganic electrocatalysts and their nanostructures for energy conversion applications, Energy Environ. Sci. 7 (2014) 3519–3542, https://doi.org/10.1039/c4ee01760a.

[23] K.A. Adegoke, S.G. Radhakrishnan, C.L. Gray, B. Sowa, C. Morais, P. Rayess, E. R. Rohwer, C. Comminges, K.B. Kokoh, E. Roduner, Highly efficient formic acid and carbon dioxide electro-reduction to alcohols on indium oxide electrodes, Sustain. Energy Fuels. 4 (2020) 4030–4038, https://doi.org/10.1039/d0se00623h.

[24] Y. Hori, Electrochemical CO_2 reduction on metal electrodes, Mod. Asp. Electrochem. 42 (2008) 89–189, https://doi.org/10.1007/978-0-387-49489-0_3.

[25] Y. Kwon, J. Lee, Formic acid from carbon dioxide on nanolayered electrocatalyst, Electrocatalysis 1 (2010) 108–115, https://doi.org/10.1007/s12678-010-0017-y.

[26] N.S. Spinner, J.A. Vega, W.E. Mustain, Recent progress in the electrochemical conversion and utilization of CO_2, Catal. Sci. Technol. 2 (2012) 19–28, https://doi.org/10.1039/c1cy00314c.

[27] J.W. Maina, C. Pozo-Gonzalo, J.A. Schütz, J. Wang, L.F. Dumée, Tuning CO_2 conversion product selectivity of metal organic frameworks derived hybrid carbon photoelectrocatalytic reactors, Carbon N. Y 148 (2019) 80–90, https://doi.org/10.1016/j.carbon.2019.03.043.

[28] A.K. Ipadeola, K. Eid, A.M. Abdullah, K.I. Ozoemena, Pd-nanoparticles embedded metal–organic framework-derived hierarchical porous carbon nanosheets as efficient electrocatalysts for carbon monoxide oxidation in different electrolytes, Langmuir 38 (2022) 11109–11120, https://doi.org/10.1021/acs.langmuir.2c01841.

[29] S. Zhang, W. Xia, Q. Yang, Y. Valentino Kaneti, X. Xu, S.M. Alshehri, T. Ahamad, M.S.A. Hossain, J. Na, J. Tang, Y. Yamauchi, Core-shell motif construction: highly graphitic nitrogen-doped porous carbon electrocatalysts using MOF-derived carbon@COF heterostructures as sacrificial templates, Chem. Eng. J. 396 (2020), 125154, https://doi.org/10.1016/j.cej.2020.125154.

[30] I. Choi, Y.E. Jung, S.J. Yoo, J.Y. Kim, H.-J. Kim, C.Y. Lee, J.H. Jang, Facile Synthesis of M-MOF-74 (M=Co, Ni, Zn) and its Application as an ElectroCatalyst for Electrochemical CO_2 Conversion and H_2 Production, J. Electrochem. Sci. Technol. 8 (2017) 61–68, https://doi.org/10.5229/JECST.2017.8.1.61.

[31] D. Hexiang, G. Sergio, C.K.E. V, F. Cory, H. Hiroyasu, G. Mohamad, W.A.C. Felipe, L. Zheng, A. Shunsuke, K. Hiroyoshi, O. Michael, T. Osamu, S.J. Fraser, Y.O. M, Large-Pore Apertures in a Series of Metal-Organic Frameworks, Science 80 (336) (2012) 1018–1023, https://doi.org/10.1126/science.1220131.

[32] H. Furukawa, K.E. Cordova, M. O'Keeffe, O.M. Yaghi, The chemistry and applications of metal-organic frameworks, Science 80 (2013) 341, https://doi.org/10.1126/science.1230444.

[33] J. Gascon, A. Corma, F. Kapteijn, F.X. Llabrés, I. Xamena, Metal organic framework catalysis: Quo vadis? ACS Catal. 4 (2014) 361–378, https://doi.org/10.1021/cs400959k.

[34] L.B. Vilhelmsen, K.S. Walton, D.S. Sholl, Structure and Mobility of Metal Clusters in MOFs: Au, Pd, and AuPd Clusters in MOF-74, J. Am. Chem. Soc. 134 (2012) 12807–12816, https://doi.org/10.1021/ja305004a.

[35] Y. Ma, H. Peng, J. Liu, Y. Wang, X. Hao, X. Feng, S.U. Khan, H. Tan, Y. Li, Polyoxometalate-based metal–organic frameworks for selective oxidation of aryl alkenes to aldehydes, Inorg. Chem. 57 (2018) 4109–4116, https://doi.org/10.1021/acs.inorgchem.8b00282.

[36] Q.L. Zhu, Q. Xu, Metal-organic framework composites, Chem. Soc. Rev. 43 (2014) 5468–5512, https://doi.org/10.1039/c3cs60472a.

[37] J. Jiang, O.M. Yaghi, Brønsted acidity in metal–organic frameworks, Chem. Rev. 115 (2015) 6966–6997, https://doi.org/10.1021/acs.chemrev.5b00221.

[38] H. Kobayashi, Y. Mitsuka, H. Kitagawa, Metal nanoparticles covered with a metal–organic framework: from one-pot synthetic methods to synergistic energy storage and conversion functions, Inorg. Chem. 55 (2016) 7301–7310, https://doi.org/10.1021/acs.inorgchem.6b00911.

[39] Q. Yang, Q. Xu, H.L. Jiang, Metal-organic frameworks meet metal nanoparticles: Synergistic effect for enhanced catalysis, Chem. Soc. Rev. 46 (2017) 4774–4808, https://doi.org/10.1039/c6cs00724d.

[40] B.D. McCarthy, A.M. Beiler, B.A. Johnson, T. Liseev, A.T. Castner, S. Ott, Analysis of electrocatalytic metal-organic frameworks, Coord. Chem. Rev. 406 (2020), 213137, https://doi.org/10.1016/j.ccr.2019.213137.

[41] B. Ma, T.T. Chen, Q.Y. Li, H.N. Qin, X.Y. Dong, S.Q. Zang, Bimetal-organic-framework-derived nanohybrids Cu0.9Co2.1S_4@MoS_2 for high-performance visible-light-catalytic hydrogen evolution reaction, ACS Appl. Energy Mater. 2 (2019) 1134–1148, https://doi.org/10.1021/acsaem.8b01691.

[42] H.F. Wang, L. Chen, H. Pang, S. Kaskel, Q. Xu, MOF-derived electrocatalysts for oxygen reduction, oxygen evolution and hydrogen evolution reactions, Chem. Soc. Rev. 49 (2020) 1414–1448, https://doi.org/10.1039/c9cs00906j.

[43] L. Du, L. Xing, G. Zhang, S. Sun, Metal-organic framework derived carbon materials for electrocatalytic oxygen reactions: Recent progress and future perspectives, Carbon N. Y 156 (2020) 77–92, https://doi.org/10.1016/j.carbon.2019.09.029.

[44] Y.-W. Li, W.-J. Zhang, J. Li, H.-Y. Ma, H.-M. Du, D.-C. Li, S.-N. Wang, J.-S. Zhao, J.-M. Dou, L. Xu, Fe-MOF-Derived Efficient ORR/OER Bifunctional Electrocatalyst for Rechargeable Zinc–Air Batteries, ACS Appl. Mater. Interfaces 12 (2020) 44710–44719, https://doi.org/10.1021/acsami.0c11945.

[45] Y. Jing, Y. Cheng, L. Wang, Y. Liu, B. Yu, C. Yang, MOF-derived Co, Fe, and Ni co-doped N-enriched hollow carbon as efficient electrocatalyst for oxygen reduction reaction, Chem. Eng. J. 397 (2020), 125539, https://doi.org/10.1016/j.cej.2020.125539.

[46] K.A. Adegoke, N.W. Maxakato, Porous metal−organic framework (MOF)-based and MOF-derived electrocatalytic materials for energy conversion, Mater. Today Energy (2021), 100816, https://doi.org/10.1016/j.mtener.2021.100816.

[47] C. Wang, Y.V. Kaneti, Y. Bando, J. Lin, C. Liu, J. Li, Y. Yamauchi, Metal-organic framework-derived one-dimensional porous or hollow carbon-based nanofibers for energy storage and conversion, Mater. Horiz. 5 (2018) 394–407, https://doi.org/10.1039/c8mh00133b.

[48] R.R. Salunkhe, Y.V. Kaneti, Y. Yamauchi, Metal-organic framework-derived nanoporous metal oxides toward supercapacitor applications: progress and prospects, ACS Nano 11 (2017) 5293–5308, https://doi.org/10.1021/acsnano.7b02796.

[49] K.A. Adegoke, N.W. Maxakato, Empirical analysis and recent advances in metal-organic framework-derived electrocatalysts for oxygen reduction, hydrogen and oxygen evolution reactions, Mater. Chem. Phys. (2022), 126438, https://doi.org/10.1016/j.matchemphys.2022.126438.

[50] C. Costentin, M. Robert, J.M. Savéant, Catalysis of the electrochemical reduction of carbon dioxide, Chem. Soc. Rev. 42 (2013) 2423–2436, https://doi.org/10.1039/c2cs35360a.

[51] P. De Luna, R. Quintero-Bermudez, C.T. DInh, M.B. Ross, O.S. Bushuyev, P. Todorović, T. Regier, S.O. Kelley, P. Yang, E.H. Sargent, Catalyst electro-redeposition controls morphology and oxidation state for selective carbon dioxide reduction, Nat. Catal. 1 (2018) 103–110, https://doi.org/10.1038/s41929-017-0018-9.

[52] M. Liu, Y. Pang, B. Zhang, P. De Luna, O. Voznyy, J. Xu, X. Zheng, C.T. Dinh, F. Fan, C. Cao, F.P.G. De Arquer, T.S. Safaei, A. Mepham, A. Klinkova, E. Kumacheva, T. Filleter, D. Sinton, S.O. Kelley, E.H. Sargent, Enhanced electrocatalytic CO_2 reduction via field-induced reagent concentration, Nature 537 (2016) 382–386, https://doi.org/10.1038/nature19060.

[53] H. Yang, Y. Huang, J. Deng, Y. Wu, N. Han, C. Zha, L. Li, Y. Li, Selective electrocatalytic CO_2 reduction enabled by SnO_2 nanoclusters, J. Energy Chem. 37 (2019) 93–96, https://doi.org/10.1016/j.jechem.2018.12.004.

[54] W.C. Chueh, C. Falter, M. Abbott, D. Scipio, P. Furler, S.M. Haile, A. Steinfeld, High-flux solar-driven thermochemical dissociation of CO_2 and H_2O using nonstoichiometric ceria, Science 80 (330) (2010) 1797–1801, https://doi.org/10.1126/science.1197834.

[55] Y. Zhang, Q. Zhu, X. Lin, Z. Xu, J. Liu, Z. Wang, J. Zhou, K. Cen, A novel thermochemical cycle for the dissociation of CO_2 and H_2O using sustainable energy sources, Appl. Energy 108 (2013) 1–7, https://doi.org/10.1016/j.apenergy.2013.03.019.

[56] Q. Jiang, Z. Chen, J. Tong, M. Yang, Z. Jiang, C. Li, Catalytic function of IrOx in the two-step thermochemical CO_2-splitting reaction at high temperatures, ACS Catal. 6 (2016) 1172–1180, https://doi.org/10.1021/acscatal.5b01774.

[57] B. Alotaibi, X. Kong, S. Vanka, S.Y. Woo, A. Pofelski, F. Oudjedi, S. Fan, M. G. Kibria, G.A. Botton, W. Ji, H. Guo, Z. Mi, Photochemical Carbon Dioxide Reduction on Mg-Doped Ga(In)N Nanowire Arrays under Visible Light Irradiation, ACS Energy Lett. 1 (2016) 246–252, https://doi.org/10.1021/acsenergylett.6b00119.

[58] J. Michl, Photochemical CO_2 reduction: towards an artificial leaf, Nat. Chem. 3 (2011) 268–269, https://doi.org/10.1038/nchem.1021.

[59] J. Wu, Y. Huang, W. Ye, Y. Li, CO_2 reduction: from the electrochemical to photochemical approach, Adv. Sci. 4 (2017) 1–29, https://doi.org/10.1002/advs.201700194.

[60] S. Castro, J. Albo, A. Irabien, Photoelectrochemical Reactors for CO_2 Utilization, ACS Sustain. Chem. Eng. 6 (2018) 15877–15894, https://doi.org/10.1021/acssuschemeng.8b03706.

[61] G. Sahara, H. Kumagai, K. Maeda, N. Kaeffer, V. Artero, M. Higashi, R. Abe, O. Ishitani, Photoelectrochemical Reduction of CO_2 Coupled to Water Oxidation Using a Photocathode with a Ru(II)-Re(I) Complex Photocatalyst and a CoOx/TaON Photoanode, J. Am. Chem. Soc. 138 (2016) 14152–14158, https://doi.org/10.1021/jacs.6b09212.

[62] Y. Hu, F. Chen, P. Ding, H. Yang, J. Chen, C. Zha, Y. Li, Designing effective Si/Ag interface via controlled chemical etching for photoelectrochemical CO_2 reduction, J. Mater. Chem. A. 6 (2018) 21906–21912, https://doi.org/10.1039/c8ta05420g.

[63] W. Zhu, R. Michalsky, Ö. Metin, H. Lv, S. Guo, C.J. Wright, X. Sun, A.A. Peterson, S. Sun, Monodisperse Au nanoparticles for selective electrocatalytic reduction of CO_2 to CO, J. Am. Chem. Soc. 135 (2013) 16833–16836, https://doi.org/10.1021/ja409445p.

[64] M. Rumayor, A. Dominguez-Ramos, A. Irabien, Formic acid manufacture: carbon dioxide utilization alternatives, Appl. Sci. 8 (2018) 914, https://doi.org/10.3390/app8060914.

[65] D.S. Laitar, P. Müller, J.P. Sadighi, Efficient homogeneous catalysis in the reduction of CO_2 to CO, J. Am. Chem. Soc. 127 (2005) 17196–17197, https://doi.org/10.1021/ja0566679.

[66] S. Liang, N. Altaf, L. Huang, Y. Gao, Q. Wang, Electrolytic cell design for electrochemical CO_2 reduction, J. CO_2 Util. 35 (2020) 90–105, https://doi.org/10.1016/j.jcou.2019.09.007.

[67] B. Kumar, M. Llorente, J. Froehlich, T. Dang, A. Sathrum, C.P. Kubiak, Photochemical and photoelectrochemical reduction of CO_2, Annu. Rev. Phys. Chem. 63 (2012) 541–569, https://doi.org/10.1146/annurev-physchem-032511-143759.

[68] S. Kaneco, H. Katsumata, T. Suzuki, K. Ohta, Photoelectrocatalytic reduction of CO_2 in LiOH/methanol at metal-modified p-InP electrodes, Appl. Catal. B Environ. 64 (2006) 139–145, https://doi.org/10.1016/j.apcatb.2005.11.012.

[69] E.E. Barton, D.M. Rampulla, A.B. Bocarsly, Selective solar-driven reduction of CO_2 to methanol using a catalyzed p-GaP based photoelectrochemical cell, J. Am. Chem. Soc. 130 (2008) 6342–6344, https://doi.org/10.1021/ja0776327.

[70] N. Furuya, K. Matsui, Electroreduction of carbon dioxide on gas-diffusion electrodes modified by metal phthalocyanines, J. Electroanal. Chem. 271 (1989) 181–191, https://doi.org/10.1016/0022-0728(89)80074-9.

[71] T. Yamamoto, D.A. Tryk, A. Fujishimal, H. Ohata, Production of syngas plus oxygen from CO_2 in a gas-diffusion electrode-based electrolytic cell, Electrochim. Acta 47 (2002) 3327–3334, https://doi.org/10.1016/S0013-4686(02)00253-0.

[72] I. Omae, Aspects of carbon dioxide utilization, Catal. Today 115 (2006) 33–52, https://doi.org/10.1016/j.cattod.2006.02.024.

[73] R.L. Cook, R.C. MacDuff, A.F. Sammells, High rate gas phase CO_2 reduction to ethylene and methane using gas diffusion electrodes, J. Electrochem. Soc. 137 (1990) 607–608, https://doi.org/10.1149/1.2086515.

[74] L. Han, W. Zhou, C. Xiang, High-rate electrochemical reduction of carbon monoxide to ethylene using cu-nanoparticle-based gas diffusion electrodes, ACS Energy Lett. 3 (2018) 855–860, https://doi.org/10.1021/acsenergylett.8b00164.

[75] S. Kaneco, H. Katsumata, T. Suzuki, K. Ohta, Electrochemical reduction of CO_2 to methane at the Cu electrode in methanol with sodium supporting salts and its comparison with other alkaline salts, Energy Fuels 20 (2006) 409–414, https://doi.org/10.1021/ef050274d.

[76] E. Barton Cole, P.S. Lakkaraju, D.M. Rampulla, A.J. Morris, E. Abelev, A. B. Bocarsly, Using a one-electron shuttle for the multielectron reduction of CO_2 to methanol: Kinetic, mechanistic, and structural insights, J. Am. Chem. Soc. 132 (2010) 11539–11551, https://doi.org/10.1021/ja1023496.

[77] Z.M. Detweiler, J.L. White, S.L. Bernasek, A.B. Bocarsly, Anodized indium metal electrodes for enhanced carbon dioxide reduction in aqueous electrolyte, Langmuir 30 (2014) 7593–7600, https://doi.org/10.1021/la501245p.

[78] O. Martin, J. Pérez-Ramírez, New and revisited insights into the promotion of methanol synthesis catalysts by CO_2, Catal. Sci. Technol. 3 (2013) 3343–3352, https://doi.org/10.1039/c3cy00573a.

[79] P.K. Giesbrecht, D.E. Herbert, Electrochemical reduction of carbon dioxide to methanol in the presence of benzannulated dihydropyridine additives, ACS Energy Lett. 2 (2017) 549–555, https://doi.org/10.1021/acsenergylett.7b00047.

[80] X. Ren, T.E. Springer, T.A. Zawodzinski, S. Gottesfeld, Methanol transport through nation membranes. electro-osmotic drag effects on potential step measurements, J. Electrochem. Soc. 147 (2000) 466, https://doi.org/10.1149/1.1393219.

[81] D.P. Summers, S. Leach, K.W. Frese, The electrochemical reduction of aqueous carbon dioxide to methanol at molybdenum electrodes with low overpotentials, J. Electroanal. Chem. 205 (1986) 219–232, https://doi.org/10.1016/0022-0728(86)90233-0.

[82] R. Kortlever, C. Balemans, Y. Kwon, M.T.M. Koper, Electrochemical CO_2 reduction to formic acid on a Pd-based formic acid oxidation catalyst, Catal. Today 244 (2015) 58–62, https://doi.org/10.1016/j.cattod.2014.08.001.

[83] G.K.S. Prakash, F.A. Viva, G.A. Olah, Electrochemical reduction of CO_2 over Sn-Nafion ® coated electrode for a fuel-cell-like device, J. Power Sources 223 (2013) 68–73, https://doi.org/10.1016/j.jpowsour.2012.09.036.

[84] X. Lu, D.Y.C. Leung, H. Wang, M.K.H. Leung, J. Xuan, Electrochemical reduction of carbon dioxide to formic acid, ChemElectroChem 1 (2014) 836–849, https://doi.org/10.1002/celc.201300206.

[85] T. Saeki, K. Hashimoto, N. Kimura, K. Omata, A. Fujishima, Electrochemical reduction of CO_2 with high current density in a CO_2 + methanol medium at various metal electrodes, J. Electroanal. Chem. 404 (1996) 299–302, https://doi.org/10.1016/0022-0728(95)04374-8.

[86] D. Yuan, C. Yan, B. Lu, H. Wang, C. Zhong, Q. Cai, Electrochemical activation of carbon dioxide for synthesis of dimethyl carbonate in an ionic liquid, Electrochim. Acta 54 (2009) 2912–2915, https://doi.org/10.1016/j.electacta.2008.11.006.

[87] B. Lu, X. Wang, Y. Li, J. Sun, J. Zhao, Q. Cai, Electrochemical conversion of CO_2 into dimethyl carbonate in a functionalized ionic liquid, J. CO_2 Util. 3–4 (2013) 98–101, https://doi.org/10.1016/j.jcou.2013.10.001.

[88] P.G. Jessop, Y. Hsiao, T. Ikariya, R. Noyori, Homogeneous catalysis in supercritical fluids: hydrogenation of supercritical carbon dioxide to formic acid, alkyl formates, and formamides, J. Am. Chem. Soc. 118 (1996) 344–355, https://doi.org/10.1021/ja953097b.

[89] H. Konnerth, B.M. Matsagar, S.S. Chen, M.H.G. Prechtl, F.K. Shieh, K.C.W. Wu, Metal-organic framework (MOF)-derived catalysts for fine chemical production, Coord. Chem. Rev. 416 (2020), https://doi.org/10.1016/j.ccr.2020.213319.

[90] R.V. Jagadeesh, K. Murugesan, A.S. Alshammari, H. Neumann, M.M. Pohl, J. Radnik, M. Beller, MOF-derived cobalt nanoparticles catalyze a general synthesis of amines, Science 80 (358) (2017) 326–332, https://doi.org/10.1126/science.aan6245.

[91] X. Liu, S. Cheng, J. Long, W. Zhang, X. Liu, D. Wei, MOFs-Derived Co@CN bi-functional catalysts for selective transfer hydrogenation of α,β-unsaturated aldehydes without use of base additives, Mater. Chem. Front. 1 (2017) 2005–2012, https://doi.org/10.1039/c7qm00189d.

[92] W. Zuo, G. Yu, Z. Dong, A MOF-derived nickel based N-doped mesoporous carbon catalyst with high catalytic activity for the reduction of nitroarenes, RSC Adv. 6 (2016) 11749–11753, https://doi.org/10.1039/c5ra23082a.

[93] X. Guo, X. Chen, D. Su, C. Liang, Preparation of Ni/C Core-shell Nanoparticles through MOF Pyrolysis for Phenylacetylene Hydrogenation Reaction, Acta Chim. Sin. 76 (2018) 22–29, https://doi.org/10.6023/A17070339.

[94] N. Stock, S. Biswas, Synthesis of metal-organic frameworks (MOFs): routes to various MOF topologies, morphologies, and composites, Chem. Rev. 112 (2012) 933–969, https://doi.org/10.1021/cr200304e.

[95] W. Chaikittisilp, K. Ariga, Y. Yamauchi, A new family of carbon materials: synthesis of MOF-derived nanoporous carbons and their promising applications, J. Mater. Chem. A 1 (2013) 14–19, https://doi.org/10.1039/c2ta00278g.

[96] X. Wang, Y. Li, Nanoporous carbons derived from MOFs as metal-free catalysts for selective aerobic oxidations, J. Mater. Chem. A 4 (2016) 5247–5257, https://doi.org/10.1039/c6ta00324a.

[97] Y.Z. Chen, G. Cai, Y. Wang, Q. Xu, S.H. Yu, H.L. Jiang, Palladium nanoparticles stabilized with N-doped porous carbons derived from metal-organic frameworks for selective catalysis in biofuel upgrade: The role of catalyst wettability, Green. Chem. 18 (2016) 1212–1217, https://doi.org/10.1039/c5gc02530c.

[98] W. Dong, L. Zhang, C. Wang, C. Feng, N. Shang, S. Gao, C. Wang, Palladium nanoparticles embedded in metal-organic framework derived porous carbon: Synthesis and application for efficient Suzuki-Miyaura coupling reactions, RSC Adv. 6 (2016) 37118–37123, https://doi.org/10.1039/c6ra00378h.

[99] C. Van Nguyen, J.R. Boo, C.H. Liu, T. Ahamad, S.M. Alshehri, B.M. Matsagar, K.C. W. Wu, Oxidation of biomass-derived furans to maleic acid over nitrogen-doped carbon catalysts under acid-free conditions, Catal. Sci. Technol. 10 (2020) 1498–1506, https://doi.org/10.1039/c9cy02364j.

[100] W. Zhang, X. Jiang, Y. Zhao, A. Carné-Sánchez, V. Malgras, J. Kim, J.H. Kim, S. Wang, J. Liu, J. Sen Jiang, Y. Yamauchi, M. Hu, Hollow carbon nanobubbles: Monocrystalline MOF nanobubbles and their pyrolysis, Chem. Sci. 8 (2017) 3538–3546, https://doi.org/10.1039/c6sc04903f.

[101] S. Yang, L. Peng, P. Huang, X. Wang, Y. Sun, C. Cao, W. Song, Nitrogen, phosphorus, and sulfur Co-doped hollow carbon shell as superior metal-free catalyst for selective oxidation of aromatic alkanes, Angew. Chem. - Int. Ed. 55 (2016) 4016–4020, https://doi.org/10.1002/anie.201600455.

[102] W. Zhong, H. Liu, C. Bai, S. Liao, Y. Li, Base-free oxidation of alcohols to esters at room temperature and atmospheric conditions using nanoscale Co-based catalysts, ACS Catal. 5 (2015) 1850–1856, https://doi.org/10.1021/cs502101c.

[103] M.H. Yap, K.L. Fow, G.Z. Chen, Synthesis and applications of MOF-derived porous nanostructures, Green. Energy Environ. 2 (2017) 218–245, https://doi.org/10.1016/j.gee.2017.05.003.

[104] Y.Y. Huang, H. Konnerth, J.Y. Yeh, M.H.G. Prechtl, C.Y. Wen, K.C.W. Wu, De novo synthesis of Cr-embedded MOF-199 and derived porous CuO/$CuCr_2O_4$ composites for enhanced phenol hydroxylation, Green. Chem. 21 (2019) 1889–1894, https://doi.org/10.1039/c8gc03348j.

[105] J. Long, K. Shen, L. Chen, Y. Li, Multimetal-MOF-derived transition metal alloy NPs embedded in an N-doped carbon matrix: Highly active catalysts for hydrogenation reactions, J. Mater. Chem. A 4 (2016) 10254–10262, https://doi.org/10.1039/c6ta00157b.

[106] Y. Te Liao, J.E. Chen, Y. Isida, T. Yonezawa, W.C. Chang, S.M. Alshehri, Y. Yamauchi, K.C.W. Wu, De novo synthesis of gold-nanoparticle-embedded, nitrogen-doped nanoporous carbon nanoparticles (Au@NC) with enhanced reduction ability, ChemCatChem 8 (2016) 502–509, https://doi.org/10.1002/cctc.201501020.

[107] B.N. Bhadra, S.H. Jhung, Well-dispersed Ni or MnO nanoparticles on mesoporous carbons: preparation via carbonization of bimetallic MOF-74s for highly reactive redox catalysts, Nanoscale 10 (2018) 15035–15047, https://doi.org/10.1039/c8nr04262d.

[108] H. Niu, S. Liu, Y. Cai, F. Wu, X. Zhao, MOF derived porous carbon supported Cu/Cu_2O composite as high performance non-noble catalyst, Microporous Mesoporous Mater. 219 (2016) 48–53, https://doi.org/10.1016/j.micromeso.2015.07.027.

[109] B. Tang, W.C. Song, E.C. Yang, X.J. Zhao, MOF-derived Ni-based nanocomposites as robust catalysts for chemoselective hydrogenation of functionalized nitro compounds, RSC Adv. 7 (2017) 1531–1539, https://doi.org/10.1039/c6ra26699a.

[110] X. Yao, C. Bai, J. Chen, Y. Li, Efficient and selective green oxidation of alcohols by MOF-derived magnetic nanoparticles as a recoverable catalyst, RSC Adv. 6 (2016) 26921–26928, https://doi.org/10.1039/c6ra01617k.

[111] Q. Guan, G.B. Wang, L. Le Zhou, W.Y. Li, Y. Bin Dong, Nanoscale covalent organic frameworks as theranostic platforms for oncotherapy: Synthesis, functionalization, and applications, Nanoscale Adv. 2 (2020) 3656–3733, https://doi.org/10.1039/d0na00537a.

[112] L. Jiao, J.Y.R. Seow, W.S. Skinner, Z.U. Wang, H.L. Jiang, Metal–organic frameworks: structures and functional applications, Mater. Today 27 (2019) 43–68, https://doi.org/10.1016/j.mattod.2018.10.038.

[113] M. Yang, L. Jiao, H. Dong, L. Zhou, C. Teng, D. Yan, T.N. Ye, X. Chen, Y. Liu, H. L. Jiang, Conversion of bimetallic MOF to Ru-doped Cu electrocatalysts for efficient hydrogen evolution in alkaline media, Sci. Bull. 66 (2021) 257–264, https://doi.org/10.1016/j.scib.2020.06.036.

[114] Y. Zhang, L. Jiao, W. Yang, C. Xie, H.L. Jiang, Rational Fabrication of Low-Coordinate Single-Atom Ni Electrocatalysts by MOFs for Highly Selective CO_2 Reduction, Angew. Chem. - Int. Ed. 60 (2021) 7607–7611, https://doi.org/10.1002/anie.202016219.

[115] T. Najam, N. Ahmad Khan, S.S. Ahmad Shah, K. Ahmad, M. Sufyan Javed, S. Suleman, M. Sohail Bashir, M.A. Hasnat, M.M. Rahman, Metal-Organic Frameworks Derived Electrocatalysts for Oxygen and Carbon Dioxide Reduction Reaction, Chem. Rec. n/a (2022), e202100329, https://doi.org/10.1002/tcr.202100329.

[116] Q. Xue, Z. Zhang, B.K.Y. Ng, P. Zhao, B.T.W. Lo, Recent advances in the engineering of single-atom catalysts through metal–organic frameworks, Top. Curr. Chem. 379 (2021) 11, https://doi.org/10.1007/s41061-021-00324-y.

[117] X. Zhang, J. Han, J. Guo, Z. Tang, Engineering nanoscale metal-organic frameworks for heterogeneous catalysis, Small Struct. 2 (2021) 2000141, https://doi.org/10.1002/sstr.202000141.

[118] B. Zhang, Y. Zheng, T. Ma, C. Yang, Y. Peng, Z. Zhou, M. Zhou, S. Li, Y. Wang, C. Cheng, Designing MOF Nanoarchitectures for Electrochemical Water Splitting, Adv. Mater. 33 (2021) 2006042, https://doi.org/10.1002/adma.202006042.

[119] I. Hod, M.D. Sampson, P. Deria, C.P. Kubiak, O.K. Farha, J.T. Hupp, Fe-porphyrin-based metal-organic framework films as high-surface concentration,

heterogeneous catalysts for electrochemical reduction of CO_2, ACS Catal. 5 (2015) 6302–6309, https://doi.org/10.1021/acscatal.5b01767.
[120] X. Chen, D.D. Ma, B. Chen, K. Zhang, R. Zou, X.T. Wu, Q.L. Zhu, Metal–organic framework-derived mesoporous carbon nanoframes embedded with atomically dispersed Fe–Nx active sites for efficient bifunctional oxygen and carbon dioxide electroreduction, Appl. Catal. B Environ. 267 (2020), https://doi.org/10.1016/j.apcatb.2020.118720.
[121] P. Shao, L. Yi, S. Chen, T. Zhou, J. Zhang, Metal-organic frameworks for electrochemical reduction of carbon dioxide: The role of metal centers, J. Energy Chem. 40 (2020) 156–170, https://doi.org/10.1016/j.jechem.2019.04.013.
[122] N. Kornienko, Y. Zhao, C.S. Kley, C. Zhu, D. Kim, S. Lin, C.J. Chang, O.M. Yaghi, P. Yang, Metal-organic frameworks for electrocatalytic reduction of carbon dioxide, J. Am. Chem. Soc. 137 (2015) 14129–14135, https://doi.org/10.1021/jacs.5b08212.
[123] X. Kang, Q. Zhu, X. Sun, J. Hu, J. Zhang, Z. Liu, B. Han, Highly efficient electrochemical reduction of CO_2 to CH_4 in an ionic liquid using a metal-organic framework cathode, Chem. Sci. 7 (2016) 266–273, https://doi.org/10.1039/c5sc03291a.
[124] Y.L. Qiu, H.X. Zhong, T.T. Zhang, W. Bin Xu, P.P. Su, X.F. Li, H.M. Zhang, Selective electrochemical reduction of carbon dioxide using Cu based metal organic framework for CO_2 capture, ACS Appl. Mater. Interfaces 10 (2018) 2480–2489, https://doi.org/10.1021/acsami.7b15255.
[125] X. Zhang, Z. Wu, X. Zhang, L. Li, Y. Li, H. Xu, X. Li, X. Yu, Z. Zhang, Y. Liang, H. Wang, Highly selective and active CO_2 reduction electrocatalysts based on cobalt phthalocyanine/carbon nanotube hybrid structures, Nat. Commun. 8 (2017) 1–8, https://doi.org/10.1038/ncomms14675.
[126] K. Zhang, W. Guo, Z. Liang, R. Zou, Metal-organic framework based nanomaterials for electrocatalytic oxygen redox reaction, Sci. China Chem. 62 (2019) 417–429, https://doi.org/10.1007/s11426-018-9441-4.
[127] Y. Zheng, P. Cheng, J. Xu, J. Han, D. Wang, C. Hao, H.R. Alanagh, C. Long, X. Shi, Z. Tang, MOF-derived nitrogen-doped nanoporous carbon for electroreduction of CO_2 to CO: The calcining temperature effect and the mechanism, Nanoscale 11 (2019) 4911–4917, https://doi.org/10.1039/c8nr10236h.
[128] Y.S. Cheng, X.P. Chu, M. Ling, N. Li, K.L. Wu, F.H. Wu, H. Li, G. Yuan, X.W. Wei, An MOF-derived copper@nitrogen-doped carbon composite: The synergistic effects of N-types and copper on selective CO_2 electroreduction, Catal. Sci. Technol. 9 (2019) 5668–5675, https://doi.org/10.1039/c9cy01131e.
[129] H. Zhang, J. Li, Q. Tan, L. Lu, Z. Wang, G. Wu, Metal–organic frameworks and their derived materials as electrocatalysts and photocatalysts for CO_2 reduction: progress, challenges, and perspectives, Chem. - A Eur. J. 24 (2018) 18137–18157, https://doi.org/10.1002/chem.201803083.
[130] Y. Pan, R. Lin, Y. Chen, S. Liu, W. Zhu, X. Cao, W. Chen, K. Wu, W.C. Cheong, Y. Wang, L. Zheng, J. Luo, Y. Lin, Y. Liu, C. Liu, J. Li, Q. Lu, X. Chen, D. Wang, Q. Peng, C. Chen, Y. Li, Design of Single-Atom Co-N5 Catalytic Site: A Robust Electrocatalyst for CO_2 Reduction with Nearly 100% CO Selectivity and Remarkable Stability, J. Am. Chem. Soc. 140 (2018) 4218–4221, https://doi.org/10.1021/jacs.8b00814.
[131] C. Gao, S. Chen, Y. Wang, J. Wang, X. Zheng, J. Zhu, L. Song, W. Zhang, Y. Xiong, Heterogeneous Single-Atom Catalyst for Visible-Light-Driven High-Turnover CO_2 Reduction: The Role of Electron Transfer, Adv. Mater. 30 (2018) 1–9, https://doi.org/10.1002/adma.201704624.
[132] M.M. Millet, G. Algara-Siller, S. Wrabetz, A. Mazheika, F. Girgsdies, D. Teschner, F. Seitz, A. Tarasov, S.V. Levchenko, R. Schlögl, E. Frei, Ni Single Atom Catalysts for CO_2 Activation, J. Am. Chem. Soc. (2019), https://doi.org/10.1021/jacs.8b11729.
[133] X. Su, X.F. Yang, Y. Huang, B. Liu, T. Zhang, Single-atom catalysis toward efficient CO_2 conversion to CO and formate products, Acc. Chem. Res. 52 (2019) 656–664, https://doi.org/10.1021/acs.accounts.8b00478.
[134] P. Lamagni, M. Miola, J. Catalano, M.S. Hvid, M.A.H. Mamakhel, M. Christensen, M.R. Madsen, H.S. Jeppesen, X.M. Hu, K. Daasbjerg, T. Skrydstrup, N. Lock, Restructuring metal–organic frameworks to nanoscale bismuth electrocatalysts for highly active and selective CO_2 reduction to formate, Adv. Funct. Mater. 30 (2020) 1–11, https://doi.org/10.1002/adfm.201910408.
[135] F. Yang, A. Chen, P.L. Deng, Y. Zhou, Z. Shahid, H. Liu, B.Y. Xia, Highly efficient electroconversion of carbon dioxide into hydrocarbons by cathodized copper-organic frameworks, Chem. Sci. 10 (2019) 7975–7981, https://doi.org/10.1039/c9sc02605c.
[136] K. Zhao, Y. Liu, X. Quan, S. Chen, H. Yu, CO_2 Electroreduction at Low Overpotential on Oxide-Derived Cu/Carbons Fabricated from Metal Organic Framework, ACS Appl. Mater. Interfaces 9 (2017) 5302–5311, https://doi.org/10.1021/acsami.6b15402.
[137] M. Peng, S. Ci, P. Shao, P. Cai, Z. Wen, Cu_3 P/C Nanocomposites for Efficient Electrocatalytic CO_2 Reduction and Zn–CO_2 Battery, J. Nanosci. Nanotechnol. 19 (2019) 3232–3236, https://doi.org/10.1166/jnn.2019.16589.
[138] X. Sun, L. Lu, Q. Zhu, C. Wu, D. Yang, C. Chen, B. Han, MoP Nanoparticles Supported on Indium-Doped Porous Carbon: Outstanding Catalysts for Highly Efficient CO_2 Electroreduction, Angew. Chem. - Int. Ed. 57 (2018) 2427–2431, https://doi.org/10.1002/anie.201712221.
[139] W. Guo, X. Sun, C. Chen, D. Yang, L. Lu, Y. Yang, B. Han, Metal-organic framework-derived indium-copper bimetallic oxide catalysts for selective aqueous electroreduction of CO_2, Green. Chem. 21 (2019) 503–508, https://doi.org/10.1039/c8gc03261k.
[140] J.X. Wu, S.Z. Hou, X. Da Zhang, M. Xu, H.F. Yang, P.S. Cao, Z.Y. Gu, Cathodized copper porphyrin metal-organic framework nanosheets for selective formate and acetate production from CO_2 electroreduction, Chem. Sci. 10 (2019) 2199–2205, https://doi.org/10.1039/c8sc04344b.
[141] Y.Z. Chen, R. Zhang, L. Jiao, H.L. Jiang, Metal–organic framework-derived porous materials for catalysis, Coord. Chem. Rev. 362 (2018) 1–23, https://doi.org/10.1016/j.ccr.2018.02.008.
[142] H. Bin Wu, X.W. Lou, Metal-organic frameworks and their derived materials for electrochemical energy storage and conversion: Promises and challenges, Sci. Adv. 3 (2017) 1–17, https://doi.org/10.1126/sciadv.aap9252.
[143] H. Tan, C. Ma, L. Gao, Q. Li, Y. Song, F. Xu, T. Wang, L. Wang, Metal-organic framework-derived copper nanoparticle@carbon nanocomposites as peroxidase mimics for colorimetric sensing of ascorbic acid, Chem. - A Eur. J. 20 (2014) 16377–16383, https://doi.org/10.1002/chem.201404960.
[144] G. Yu, J. Sun, F. Muhammad, P. Wang, G. Zhu, Cobalt-based metal organic framework as precursor to achieve superior catalytic activity for aerobic epoxidation of styrene, RSC Adv. 4 (2014) 38804–38811, https://doi.org/10.1039/c4ra03746d.
[145] C. Bai, X. Yao, Y. Li, Easy access to amides through aldehydic C-H bond functionalization catalyzed by heterogeneous Co-based catalysts, ACS Catal. 5 (2015) 884–891, https://doi.org/10.1021/cs501822r.
[146] J.A. Rodriguez, P. Liu, D.J. Stacchiola, S.D. Senanayake, M.G. White, J.G. Chen, Hydrogenation of CO_2 to Methanol: Importance of Metal-Oxide and Metal-Carbide Interfaces in the Activation of CO_2, ACS Catal. 5 (2015) 6696–6706, https://doi.org/10.1021/acscatal.5b01755.
[147] R. Lippi, S.C. Howard, H. Barron, C.D. Easton, I.C. Madsen, L.J. Waddington, C. Vogt, M.R. Hill, C.J. Sumby, C.J. Doonan, D.F. Kennedy, Highly active catalyst for CO_2 methanation derived from a metal organic framework template, J. Mater. Chem. A 5 (2017) 12990–12997, https://doi.org/10.1039/c7ta00958e.
[148] J. Liu, D.D. Zhu, C.X. Guo, A. Vasileff, S.Z. Qiao, Design strategies toward advanced mof-derived electrocatalysts for energy-conversion reactions, Adv. Energy Mater. 7 (2017) 1–26, https://doi.org/10.1002/aenm.201700518.
[149] X. Cao, C. Tan, M. Sindoro, H. Zhang, Hybrid micro-/nano-structures derived from metal-organic frameworks: Preparation and applications in energy storage and conversion, Chem. Soc. Rev. 46 (2017) 2660–2677, https://doi.org/10.1039/c6cs00426a.
[150] J.K. Sun, Q. Xu, Functional materials derived from open framework templates/precursors: Synthesis and applications, Energy Environ. Sci. 7 (2014) 2071–2100, https://doi.org/10.1039/c4ee00517a.
[151] B. Liu, H. Shioyama, T. Akita, Q. Xu, Metal-organic framework as a template for porous carbon synthesis, J. Am. Chem. Soc. 130 (2008) 5390–5391, https://doi.org/10.1021/ja7106146.
[152] Y. Yang, Z. Lun, G. Xia, F. Zheng, M. He, Q. Chen, Non-precious alloy encapsulated in nitrogen-doped graphene layers derived from MOFs as an active and durable hydrogen evolution reaction catalyst, Energy Environ. Sci. 8 (2015) 3563–3571, https://doi.org/10.1039/c5ee02460a.
[153] B. Liu, X. Zhang, H. Shioyama, T. Mukai, T. Sakai, Q. Xu, Converting cobalt oxide subunits in cobalt metal-organic framework into agglomerated Co_3O_4 nanoparticles as an electrode material for lithium ion battery, J. Power Sources 195 (2010) 857–861, https://doi.org/10.1016/j.jpowsour.2009.08.058.
[154] H.-L. Jiang, B. Liu, Y.-Q. Lan, K. Kuratani, T. Akita, H. Shioyama, F. Zong, Q. Xu, From Metal–Organic Framework to Nanoporous Carbon: Toward a Very High Surface Area and Hydrogen Uptake, J. Am. Chem. Soc. 133 (2011) 11854–11857, https://doi.org/10.1021/ja203184k.
[155] Z. Liang, T. Qiu, S. Gao, R. Zhong, R. Zou, Multi-Scale Design of Metal–Organic Framework-Derived Materials for Energy Electrocatalysis, Adv. Energy Mater. 12 (2022) 2003410, https://doi.org/10.1002/aenm.202003410.
[156] S. Gadipelli, W. Travis, W. Zhou, Z. Guo, A thermally derived and optimized structure from ZIF-8 with giant enhancement in CO_2 uptake, Energy Environ. Sci. 7 (2014) 2232–2238, https://doi.org/10.1039/C4EE01009D.
[157] K.A. Adegoke, S.O. Akinnawo, O.S. Bello, N.W. Maxakato, R.O. Adegoke, Chapter 6 - MOF-based electrocatalysts for oxygen evolution reactions, in: R.K. Gupta, T. A. Nguyen, G.B.T.-M.-O.F.-B.N. for E.C., S. Yasin (Eds.), Micro Nano Technol, Elsevier, 2022, pp. 107–134, https://doi.org/10.1016/B978-0-323-91179-5.00006-1.
[158] Y.-J. Li, J.-M. Fan, M.-S. Zheng, Q.-F. Dong, A novel synergistic composite with multi-functional effects for high-performance Li–S batteries, Energy Environ. Sci. 9 (2016) 1998–2004, https://doi.org/10.1039/C6EE00104A.
[159] L.-F. Chen, Q. Xu, Converting MOFs into amination catalysts, Science 80 (358) (2017) 304–305, https://doi.org/10.1126/science.aap8004.
[160] Q. Lai, Y. Zhao, Y. Liang, J. He, J. Chen, In Situ Confinement Pyrolysis Transformation of ZIF-8 to Nitrogen-Enriched Meso-Microporous Carbon Frameworks for Oxygen Reduction, Adv. Funct. Mater. 26 (2016) 8334–8344, https://doi.org/10.1002/adfm.201603607.
[161] Z. Liang, R. Zhao, T. Qiu, R. Zou, Q. Xu, Metal-organic framework-derived materials for electrochemical energy applications, EnergyChem 1 (2019), 100001, https://doi.org/10.1016/j.enchem.2019.100001.
[162] S.L. Li, Q. Xu, Metal–organic frameworks as platforms for clean energy, Energy Environ. Sci. 6 (2013) 1656–1683, https://doi.org/10.1039/C3EE40507A.
[163] W. Xia, A. Mahmood, R. Zou, Q. Xu, Metal-organic frameworks and their derived nanostructures for electrochemical energy storage and conversion, Energy Environ. Sci. 8 (2015) 1837–1866, https://doi.org/10.1039/c5ee00762c.
[164] Y.V. Kaneti, J. Tang, R.R. Salunkhe, X. Jiang, A. Yu, K.C.W. Wu, Y. Yamauchi, Nanoarchitectured design of porous materials and nanocomposites from metal-organic frameworks, Adv. Mater. 29 (2017), https://doi.org/10.1002/adma.201604898.
[165] H. Zhang, H. Osgood, X. Xie, Y. Shao, G. Wu, Engineering nanostructures of PGM-free oxygen-reduction catalysts using metal-organic frameworks, Nano Energy 31 (2017) 331–350, https://doi.org/10.1016/j.nanoen.2016.11.033.

[166] B.Y. Guan, X.Y. Yu, H. Bin Wu, X.W.D. Lou, Complex nanostructures from materials based on metal–organic frameworks for electrochemical energy storage and conversion, Adv. Mater. 29 (2017) 1703614, https://doi.org/10.1002/adma.201703614.
[167] Z. Li, M. Song, W. Zhu, W. Zhuang, X. Du, L. Tian, MOF-derived hollow heterostructures for advanced electrocatalysis, in: Coord. Chem. Rev, 439, 2021, https://doi.org/10.1016/j.ccr.2021.213946.
[168] X.F. Lu, Y. Fang, D. Luan, X.W.D. Lou, Metal−organic frameworks derived functional materials for electrochemical energy storage and conversion: a mini review, Nano Lett. 21 (2021) 1555–1565, https://doi.org/10.1021/acs.nanolett.0c04898.
[169] X.F. Lu, B.Y. Xia, S.Q. Zang, X.W. Lou, Metal–organic frameworks based electrocatalysts for the oxygen reduction reaction, Angew. Chem. - Int. Ed. 59 (2020) 4634–4650, https://doi.org/10.1002/anie.201910309.
[170] C. Dey, T. Kundu, B.P. Biswal, A. Mallick, R. Banerjee, Crystalline metal-Organic frameworks (MOFs): Synthesis, structure and function, Acta Crystallogr. Sect. B Struct. Sci. Cryst. Eng. Mater. 70 (2014) 3–10, https://doi.org/10.1107/S2052520613029557.
[171] H. Zhang, J. Nai, L. Yu, X.W. (David) Lou, Metal-organic-framework-based materials as platforms for renewable energy and environmental applications, Joule 1 (2017) 77–107, https://doi.org/10.1016/j.joule.2017.08.008.
[172] A. Indra, T. Song, U. Paik, Metal organic framework derived materials: progress and prospects for the energy conversion and storage, Adv. Mater. 30 (2018) 1705146, https://doi.org/10.1002/adma.201705146.
[173] K.A. Adegoke, N.W. Maxakato, Porous metal-organic framework (MOF)-based and MOF-derived electrocatalytic materials for energy conversion, Mater. Today Energy 21 (2021), 100816, https://doi.org/10.1016/j.mtener.2021.100816.
[174] C. Zhao, X. Dai, T. Yao, W. Chen, X. Wang, J. Wang, J. Yang, S. Wei, Y. Wu, Y. Li, Ionic exchange of metal–organic frameworks to access single nickel sites for efficient electroreduction of CO_2, J. Am. Chem. Soc. 139 (2017) 8078–8081, https://doi.org/10.1021/jacs.7b02736.
[175] X. Wang, Z. Chen, X. Zhao, T. Yao, W. Chen, R. You, C. Zhao, G. Wu, J. Wang, W. Huang, J. Yang, X. Hong, S. Wei, Y. Wu, Y. Li, Regulation of Coordination Number over Single Co Sites: Triggering the Efficient Electroreduction of CO_2, Angew. Chem. - Int. Ed. 57 (2018) 1944–1948, https://doi.org/10.1002/anie.201712451.
[176] J. Nai, B.Y. Guan, L. Yu, X. Wen David Lou, Oriented assembly of anisotropic nanoparticles into frame-like superstructures, Sci. Adv. 3 (2017), e1700732, https://doi.org/10.1126/sciadv.1700732.
[177] Z. Yang, B. Chen, W. Chen, Y. Qu, F. Zhou, C. Zhao, Q. Xu, Q. Zhang, X. Duan, Y. Wu, Directly transforming copper (I) oxide bulk into isolated single-atom copper sites catalyst through gas-transport approach, Nat. Commun. 10 (2019) 1–7, https://doi.org/10.1038/s41467-019-11796-4.
[178] X.F. Lu, L.F. Gu, J.W. Wang, J.X. Wu, P.Q. Liao, G.R. Li, Bimetal-Organic Framework Derived $CoFe_2O_4$/C Porous Hybrid Nanorod Arrays as High-Performance Electrocatalysts for Oxygen Evolution Reaction, Adv. Mater. 29 (2017), https://doi.org/10.1002/adma.201604437.
[179] X.F. Lu, Y. Chen, S. Wang, S. Gao, X.W. Lou, Interfacing manganese oxide and cobalt in porous graphitic carbon polyhedrons boosts oxygen electrocatalysis for zn–air batteries, Adv. Mater. 31 (2019) 1902339, https://doi.org/10.1002/adma.201902339.
[180] J. Li, M. Chen, D.A. Cullen, S. Hwang, M. Wang, B. Li, K. Liu, S. Karakalos, M. Lucero, H. Zhang, C. Lei, H. Xu, G.E. Sterbinsky, Z. Feng, D. Su, K.L. More, G. Wang, Z. Wang, G. Wu, Atomically dispersed manganese catalysts for oxygen reduction in proton-exchange membrane fuel cells, Nat. Catal. 1 (2018) 935–945, https://doi.org/10.1038/s41929-018-0164-8.
[181] X.F. Lu, L. Yu, X.W. Lou, Highly crystalline Ni-doped FeP/carbon hollow nanorods as all-pH efficient and durable hydrogen evolving electrocatalysts, Sci. Adv. 5 (2019) eaav6009, https://doi.org/10.1126/sciadv.aav6009.
[182] Y. Fang, X.Y. Yu, X.W.D. Lou, Formation of Hierarchical Cu-Doped $CoSe_2$ Microboxes via Sequential Ion Exchange for High-Performance Sodium-Ion Batteries, Adv. Mater. 30 (2018) 1706668, https://doi.org/10.1002/adma.201706668.
[183] Y. Fang, D. Luan, Y. Chen, S. Gao, X.W. Lou, Synthesis of Copper-Substituted CoS_2@CuxS Double-Shelled Nanoboxes by Sequential Ion Exchange for Efficient Sodium Storage, Angew. Chem. - Int. Ed. 59 (2020) 2644–2648, https://doi.org/10.1002/anie.201912924.
[184] Y. Jia, K. Jiang, H. Wang, X. Yao, The role of defect sites in nanomaterials for electrocatalytic energy conversion, Chem 5 (2019) 1371–1397, https://doi.org/10.1016/j.chempr.2019.02.008.
[185] S. Liu, L. Kang, J. Zhang, E. Jung, S. Lee, S.C. Jun, Structural engineering and surface modification of MOF-derived cobalt-based hybrid nanosheets for flexible solid-state supercapacitors, Energy Storage Mater. 32 (2020) 167–177, https://doi.org/10.1016/j.ensm.2020.07.017.
[186] Z. Wang, S.M. Cohen, Postsynthetic modification of metal–organic frameworks, Chem. Soc. Rev. 38 (2009) 1315–1329, https://doi.org/10.1039/b802258p.
[187] M. Kalaj, S.M. Cohen, Postsynthetic modification: an enabling technology for the advancement of metal-organic frameworks, ACS Cent. Sci. 6 (2020) 1046–1057, https://doi.org/10.1021/acscentsci.0c00690.
[188] A. Kirchon, L. Feng, H.F. Drake, E.A. Joseph, H.C. Zhou, From fundamentals to applications: a toolbox for robust and multifunctional MOF materials, Chem. Soc. Rev. 47 (2018) 8611–8638, https://doi.org/10.1039/c8cs00688a.
[189] S.M. Cohen, The Postsynthetic Renaissance in Porous Solids, J. Am. Chem. Soc. 139 (2017) 2855–2863, https://doi.org/10.1021/jacs.6b11259.
[190] W. Li, Metal–organic framework membranes: Production, modification, and applications, Prog. Mater. Sci. 100 (2019) 21–63, https://doi.org/10.1016/j.pmatsci.2018.09.003.
[191] J. Gandara-Loe, L. Pastor-Perez, L.F. Bobadilla, J.A. Odriozola, T.R. Reina, Understanding the opportunities of metal-organic frameworks (MOFs) for CO_2 capture and gas-phase CO_2 conversion processes: a comprehensive overview, React. Chem. Eng. 6 (2021) 787–814, https://doi.org/10.1039/d1re00034a.
[192] C. Zhu, Y. Peng, W. Yang, Modification strategies for metal-organic frameworks targeting at membrane-based gas separations, Green. Chem. Eng. 2 (2021) 17–26, https://doi.org/10.1016/j.gce.2020.11.005.
[193] L. Jiao, R. Zhang, G. Wan, W. Yang, X. Wan, H. Zhou, J. Shui, S.H. Yu, H.L. Jiang, Nanocasting SiO2 into metal–organic frameworks imparts dual protection to high-loading Fe single-atom electrocatalysts, Nat. Commun. 11 (2020), https://doi.org/10.1038/s41467-020-16715-6.
[194] X. Zhang, D. Xue, S. Jiang, H. Xia, Y. Yang, W. Yan, J. Hu, J. Zhang, Rational confinement engineering of MOF-derived carbon-based electrocatalysts toward CO_2 reduction and O2 reduction reactions, InfoMat 4 (2022), e12257, https://doi.org/10.1002/inf2.12257.
[195] T.W. Hansen, A.T. Delariva, S.R. Challa, A.K. Datye, Sintering of catalytic nanoparticles: Particle migration or ostwald ripening, Acc. Chem. Res. 46 (2013) 1720–1730, https://doi.org/10.1021/ar3002427.
[196] L.-P. Yuan, T. Tang, J.-S. Hu, L.-J. Wan, Confinement strategies for precise synthesis of efficient electrocatalysts from the macroscopic to the atomic level, Acc. Mater. Res. 2 (2021) 907–919, https://doi.org/10.1021/accountsmr.1c00135.
[197] S.B. Simonsen, I. Chorkendorff, S. Dahl, M. Skoglundh, J. Sehested, S. Helveg, Direct observations of oxygen-induced platinum nanoparticle ripening studied by in situ TEM, J. Am. Chem. Soc. 132 (2010) 7968–7975, https://doi.org/10.1021/ja910094r.
[198] Y. Lykhach, S.M. Kozlov, T. Skála, A. Tovt, V. Stetsovych, N. Tsud, F. Dvořák, V. Johánek, A. Neitzel, J. Mysliveček, S. Fabris, V. Matolín, K.M. Neyman, J. Libuda, Counting electrons on supported nanoparticles, Nat. Mater. 15 (2016) 284–288, https://doi.org/10.1038/nmat4500.
[199] I.V. Yudanov, A. Genest, S. Schauermann, H.-J. Freund, N. Rösch, Size Dependence of the Adsorption Energy of CO on Metal Nanoparticles: A DFT Search for the Minimum Value, Nano Lett. 12 (2012) 2134–2139, https://doi.org/10.1021/nl300515z.
[200] X. Han, X. Ling, Y. Wang, T. Ma, C. Zhong, W. Hu, Y. Deng, Generation of nanoparticle, atomic-cluster, and single-atom cobalt catalysts from zeolitic imidazole frameworks by spatial isolation and their use in zinc–air batteries, Angew. Chem. - Int. Ed. 58 (2019) 5359–5364, https://doi.org/10.1002/anie.201901109.
[201] P. Yin, T. Yao, Y. Wu, L. Zheng, Y. Lin, W. Liu, H. Ju, J. Zhu, X. Hong, Z. Deng, G. Zhou, S. Wei, Y. Li, Single Cobalt Atoms with Precise N-Coordination as Superior Oxygen Reduction Reaction Catalysts, Angew. Chem. - Int. Ed. 55 (2016) 10800–10805, https://doi.org/10.1002/anie.201604802.
[202] M. Chen, Y. He, J.S. Spendelow, G. Wu, Atomically dispersed metal catalysts for oxygen reduction, ACS Energy Lett. 4 (2019) 1619–1633, https://doi.org/10.1021/acsenergylett.9b00804.
[203] S. Ji, Y. Chen, X. Wang, Z. Zhang, D. Wang, Y. Li, Chemical synthesis of single atomic site catalysts, Chem. Rev. 120 (2020) 11900–11955, https://doi.org/10.1021/acs.chemrev.9b00818.
[204] Y.N. Gong, L. Jiao, Y. Qian, C.Y. Pan, L. Zheng, X. Cai, B. Liu, S.H. Yu, H.L. Jiang, Regulating the coordination environment of MOF-templated single-atom nickel electrocatalysts for boosting CO_2 Reduction, Angew. Chem. - Int. Ed. 59 (2020) 2705–2709, https://doi.org/10.1002/anie.201914977.
[205] X. Yang, J. Cheng, X. Yang, Y. Xu, W. Sun, N. Liu, J. Liu, Boosting Electrochemical CO_2 Reduction by Controlling Coordination Environment in Atomically Dispersed Ni@NxCy Catalysts, ACS Sustain, Chem. Eng. 9 (2021) 6438–6445, https://doi.org/10.1021/acssuschemeng.1c01364.
[206] C. Costentin, M. Robert, J.M. Savéant, Molecular catalysis of electrochemical reactions, Curr. Opin. Electrochem 2 (2017) 26–31, https://doi.org/10.1016/j.coelec.2017.02.006.
[207] R. Kortlever, J. Shen, K.J.P. Schouten, F. Calle-Vallejo, M.T.M. Koper, Catalysts and reaction pathways for the electrochemical reduction of carbon dioxide, J. Phys. Chem. Lett. 6 (2015) 4073–4082, https://doi.org/10.1021/acs.jpclett.5b01559.
[208] J.T. Feaster, C. Shi, E.R. Cave, T. Hatsukade, D.N. Abram, K.P. Kuhl, C. Hahn, J. K. Nørskov, T.F. Jaramillo, Understanding Selectivity for the Electrochemical Reduction of Carbon Dioxide to Formic Acid and Carbon Monoxide on Metal Electrodes, ACS Catal. 7 (2017) 4822–4827, https://doi.org/10.1021/acscatal.7b00687.
[209] H.A. Hansen, J.B. Varley, A.A. Peterson, J.K. Nørskov, Understanding trends in the electrocatalytic activity of metals and enzymes for CO_2 reduction to CO, J. Phys. Chem. Lett. 4 (2013) 388–392, https://doi.org/10.1021/jz3021155.
[210] W. Ni, Y. Xue, X. Zang, C. Li, H. Wang, Z. Yang, Y.M. Yan, Fluorine Doped Cagelike Carbon Electrocatalyst: An Insight into the Structure-Enhanced CO Selectivity for CO_2 Reduction at High Overpotential, ACS Nano 14 (2020) 2014–2023, https://doi.org/10.1021/acsnano.9b08528.
[211] Q. Li, Z. Wang, M. Zhang, P. Hou, P. Kang, Nitrogen doped tin oxide nanostructured catalysts for selective electrochemical reduction of carbon dioxide to formate, J. Energy Chem. 26 (2017) 825–829, https://doi.org/10.1016/j.jechem.2017.08.010.
[212] A.S. Varela, W. Ju, A. Bagger, P. Franco, J. Rossmeisl, P. Strasser, Electrochemical reduction of CO_2 on metal-nitrogen-doped carbon catalysts, http s, Doi. Org/

10.1021/Acscatal. 9B01405, ACS Catal. 9 (2019) 7270–7284. http s, Doi. Org/10.1021/Acscatal. 9B01405.
[213] J. Li, P. Yan, K. Li, J. You, H. Wang, W. Cui, W. Cen, Y. Chu, F. Dong, Cu supported on polymeric carbon nitride for selective CO_2 reduction into CH_4: A combined kinetics and thermodynamics investigation, J. Mater. Chem. A 7 (2019) 17014–17021, https://doi.org/10.1039/c9ta05112k.
[214] X. Nie, M.R. Esopi, M.J. Janik, A. Asthagiri, Selectivity of CO_2 reduction on copper electrodes: The role of the kinetics of elementary steps, Angew. Chem. - Int. Ed. 52 (2013) 2459–2462, https://doi.org/10.1002/anie.201208320.
[215] H. Zhang, X. Chang, J.G. Chen, W.A. Goddard, B. Xu, M.J. Cheng, Q. Lu, Computational and experimental demonstrations of one-pot tandem catalysis for electrochemical carbon dioxide reduction to methane, Nat. Commun. 10 (2019) 1–9, https://doi.org/10.1038/s41467-019-11292-9.
[216] Y. Zheng, A. Vasileff, X. Zhou, Y. Jiao, M. Jaroniec, S.Z. Qiao, Understanding the Roadmap for Electrochemical Reduction of CO_2 to Multi-Carbon Oxygenates and Hydrocarbons on Copper-Based Catalysts, J. Am. Chem. Soc. 141 (2019) 7646–7659, https://doi.org/10.1021/jacs.9b02124.
[217] L. Fan, C. Xia, F. Yang, J. Wang, H. Wang, Y. Lu, Strategies in catalysts and electrolyzer design for electrochemical CO_2 reduction toward C_2+ products, Sci. Adv. 6 (2020), https://doi.org/10.1126/sciadv.aay3111.
[218] F. Calle-Vallejo, M.T.M. Koper, Accounting for bifurcating pathways in the screening for CO_2 reduction catalysts, ACS Catal. 7 (2017) 7346–7351, https://doi.org/10.1021/acscatal.7b02917.
[219] L. Wang, S. Nitopi, A.B. Wong, J.L. Snider, A.C. Nielander, C.G. Morales-Guio, M. Orazov, D.C. Higgins, C. Hahn, T.F. Jaramillo, Electrochemically converting carbon monoxide to liquid fuels by directing selectivity with electrode surface area, Nat. Catal. 2 (2019) 702–708, https://doi.org/10.1038/s41929-019-0301-z.
[220] Y. Momose, K. Sato, O. Ohno, Electrochemical reduction of CO_2 at copper electrodes and its relationship to the metal surface characteristics, Surf. Interface Anal. 34 (2002) 615–618, https://doi.org/10.1002/sia.1372.
[221] X. Zhi, Y. Jiao, Y. Zheng, A. Vasileff, S.Z. Qiao, Selectivity roadmap for electrochemical CO_2 reduction on copper-based alloy catalysts, Nano Energy 71 (2020), 104601, https://doi.org/10.1016/j.nanoen.2020.104601.
[222] M.A. Tekalgne, H.H. Do, A. Hasani, Q. Van Le, H.W. Jang, S.H. Ahn, S.Y. Kim, Two-dimensional materials and metal-organic frameworks for the CO_2 reduction reaction, Mater. Today Adv. 5 (2020), 100038, https://doi.org/10.1016/j.mtadv.2019.100038.
[223] X. Su, Y. Sun, L. Jin, L. Zhang, Y. Yang, P. Kerns, B. Liu, S. Li, J. He, Hierarchically porous Cu/Zn bimetallic catalysts for highly selective CO_2 electroreduction to liquid C_2 products, Appl. Catal. B Environ. 269 (2020), 118800, https://doi.org/10.1016/j.apcatb.2020.118800.
[224] F. Zhang, A.C. Co, Direct Evidence of Local pH Change and the Role of Alkali Cation during CO_2 Electroreduction in Aqueous Media, Angew. Chem. - Int. Ed. 59 (2020) 1674–1681, https://doi.org/10.1002/anie.201912637.
[225] L. Ai, J. Su, M. Wang, J. Jiang, Bamboo-Structured Nitrogen-Doped Carbon Nanotube Coencapsulating Cobalt and Molybdenum Carbide Nanoparticles: An Efficient Bifunctional Electrocatalyst for Overall Water Splitting, ACS Sustain. Chem. Eng. 6 (2018) 9912–9920, https://doi.org/10.1021/acssuschemeng.8b01120.
[226] L. Zhang, I. Merino-Garcia, J. Albo, C.M. Sánchez-Sánchez, Electrochemical CO_2 reduction reaction on cost-effective oxide-derived copper and transition metal–nitrogen–carbon catalysts, Curr. Opin. Electrochem 23 (2020) 65–73, https://doi.org/10.1016/j.coelec.2020.04.005.
[227] A.S. Varela, W. Ju, T. Reier, P. Strasser, Tuning the Catalytic Activity and Selectivity of Cu for CO_2 Electroreduction in the Presence of Halides, ACS Catal. 6 (2016) 2136–2144, https://doi.org/10.1021/acscatal.5b02550.
[228] Y. Hori, H. Wakebe, T. Tsukamoto, O. Koga, Electrocatalytic process of CO selectivity in electrochemical reduction of CO_2 at metal electrodes in aqueous media, Electrochim. Acta 39 (1994) 1833–1839, https://doi.org/10.1016/0013-4686(94)85172-7.
[229] W. Ma, S. Xie, T. Liu, Q. Fan, J. Ye, F. Sun, Z. Jiang, Q. Zhang, J. Cheng, Y. Wang, Electrocatalytic reduction of CO_2 to ethylene and ethanol through hydrogen-assisted C–C coupling over fluorine-modified copper, Nat. Catal. 3 (2020) 478–487, https://doi.org/10.1038/s41929-020-0450-0.
[230] Q. Hu, Z. Han, X. Wang, G. Li, Z. Wang, X. Huang, H. Yang, X. Ren, Q. Zhang, J. Liu, C. He, Facile Synthesis of Sub-Nanometric Copper Clusters by Double Confinement Enables Selective Reduction of Carbon Dioxide to Methane, Angew. Chem. - Int. Ed. 59 (2020) 19054–19059, https://doi.org/10.1002/anie.202009277.
[231] D.H. Won, H. Shin, J. Koh, J. Chung, H.S. Lee, H. Kim, S.I. Woo, Highly Efficient, Selective, and Stable CO_2 Electroreduction on a Hexagonal Zn Catalyst, Angew. Chem. - Int. Ed. 55 (2016) 9297–9300, https://doi.org/10.1002/anie.201602888.
[232] H.S. Jeon, I. Sinev, F. Scholten, N.J. Divins, I. Zegkinoglou, L. Pielsticker, B. R. Cuenya, Operando evolution of the structure and oxidation state of size-controlled Zn nanoparticles during CO_2 electroreduction, J. Am. Chem. Soc. 140 (2018) 9383–9386, https://doi.org/10.1021/jacs.8b05258.
[233] D. Ren, B.S.H. Ang, B.S. Yeo, Tuning the selectivity of carbon dioxide electroreduction toward ethanol on oxide-derived Cu_xZn catalysts, ACS Catal. 6 (2016) 8239–8247, https://doi.org/10.1021/acscatal.6b02162.
[234] G. Keerthiga, R. Chetty, Electrochemical reduction of carbon dioxide on zinc-modified copper electrodes, J. Electrochem. Soc. 164 (2017) H164–H169, https://doi.org/10.1149/2.0421704jes.
[235] J. Albo, A. Sáez, J. Solla-Gullón, V. Montiel, A. Irabien, Production of methanol from CO_2 electroreduction at Cu_2O and Cu_2O/ZnO-based electrodes in aqueous solution, Appl. Catal. B Environ. 176–177 (2015) 709–717, https://doi.org/10.1016/j.apcatb.2015.04.055.
[236] S. Sarfraz, A.T. Garcia-Esparza, A. Jedidi, L. Cavallo, K. Takanabe, Cu-Sn Bimetallic Catalyst for Selective Aqueous Electroreduction of CO_2 to CO, ACS Catal. 6 (2016) 2842–2851, https://doi.org/10.1021/acscatal.6b00269.
[237] M. Morimoto, Y. Takatsuji, R. Yamasaki, H. Hashimoto, I. Nakata, T. Sakakura, T. Haruyama, Electrodeposited Cu-Sn Alloy for Electrochemical CO_2 Reduction to CO/HCOO−, Electrocatalysis 9 (2018) 323–332, https://doi.org/10.1007/s12678-017-0434-2.
[238] F. Li, L. Chen, G.P. Knowles, D.R. MacFarlane, J. Zhang, Hierarchical Mesoporous SnO_2 Nanosheets on Carbon Cloth: A Robust and Flexible Electrocatalyst for CO_2 Reduction with High Efficiency and Selectivity, Angew. Chem. - Int. Ed. 56 (2017) 505–509, https://doi.org/10.1002/anie.201608279.
[239] H. Zhong, F. Meng, Q. Zhang, K. Liu, X. Zhang, Highly efficient and selective CO_2 electro-reduction with atomic Fe-C-N hybrid coordination on porous carbon nematosphere, Nano Res 12 (2019) 2318–2323, https://doi.org/10.1007/s12274-019-2339-2.
[240] H. Song, M. Im, J.T. Song, J.A. Lim, B.S. Kim, Y. Kwon, S. Ryu, J. Oh, Effect of mass transfer and kinetics in ordered Cu-mesostructures for electrochemical CO_2 reduction, Appl. Catal. B Environ. 232 (2018) 391–396, https://doi.org/10.1016/j.apcatb.2018.03.071.
[241] A. Dutta, M. Rahaman, N.C. Luedi, M. Mohos, P. Broekmann, Morphology matters: tuning the product distribution of CO_2 electroreduction on oxide-derived Cu foam catalysts, ACS Catal. 6 (2016) 3804–3814, https://doi.org/10.1021/acscatal.6b00770.
[242] A.S. Hall, Y. Yoon, A. Wuttig, Y. Surendranath, Mesostructure-induced selectivity in CO_2 reduction catalysis, J. Am. Chem. Soc. 137 (2015) 14834–14837, https://doi.org/10.1021/jacs.5b08259.
[243] Z. Pan, K. Wang, K. Ye, Y. Wang, H.Y. Su, B. Hu, J. Xiao, T. Yu, Y. Wang, S. Song, Intermediate adsorption states switch to selectively catalyze electrochemical Co_2 reduction, ACS Catal. 10 (2020) 3871–3880, https://doi.org/10.1021/acscatal.9b05115.
[244] J.J. Lv, M. Jouny, W. Luc, W. Zhu, J.J. Zhu, F. Jiao, A highly porous copper electrocatalyst for carbon dioxide reduction, Adv. Mater. 30 (2018), https://doi.org/10.1002/adma.201803111.
[245] M. Ma, K. Djanashvili, W.A. Smith, Controllable hydrocarbon formation from the electrochemical reduction of CO_2 over Cu nanowire arrays, Angew. Chem. - Int. Ed. 55 (2016) 6680–6684, https://doi.org/10.1002/anie.201601282.
[246] K.D. Yang, W.R. Ko, J.H. Lee, S.J. Kim, H. Lee, M.H. Lee, K.T. Nam, Morphology-Directed Selective Production of Ethylene or Ethane from CO_2 on a Cu Mesopore Electrode, Angew. Chem. - Int. Ed. 56 (2017) 796–800, https://doi.org/10.1002/anie.201610432.
[247] F. Li, G.H. Gu, C. Choi, P. Kolla, S. Hong, T.S. Wu, Y.L. Soo, J. Masa, S. Mukerjee, Y. Jung, J. Qiu, Z. Sun, Highly stable two-dimensional bismuth metal-organic frameworks for efficient electrochemical reduction of CO_2, Appl. Catal. B Environ. 277 (2020), https://doi.org/10.1016/j.apcatb.2020.119241.
[248] D. Narváez-Celada, A.S. Varela, CO_2 electrochemical reduction on metal–organic framework catalysts: current status and future directions, J. Mater. Chem. A 10 (2022) 5899–5917, https://doi.org/10.1039/D1TA10440C.
[249] Y. Zhang, S.-X. Guo, X. Zhang, A.M. Bond, J. Zhang, Mechanistic understanding of the electrocatalytic CO_2 reduction reaction – New developments based on advanced instrumental techniques, Nano Today 31 (2020), 100835, https://doi.org/10.1016/j.nantod.2019.100835.
[250] Y. Lum, J.W. Ager, Evidence for product-specific active sites on oxide-derived Cu catalysts for electrochemical CO_2 reduction, Nat. Catal. 2 (2019) 86–93, https://doi.org/10.1038/s41929-018-0201-7.
[251] S.L. Shannon, J.G. Goodwin, Characterization of catalytic surfaces by isotopic-transient kinetics during steady-state reaction, Chem. Rev. 95 (1995) 677–695, https://doi.org/10.1021/cr00035a011.
[252] X.C. Lin, Probing transient molecular structures in photochemical processes using laser-initiated time-resolved X-ray absorption spectroscopy, Annu. Rev. Phys. Chem. 56 (2005) 221–254, https://doi.org/10.1146/annurev.physchem.56.092503.141310.
[253] G. Smolentsev, V. Sundström (Eds.), Time-Resolv. X-ray Absorpt. Spectrosc. study Mol. Syst. Relev. Artif. Photosynth., Coord. Chem. Rev. 304–305 (2015) 117–132, https://doi.org/10.1016/j.ccr.2015.03.001.
[254] S.S.A. Shah, T. Najam, M. Wen, S.-Q. Zang, A. Waseem, H.-L. Jiang, Metal–organic framework-based electrocatalysts for CO_2 reduction, Small Struct. 3 (2022) 2100090, https://doi.org/10.1002/sstr.202100090.
[255] Y. Pan, C. Zhang, Z. Liu, C. Chen, Y. Li, Structural Regulation with Atomic-Level Precision: From Single-Atomic Site to Diatomic and Atomic Interface Catalysis, Matter 2 (2020) 78–110, https://doi.org/10.1016/j.matt.2019.11.014.
[256] J. Li, S. Sharma, X. Liu, Y.-T. Pan, J.S. Spendelow, M. Chi, Y. Jia, P. Zhang, D. A. Cullen, Z. Xi, H. Lin, Z. Yin, B. Shen, M. Muzzio, C. Yu, Y.S. Kim, A.A. Peterson, K.L. More, H. Zhu, S. Sun, Hard-Magnet $L1_0$-CoPt Nanoparticles Advance Fuel Cell Catalysis, Joule 3 (2019) 124–135, https://doi.org/10.1016/j.joule.2018.09.016.
[257] Z. Zhai, W. Yan, L. Dong, S. Deng, D.P. Wilkinson, X. Wang, L. Zhang, J. Zhang, Catalytically active sites of MOF-derived electrocatalysts: synthesis, characterization, theoretical calculations, and functional mechanisms, J. Mater. Chem. A 9 (2021) 20320–20344, https://doi.org/10.1039/D1TA02896K.
[258] K. Jiang, H. Wang, Electrocatalysis over Graphene-Defect-Coordinated Transition-Metal Single-Atom Catalysts, Chem 4 (2018) 194–195, https://doi.org/10.1016/j.chempr.2018.01.013.
[259] Y. Jia, L. Zhang, L. Zhuang, H. Liu, X. Yan, X. Wang, J. Liu, J. Wang, Y. Zheng, Z. Xiao, E. Taran, J. Chen, D. Yang, Z. Zhu, S. Wang, L. Dai, X. Yao, Identification of active sites for acidic oxygen reduction on carbon catalysts with and without nitrogen doping, Nat. Catal. 2 (2019) 688–695, https://doi.org/10.1038/s41929-019-0297-4.

[260] J. Li, M. Chen, D.A. Cullen, S. Hwang, M. Wang, B. Li, K. Liu, S. Karakalos, M. Lucero, H. Zhang, C. Lei, H. Xu, G.E. Sterbinsky, Z. Feng, D. Su, K.L. More, G. Wang, Z. Wang, G. Wu, Atomically dispersed manganese catalysts for oxygen reduction in proton-exchange membrane fuel cells, Nat. Catal. 1 (2018) 935–945, https://doi.org/10.1038/s41929-018-0164-8.
[261] X. Ao, W. Zhang, B. Zhao, Y. Ding, G. Nam, L. Soule, A. Abdelhafiz, C. Wang, M. Liu, Atomically dispersed Fe–N–C decorated with Pt-alloy core–shell nanoparticles for improved activity and durability towards oxygen reduction, Energy Environ. Sci. 13 (2020) 3032–3040, https://doi.org/10.1039/D0EE00832J.
[262] J.-X. Wu, X.-R. Zhu, T. Liang, X.-D. Zhang, S.-Z. Hou, M. Xu, Y.-F. Li, Z.-Y. Gu, Sn (101) Derived from Metal–Organic Frameworks for Efficient Electrocatalytic Reduction of CO_2, Inorg. Chem. 60 (2021) 9653–9659, https://doi.org/10.1021/acs.inorgchem.1c00946.
[263] Z. Yang, H. Wang, X. Fei, W. Wang, Y. Zhao, X. Wang, X. Tan, Q. Zhao, H. Wang, J. Zhu, L. Zhou, H. Ning, M. Wu, MOF derived bimetallic CuBi catalysts with ultra-wide potential window for high-efficient electrochemical reduction of CO_2 to formate, Appl. Catal. B Environ. 298 (2021), 120571, https://doi.org/10.1016/j.apcatb.2021.120571.
[264] A.A. Peterson, F. Abild-Pedersen, F. Studt, J. Rossmeisl, J.K. Nørskov, How copper catalyzes the electroreduction of carbon dioxide into hydrocarbon fuels, Energy Environ. Sci. 3 (2010) 1311–1315, https://doi.org/10.1039/c0ee00071j.
[265] H. Kim, D. Shin, W. Yang, D.H. Won, H.-S. Oh, M.W. Chung, D. Jeong, S.H. Kim, K.H. Chae, J.Y. Ryu, J. Lee, S.J. Cho, J. Seo, H. Kim, C.H. Choi, Identification of Single-Atom Ni Site Active toward Electrochemical CO_2 Conversion to CO, J. Am. Chem. Soc. 143 (2021) 925–933, https://doi.org/10.1021/jacs.0c11008.
[266] S. Li, X. Lu, S. Zhao, M. Ceccato, X.-M. Hu, A. Roldan, M. Liu, K. Daasbjerg, p-Block Indium Single-Atom Catalyst with Low-Coordinated In–N Motif for Enhanced Electrochemical CO_2 Reduction, ACS Catal. 12 (2022) 7386–7395, https://doi.org/10.1021/acscatal.2c01805.
[267] A. Bagger, W. Ju, A.S. Varela, P. Strasser, J. Rossmeisl, Electrochemical CO_2 Reduction: A Classification Problem, ChemPhysChem 18 (2017) 3266–3273, https://doi.org/10.1002/cphc.201700736.
[268] J.H. Montoya, A.A. Peterson, J.K. Nørskov, Insights into C-C Coupling in CO_2 Electroreduction on Copper Electrodes, ChemCatChem 5 (2013) 737–742, https://doi.org/10.1002/cctc.201200564.
[269] F. Calle-Vallejo, M.T.M. Koper, Theoretical considerations on the electroreduction of CO to C_2 Species on Cu(100) electrodes, Angew. Chem. - Int. Ed. 52 (2013) 7282–7285, https://doi.org/10.1002/anie.201301470.
[270] J. Li, P. Pršlja, T. Shinagawa, A.J. Martín Fernández, F. Krumeich, K. Artyushkova, P. Atanassov, A. Zitolo, Y. Zhou, R. García-Muelas, N. López, J. Pérez-Ramírez, F. Jaouen, Volcano Trend in Electrocatalytic CO_2 Reduction Activity over Atomically Dispersed Metal Sites on Nitrogen-Doped Carbon, ACS Catal. 9 (2019) 10426–10439, https://doi.org/10.1021/acscatal.9b02594.
[271] W. Ju, A. Bagger, G.P. Hao, A.S. Varela, I. Sinev, V. Bon, B. Roldan Cuenya, S. Kaskel, J. Rossmeisl, P. Strasser, Understanding activity and selectivity of metal-nitrogen-doped carbon catalysts for electrochemical reduction of CO_2, Nat. Commun. 8 (2017) 944, https://doi.org/10.1038/s41467-017-01035-z.
[272] G. Xing, L. Cheng, K. Li, Y. Gao, H. Tang, Y. Wang, Z. Wu, Efficient electroreduction of CO_2 by single-atom catalysts two-dimensional metal hexahydroxybenzene frameworks: A theoretical study, Appl. Surf. Sci. 550 (2021), 149389, https://doi.org/10.1016/j.apsusc.2021.149389.
[273] Z. Meng, J. Luo, W. Li, K.A. Mirica, Hierarchical Tuning of the Performance of Electrochemical Carbon Dioxide Reduction Using Conductive Two-Dimensional Metallophthalocyanine Based Metal-Organic Frameworks, J. Am. Chem. Soc. 142 (2020) 21656–21669, https://doi.org/10.1021/jacs.0c07041.
[274] Y. Tian, Y. Wang, L. Yan, J. Zhao, Z. Su, Electrochemical reduction of carbon dioxide on the two–dimensional M3(Hexaiminotriphenylene)2 sheet: A computational study, Appl. Surf. Sci. 467–468 (2019) 98–103, https://doi.org/10.1016/j.apsusc.2018.10.131.
[275] T. Bligaard, J.K. Nørskov, Ligand effects in heterogeneous catalysis and electrochemistry, Electrochim. Acta 52 (2007) 5512–5516, https://doi.org/10.1016/j.electacta.2007.02.041.
[276] X. Mao, C. Tang, T. He, D. Wijethunge, C. Yan, Z. Zhu, A. Du, Computational screening of MN4 (M = Ti–Cu) based metal organic frameworks for CO_2 reduction using the d-band centre as a descriptor, Nanoscale 12 (2020) 6188–6194, https://doi.org/10.1039/C9NR09529B.
[277] H. Zhong, M. Ghorbani-Asl, K.H. Ly, J. Zhang, J. Ge, M. Wang, Z. Liao, D. Makarov, E. Zschech, E. Brunner, I.M. Weidinger, J. Zhang, A. V. Krasheninnikov, S. Kaskel, R. Dong, X. Feng, Synergistic electroreduction of carbon dioxide to carbon monoxide on bimetallic layered conjugated metal-organic frameworks, Nat. Commun. 11 (2020) 1409, https://doi.org/10.1038/s41467-020-15141-y.
[278] W. Ren, X. Tan, W. Yang, C. Jia, S. Xu, K. Wang, S.C. Smith, C. Zhao, Isolated Diatomic Ni-Fe Metal–Nitrogen Sites for Synergistic Electroreduction of CO_2, Angew. Chem. - Int. Ed. 58 (2019) 6972–6976, https://doi.org/10.1002/anie.201901575.
[279] H. Yuan, Z. Li, Intrinsic descriptors for coordination environment and synergistic effects of metal and environment in single-atom-catalyzed carbon dioxide electroreduction, J. Phys. Chem. C. 125 (2021) 18180–18186, https://doi.org/10.1021/acs.jpcc.1c04637.
[280] Z. Xue, Y. Li, Y. Zhang, W. Geng, B. Jia, J. Tang, S. Bao, H.P. Wang, Y. Fan, Z. Wen Wei, Z. Zhang, Z. Ke, G. Li, C.Y. Su, Modulating electronic structure of metal-organic framework for efficient electrocatalytic oxygen evolution, Adv. Energy Mater. 8 (2018), https://doi.org/10.1002/aenm.201801564.
[281] S. Dou, J. Song, S. Xi, Y. Du, J. Wang, Z.F. Huang, Z.J. Xu, X. Wang, Boosting Electrochemical CO_2 Reduction on Metal–Organic Frameworks via Ligand Doping, Angew. Chem. - Int. Ed. 58 (2019) 4041–4045, https://doi.org/10.1002/anie.201814711.
[282] X. Jiang, H. Li, J. Xiao, D. Gao, R. Si, F. Yang, Y. Li, G. Wang, X. Bao, Carbon dioxide electroreduction over imidazolate ligands coordinated with Zn(II) center in ZIFs, Nano Energy 52 (2018) 345–350, https://doi.org/10.1016/j.nanoen.2018.07.047.
[283] Z. Xin, J. Liu, X. Wang, K. Shen, Z. Yuan, Y. Chen, Y.-Q. Lan, Implanting Polypyrrole in Metal-Porphyrin MOFs: Enhanced Electrocatalytic Performance for CO_2RR, ACS Appl. Mater. Interfaces 13 (2021) 54959–54966, https://doi.org/10.1021/acsami.1c15187.
[284] T. Zhan, Y. Zou, Y. Yang, X. Ma, Z. Zhang, S. Xiang, Two-dimensional Metal-organic Frameworks for Electrochemical CO_2 Reduction Reaction, ChemCatChem 14 (2022), e202101453, https://doi.org/10.1002/cctc.202101453.
[285] S.M. Cao, H.B. Chen, B.X. Dong, Q.H. Zheng, Y.X. Ding, M.J. Liu, S.L. Qian, Y. L. Teng, Z.W. Li, W.L. Liu, Nitrogen-rich metal-organic framework mediated Cu–N–C composite catalysts for the electrochemical reduction of CO_2, J. Energy Chem. 54 (2021) 555–563, https://doi.org/10.1016/j.jechem.2020.06.038.
[286] R. Wang, X. Sun, S. Ould-Chikh, D. Osadchii, F. Bai, F. Kapteijn, J. Gascon, Metal-organic-framework-mediated nitrogen-doped carbon for CO_2 electrochemical reduction, ACS Appl. Mater. Interfaces 10 (2018) 14751–14758, https://doi.org/10.1021/acsami.8b02226.
[287] Y. Guo, H. Yang, X. Zhou, K. Liu, C. Zhang, Z. Zhou, C. Wang, W. Lin, Electrocatalytic reduction of CO_2 to CO with 100% faradaic efficiency by using pyrolyzed zeolitic imidazolate frameworks supported on carbon nanotube networks, J. Mater. Chem. A 5 (2017) 24867–24873, https://doi.org/10.1039/c7ta08431e.
[288] Q. Wu, J. Gao, J. Feng, Q. Liu, Y. Zhou, S. Zhang, M. Nie, Y. Liu, J. Zhao, F. Liu, J. Zhong, Z. Kang, A CO_2 adsorption dominated carbon defect-based electrocatalyst for efficient carbon dioxide reduction, J. Mater. Chem. A 8 (2020) 1205–1211, https://doi.org/10.1039/C9TA11473D.
[289] S. Guo, S. Zhao, X. Wu, H. Li, Y. Zhou, C. Zhu, N. Yang, X. Jiang, J. Gao, L. Bai, Y. Liu, Y. Lifshitz, S.-T. Lee, Z. Kang, A Co_3O_4-CDots-C_3N_4 three component electrocatalyst design concept for efficient and tunable CO_2 reduction to syngas, Nat. Commun. 8 (2017) 1828, https://doi.org/10.1038/s41467-017-01893-7.
[290] Y. Dong, Q. Zhang, Z. Tian, B. Li, W. Yan, S. Wang, K. Jiang, J. Su, C.W. Oloman, E.L. Gyenge, R. Ge, Z. Lu, X. Ji, L. Chen, Ammonia Thermal Treatment toward Topological Defects in Porous Carbon for Enhanced Carbon Dioxide Electroreduction, Adv. Mater. 32 (2020) 2001300, https://doi.org/10.1002/adma.202001300.
[291] J.D. Yi, D.H. Si, R. Xie, Q. Yin, M. Di Zhang, Q. Wu, G.L. Chai, Y.B. Huang, R. Cao, Conductive Two-Dimensional Phthalocyanine-based Metal–Organic Framework Nanosheets for Efficient Electroreduction of CO_2, Angew. Chem. - Int. Ed. 60 (2021) 17108–17114, https://doi.org/10.1002/anie.202104564.
[292] J. Liu, D. Yang, Y. Zhou, G. Zhang, G. Xing, Y. Liu, Y. Ma, O. Terasaki, S. Yang, L. Chen, Tricycloquinazoline-Based 2D Conductive Metal–Organic Frameworks as Promising Electrocatalysts for CO_2 Reduction, Angew. Chem. - Int. Ed. 60 (2021) 14473–14479, https://doi.org/10.1002/anie.202103398.
[293] X. Li, L. Li, X. Ren, D. Wu, Y. Zhang, H. Ma, X. Sun, B. Du, Q. Wei, B. Li, Enabling Electrocatalytic N_2 Reduction to NH_3 by Y_2O_3 Nanosheet under Ambient Conditions, Ind. Eng. Chem. Res. 57 (2018) 16622–16627, https://doi.org/10.1021/acs.iecr.8b04045.
[294] C. Zhao, X. Dai, T. Yao, W. Chen, X. Wang, J. Wang, J. Yang, S. Wei, Y. Wu, Y. Li, Ionic Exchange of Metal-Organic Frameworks to Access Single Nickel Sites for Efficient Electroreduction of CO_2, J. Am. Chem. Soc. 139 (2017) 8078–8081, https://doi.org/10.1021/jacs.7b02736.
[295] Z. Ma, D. Wu, X. Han, H. Wang, L. Zhang, Z. Gao, F. Xu, K. Jiang, Ultrasonic assisted synthesis of Zn-Ni bi-metal MOFs for interconnected Ni-N-C materials with enhanced electrochemical reduction of CO_2, J. CO_2 Util. 32 (2019) 251–258, https://doi.org/10.1016/j.jcou.2019.04.006.
[296] F. Pan, H. Zhang, K. Liu, D. Cullen, K. More, M. Wang, Z. Feng, G. Wang, G. Wu, Y. Li, Unveiling Active Sites of CO_2 Reduction on Nitrogen-Coordinated and Atomically Dispersed Iron and Cobalt Catalysts, ACS Catal. 8 (2018) 3116–3122, https://doi.org/10.1021/acscatal.8b00398.
[297] X. Zhang, G. Li, D. Wu, X. Li, N. Hu, J. Chen, G. Chen, Y. Wu, Recent progress in the design fabrication of metal-organic frameworks-based nanozymes and their applications to sensing and cancer therapy, Biosens. Bioelectron. 137 (2019) 178–198, https://doi.org/10.1016/j.bios.2019.04.061.
[298] Q. Wang, D. Astruc, State of the Art and Prospects in Metal-Organic Framework (MOF)-Based and MOF-Derived Nanocatalysis, Chem. Rev. 120 (2020) 1438–1511, https://doi.org/10.1021/acs.chemrev.9b00223.
[299] H. Huang, K. Shen, F. Chen, Y. Li, Metal-organic frameworks as a good platform for the fabrication of single-atom catalysts, ACS Catal. 10 (2020) 6579–6586, https://doi.org/10.1021/acscatal.0c01459.
[300] K. Shen, X. Chen, J. Chen, Y. Li, Development of MOF-Derived Carbon-Based Nanomaterials for Efficient Catalysis, ACS Catal. 6 (2016) 5887–5903, https://doi.org/10.1021/acscatal.6b01222.
[301] F.N. Al-Rowaili, A. Jamal, M.S. Ba Shammakh, A. Rana, A Review on Recent Advances for Electrochemical Reduction of Carbon Dioxide to Methanol Using Metal-Organic Framework (MOF) and Non-MOF Catalysts: Challenges and Future Prospects, ACS Sustain. Chem. Eng. 6 (2018) 15895–15914, https://doi.org/10.1021/acssuschemeng.8b03843.
[302] D. Zhou, X. Li, H. Shang, F. Qin, W. Chen, Atomic regulation of metal-organic framework derived carbon-based single-atom catalysts for the electrochemical

CO2reduction reaction, J. Mater. Chem. A. 9 (2021) 23382–23418, https://doi.org/10.1039/d1ta06915b.
[303] Q. Wu, J. Liang, J.D. Yi, D.L. Meng, P.C. Shi, Y.B. Huang, R. Cao, Unraveling the relationship between the morphologies of metal-organic frameworks and the properties of their derived carbon materials, Dalt. Trans. 48 (2019) 7211–7217, https://doi.org/10.1039/c8dt04941f.
[304] H.X. Zhang, Q.L. Hong, J. Li, F. Wang, X. Huang, S. Chen, W. Tu, D. Yu, R. Xu, T. Zhou, J. Zhang, Isolated Square-Planar Copper Center in Boron Imidazolate Nanocages for Photocatalytic Reduction of CO_2 to CO, Angew. Chem. - Int. Ed. 58 (2019) 11752–11756, https://doi.org/10.1002/anie.201905869.
[305] X. Li, A.E. Surkus, J. Rabeah, M. Anwar, S. Dastigir, H. Junge, A. Brückner, M. Beller, Cobalt Single-Atom Catalysts with High Stability for Selective Dehydrogenation of Formic Acid, Angew. Chem. - Int. Ed. 59 (2020) 15849–15854, https://doi.org/10.1002/anie.202004125.
[306] N. Li, J. Liu, J.J. Liu, L.Z. Dong, Z.F. Xin, Y.L. Teng, Y.Q. Lan, Adenine components in biomimetic metal–organic frameworks for efficient CO_2 photoconversion, Angew. Chem. - Int. Ed. 58 (2019) 5226–5231, https://doi.org/10.1002/anie.201814729.
[307] J. Yuan, L. Xiao, G.Y. Huang, J.M. Yang, H. Bin Zhu, Fabrication of Mn,N-Codoped Carbon Electrocatalysts from a Cationic Cd(II)-based MOF Involving Anion-exchange with MnO4− Anions, ChemNanoMat 6 (2020) 1776–1781, https://doi.org/10.1002/cnma.202000397.
[308] Y. He, C. Li, X. Chen, H. Rao, Z. Shi, S. Feng, Critical aspects of metal–organic framework-based materials for solar-driven CO_2 Reduction into Valuable Fuels, Glob. Challenges 5 (2021) 2000082, https://doi.org/10.1002/gch2.202000082.
[309] L. Gong, D. Zhang, C.Y. Lin, Y. Zhu, Y. Shen, J. Zhang, X. Han, L. Zhang, Z. Xia, Catalytic Mechanisms and Design Principles for Single-Atom Catalysts in Highly Efficient CO_2 Conversion, Adv. Energy Mater. 9 (2019) 1902625, https://doi.org/10.1002/aenm.201902625.
[310] C. Chen, X. Sun, X. Yan, Y. Wu, H. Liu, Q. Zhu, B.B.A. Bediako, B. Han, Boosting CO_2 Electroreduction on N,P-Co-doped Carbon Aerogels, Angew. Chem. - Int. Ed. 59 (2020) 11123–11129, https://doi.org/10.1002/anie.202004226.
[311] M. Duguet, A. Lemarchand, Y. Benseghir, P. Mialane, M. Gomez-Mingot, C. Roch-Marchal, M. Haouas, M. Fontecave, C. Mellot-Draznieks, C. Sassoye, A. Dolbecq, Structure-directing role of immobilized polyoxometalates in the synthesis of porphyrinic Zr-based metal-organic frameworks, Chem. Commun. 56 (2020) 10143–10146, https://doi.org/10.1039/d0cc04283h.
[312] X. Cheng, J. Zhang, X. Tan, L. Zheng, D. Tan, L. Liu, G. Chen, Q. Wan, B. Zhang, F. Zhang, Z. Su, B. Han, J. Zhang, Improved photocatalytic performance of metal-organic frameworks for CO_2 conversion by ligand modification, Chem. Commun. 56 (2020) 7637–7640, https://doi.org/10.1039/d0cc02707c.
[313] F. Dvořák, M.F. Camellone, A. Tovt, N.D. Tran, F.R. Negreiros, M. Vorokhta, T. Skála, I. Matolínová, J. Mysliveček, V. Matolín, S. Fabris, Creating single-atom Pt-ceria catalysts by surface step decoration, Nat. Commun. 7 (2016) 10801, https://doi.org/10.1038/ncomms10801.
[314] B. Qiao, A. Wang, X. Yang, L.F. Allard, Z. Jiang, Y. Cui, J. Liu, J. Li, T. Zhang, Single-atom catalysis of CO oxidation using Pt1/FeOx, Nat. Chem. 3 (2011) 634–641, https://doi.org/10.1038/nchem.1095.
[315] R. Hinogami, S. Yotsuhashi, M. Deguchi, Y. Zenitani, H. Hashiba, Y. Yamada, Electrochemical reduction of carbon dioxide using a copper rubeanate metal organic framework, ECS Electrochem. Lett. 1 (2012) 17–20, https://doi.org/10.1149/2.001204eel.
[316] D.H. Nam, O.S. Bushuyev, J. Li, P. De Luna, A. Seifitokaldani, C.T. Dinh, F. P. García De Arquer, Y. Wang, Z. Liang, A.H. Proppe, C.S. Tan, P. Todorović, O. Shekhah, C.M. Gabardo, J.W. Jo, J. Choi, M.J. Choi, S.W. Baek, J. Kim, D. Sinton, S.O. Kelley, M. Eddaoudi, E.H. Sargent, Metal-Organic Frameworks Mediate Cu Coordination for Selective CO_2 Electroreduction, J. Am. Chem. Soc. 140 (2018) 11378–11386, https://doi.org/10.1021/jacs.8b06407.
[317] E. Zhang, T. Wang, K. Yu, J. Liu, W. Chen, A. Li, H. Rong, R. Lin, S. Ji, X. Zheng, Y. Wang, L. Zheng, C. Chen, D. Wang, J. Zhang, Y. Li, Bismuth single atoms resulting from transformation of metal-organic frameworks and their use as electrocatalysts for CO_2 reduction, J. Am. Chem. Soc. 141 (2019) 16569–16573, https://doi.org/10.1021/jacs.9b08259.
[318] H. Shang, T. Wang, J. Pei, Z. Jiang, D. Zhou, Y. Wang, H. Li, J. Dong, Z. Zhuang, W. Chen, D. Wang, J. Zhang, Y. Li, Design of a Single-Atom Indium$\delta+$–N_4 Interface for Efficient Electroreduction of CO_2 to Formate, Angew. Chem. - Int. Ed. 59 (2020) 22465–22469, https://doi.org/10.1002/anie.202010903.
[319] K. Zhao, X. Nie, H. Wang, S. Chen, X. Quan, H. Yu, W. Choi, G. Zhang, B. Kim, J. G. Chen, Selective electroreduction of CO_2 to acetone by single copper atoms anchored on N-doped porous carbon, Nat. Commun. 11 (2020) 2455, https://doi.org/10.1038/s41467-020-16381-8.
[320] J. Albo, D. Vallejo, G. Beobide, O. Castillo, P. Castaño, A. Irabien, Copper-based metal–organic porous materials for CO_2 electrocatalytic reduction to alcohols, ChemSusChem 10 (2017) 1100–1109, https://doi.org/10.1002/cssc.201600693.
[321] J.C. Cardoso, S. Stulp, J.F. de Brito, J.B.S. Flor, R.C.G. Frem, M.V.B. Zanoni, MOFs based on ZIF-8 deposited on TiO_2 nanotubes increase the surface adsorption of CO_2 and its photoelectrocatalytic reduction to alcohols in aqueous media, Appl. Catal. B Environ. 225 (2018) 563–573, https://doi.org/10.1016/j.apcatb.2017.12.013.
[322] L. Lin, H. Li, C. Yan, H. Li, R. Si, M. Li, J. Xiao, G. Wang, X. Bao, Synergistic Catalysis over Iron-Nitrogen Sites Anchored with Cobalt Phthalocyanine for Efficient CO_2 Electroreduction, Adv. Mater. 31 (2019) 1–7, https://doi.org/10.1002/adma.201903470.
[323] C. Gao, J. Low, R. Long, T. Kong, J. Zhu, Y. Xiong, Heterogeneous Single-Atom Photocatalysts: Fundamentals and Applications, Chem. Rev. 120 (2020) 12175–12216, https://doi.org/10.1021/acs.chemrev.9b00840.
[324] A. Wang, J. Li, T. Zhang, Heterogeneous single-atom catalysis, Nat. Rev. Chem. 2 (2018) 65–81, https://doi.org/10.1038/s41570-018-0010-1.
[325] N. Cheng, L. Zhang, K. Doyle-Davis, X. Sun, Single-Atom Catalysts: From Design to Application, Springer, Singapore, 2019, https://doi.org/10.1007/s41918-019-00050-6.
[326] Y. Ye, F. Cai, H. Li, H. Wu, G. Wang, Y. Li, S. Miao, S. Xie, R. Si, J. Wang, X. Bao, Surface functionalization of ZIF-8 with ammonium ferric citrate toward high exposure of Fe-N active sites for efficient oxygen and carbon dioxide electroreduction, Nano Energy 38 (2017) 281–289, https://doi.org/10.1016/j.nanoen.2017.05.042.
[327] C. Yan, Y. Ye, L. Lin, H. Wu, Q. Jiang, G. Wang, X. Bao, Improving CO_2 electroreduction over ZIF-derived carbon doped with Fe-N sites by an additional ammonia treatment, Catal. Today 330 (2019) 252–258, https://doi.org/10.1016/j.cattod.2018.03.062.
[328] Y. Wang, M. Wang, Z. Zhang, Q. Wang, Z. Jiang, M. Lucero, X. Zhang, X. Li, M. Gu, Z. Feng, Y. Liang, Phthalocyanine precursors to construct atomically dispersed iron electrocatalysts, ACS Catal. 9 (2019) 6252–6261, https://doi.org/10.1021/acscatal.9b01617.
[329] Z. Geng, Y. Cao, W. Chen, X. Kong, Y. Liu, T. Yao, Y. Lin, Regulating the coordination environment of Co single atoms for achieving efficient electrocatalytic activity in CO_2 reduction, Appl. Catal. B Environ. 240 (2019) 234–240, https://doi.org/10.1016/j.apcatb.2018.08.075.
[330] X. Song, H. Zhang, Y. Yang, B. Zhang, M. Zuo, X. Cao, J. Sun, C. Lin, X. Li, Z. Jiang, Bifunctional Nitrogen and Cobalt Codoped Hollow Carbon for Electrochemical Syngas Production, Adv. Sci. 5 (2018) 1800177, https://doi.org/10.1002/advs.201800177.
[331] H. Bin Yang, S.F. Hung, S. Liu, K. Yuan, S. Miao, L. Zhang, X. Huang, H.Y. Wang, W. Cai, R. Chen, J. Gao, X. Yang, W. Chen, Y. Huang, H.M. Chen, C.M. Li, T. Zhang, B. Liu, Atomically dispersed Ni(i) as the active site for electrochemical CO_2 reduction, Nat. Energy 3 (2018) 140–147, https://doi.org/10.1038/s41560-017-0078-8.
[332] H. Cheng, X. Wu, X. Li, X. Nie, S. Fan, M. Feng, Z. Fan, M. Tan, Y. Chen, G. He, Construction of atomically dispersed Cu-N4 sites via engineered coordination environment for high-efficient CO_2 electroreduction, Chem. Eng. J. 407 (2021), 126842, https://doi.org/10.1016/j.cej.2020.126842.
[333] A. Guan, Z. Chen, Y. Quan, C. Peng, Z. Wang, T.K. Sham, C. Yang, Y. Ji, L. Qian, X. Xu, G. Zheng, Boosting CO_2 Electroreduction to CH4 via Tuning Neighboring Single-Copper Sites, ACS Energy Lett. 5 (2020) 1044–1053, https://doi.org/10.1021/acsenergylett.0c00018.
[334] H. Yang, Y. Wu, G. Li, Q. Lin, Q. Hu, Q. Zhang, J. Liu, C. He, Scalable Production of Efficient Single-Atom Copper Decorated Carbon Membranes for CO_2 Electroreduction to Methanol, J. Am. Chem. Soc. 141 (2019) 12717–12723, https://doi.org/10.1021/jacs.9b04907.
[335] C. Yan, H. Li, Y. Ye, H. Wu, F. Cai, R. Si, J. Xiao, S. Miao, S. Xie, F. Yang, Y. Li, G. Wang, X. Bao, Coordinatively unsaturated nickel-nitrogen sites towards selective and high-rate CO_2 electroreduction, Energy Environ. Sci. 11 (2018) 1204–1210, https://doi.org/10.1039/c8ee00133b.
[336] J. Gu, C.S. Hsu, L. Bai, H.M. Chen, X. Hu, Atomically dispersed Fe3+ sites catalyze efficient CO_2 electroreduction to CO, Science 80 (364) (2019) 1091–1094, https://doi.org/10.1126/science.aaw7515.
[337] N. Mohd Adli, W. Shan, S. Hwang, W. Samarakoon, S. Karakalos, Y. Li, D. A. Cullen, D. Su, Z. Feng, G. Wang, G. Wu, Engineering atomically dispersed fen4 active sites for CO_2 electroreduction, Angew. Chem. - Int. Ed. 60 (2021) 1022–1032, https://doi.org/10.1002/anie.202012329.
[338] X. Li, Y. Zeng, C.W. Tung, Y.R. Lu, S. Baskaran, S.F. Hung, S. Wang, C.Q. Xu, J. Wang, T.S. Chan, H.M. Chen, J. Jiang, Q. Yu, Y. Huang, J. Li, T. Zhang, B. Liu, Unveiling the in Situ Generation of a Monovalent Fe(I) Site in the Single-Fe-Atom Catalyst for Electrochemical CO_2 Reduction, ACS Catal. 11 (2021) 7292–7301, https://doi.org/10.1021/acscatal.1c01621.
[339] P. Lu, X. Tan, H. Zhao, Q. Xiang, K. Liu, X. Zhao, X. Yin, X. Li, X. Hai, S. Xi, A.T. S. Wee, S.J. Pennycook, X. Yu, M. Yuan, J. Wu, G. Zhang, S.C. Smith, Z. Yin, Atomically Dispersed Indium Sites for Selective CO_2 Electroreduction to Formic Acid, ACS Nano 15 (2021) 5671–5678, https://doi.org/10.1021/acsnano.1c00858.
[340] H.Y. Tan, S.C. Lin, J. Wang, C.J. Chang, S.C. Haw, K.H. Lin, L.D. Tsai, H.C. Chen, H.M. Chen, MOF-Templated Sulfurization of Atomically Dispersed Manganese Catalysts Facilitating Electroreduction of CO_2 to CO, ACS Appl. Mater. Interfaces 13 (2021) 52134–52143, https://doi.org/10.1021/acsami.1c10059.
[341] Y. Zhou, L. Zheng, D. Yang, H. Yang, Q. Lu, Q. Zhang, L. Gu, X. Wang, Enhancing CO_2 Electrocatalysis on 2D Porphyrin-Based Metal–Organic Framework Nanosheets Coupled with Visible-Light, Small Methods 5 (2021), https://doi.org/10.1002/smtd.202000991.
[342] P. Lu, Y. Yang, J. Yao, M. Wang, S. Dipazir, M. Yuan, J. Zhang, X. Wang, Z. Xie, G. Zhang, Facile synthesis of single-nickel-atomic dispersed N-doped carbon framework for efficient electrochemical CO_2 reduction, Appl. Catal. B Environ. 241 (2019) 113–119, https://doi.org/10.1016/j.apcatb.2018.09.025.
[343] S. Yang, J. Zhang, L. Peng, M. Asgari, D. Stoian, I. Kochetygov, W. Luo, E. Oveisi, O. Trukhina, A.H. Clark, D.T. Sun, W.L. Queen, A metal-organic framework/polymer derived catalyst containing single-atom nickel species for electrocatalysis, Chem. Sci. 11 (2020) 10991–10997, https://doi.org/10.1039/d0sc04512h.
[344] Y. Hou, Y.L. Liang, P.C. Shi, Y.B. Huang, R. Cao, Atomically dispersed Ni species on N-doped carbon nanotubes for electroreduction of CO_2 with nearly 100% CO selectivity, Appl. Catal. B Environ. 271 (2020), 118929, https://doi.org/10.1016/j.apcatb.2020.118929.

[345] L. Jiao, W. Yang, G. Wan, R. Zhang, X. Zheng, H. Zhou, S.H. Yu, H.L. Jiang, Single-Atom Electrocatalysts from Multivariate Metal–Organic Frameworks for Highly Selective Reduction of CO_2 at Low Pressures, Angew. Chem. - Int. Ed. 59 (2020) 20589–20595, https://doi.org/10.1002/anie.202008787.
[346] Z. Chen, X. Zhang, W. Liu, M. Jiao, K. Mou, X. Zhang, L. Liu, Amination strategy to boost the CO2electroreduction current density of M-N/C single-atom catalysts to the industrial application level, Energy Environ. Sci. 14 (2021) 2349–2356, https://doi.org/10.1039/d0ee04052e.
[347] X. Wang, Y. Wang, X. Sang, W. Zheng, S. Zhang, L. Shuai, B. Yang, Z. Li, J. Chen, L. Lei, N.M. Adli, M.K.H. Leung, M. Qiu, G. Wu, Y. Hou, Dynamic Activation of Adsorbed Intermediates via Axial Traction for the Promoted Electrochemical CO_2 Reduction, Angew. Chem. - Int. Ed. 60 (2021) 4192–4198, https://doi.org/10.1002/anie.202013427.
[348] H. Wang, G. Liu, C. Chen, W. Tu, Y. Lu, S. Wu, D. O'Hare, R. Xu, Single-Ni sites embedded in multilayer nitrogen-doped graphene derived from amino-functionalized MOF for highly selective CO electroreduction, ACS Sustain. Chem. Eng. 9 (2021) 3792–3801, https://doi.org/10.1021/acssuschemeng.0c08749.
[349] Y.N. Gong, L. Jiao, Y. Qian, C.Y. Pan, L. Zheng, X. Cai, B. Liu, S.H. Yu, H.L. Jiang, Regulating the Coordination Environment of MOF-Templated Single-Atom Nickel Electrocatalysts for Boosting CO_2 Reduction, Angew. Chem. - Int. Ed. 59 (2020) 2705–2709, https://doi.org/10.1002/anie.201914977.
[350] J. Yang, Z. Qiu, C. Zhao, W. Wei, W. Chen, Z. Li, Y. Qu, J. Dong, J. Luo, Z. Li, Y. Wu, In Situ Thermal Atomization To Convert Supported Nickel Nanoparticles into Surface-Bound Nickel Single-Atom Catalysts, Angew. Chem. - Int. Ed. 57 (2018) 14095–14100, https://doi.org/10.1002/anie.201808049.
[351] S.Y. Zhang, Y.Y. Yang, Y.Q. Zheng, H.L. Zhu, Ag-doped Co_3O_4 catalyst derived from heterometallic MOF for syngas production by electrocatalytic reduction of CO_2 in water, J. Solid State Chem. 263 (2018) 44–51, https://doi.org/10.1016/j.jssc.2018.04.007.
[352] J. Liu, L. Peng, Y. Zhou, L. Lv, J. Fu, J. Lin, D. Guay, J. Qiao, Metal-Organic-Frameworks-Derived Cu/Cu_2O Catalyst with Ultrahigh Current Density for Continuous-Flow CO_2 Electroreduction, ACS Sustain. Chem. Eng. 7 (2019) 15739–15746, https://doi.org/10.1021/acssuschemeng.9b03892.
[353] C. Hu, S. Bai, L. Gao, S. Liang, J. Yang, S.D. Cheng, S.B. Mi, J. Qiu, Porosity-Induced High Selectivity for CO_2 Electroreduction to CO on Fe-Doped ZIF-Derived Carbon Catalysts, ACS Catal. 9 (2019) 11579–11588, https://doi.org/10.1021/acscatal.9b03175.
[354] J.W. Maina, C. Pozo-Gonzalo, J.A. Schütz, J. Wang, L.F. Dumée, Tuning CO_2 conversion product selectivity of metal organic frameworks derived hybrid carbon photoelectrocatalytic reactors, Carbon N. Y 148 (2019) 80–90, https://doi.org/10.1016/j.carbon.2019.03.043.
[355] X.M. Hu, H.H. Hval, E.T. Bjerglund, K.J. Dalgaard, M.R. Madsen, M.M. Pohl, E. Welter, P. Lamagni, K.B. Buhl, M. Bremholm, M. Beller, S.U. Pedersen, T. Skrydstrup, K. Daasbjerg, Selective CO_2 Reduction to CO in Water using Earth-Abundant Metal and Nitrogen-Doped Carbon Electrocatalysts, ACS Catal. 8 (2018) 6255–6264, https://doi.org/10.1021/acscatal.8b01022.
[356] V. Tripkovic, M. Vanin, M. Karamad, M.E. Björketun, K.W. Jacobsen, K. S. Thygesen, J. Rossmeisl, Electrochemical CO_2 and CO reduction on metal-functionalized porphyrin-like graphene, J. Phys. Chem. C. 117 (2013) 9187–9195, https://doi.org/10.1021/jp306172k.
[357] A.S. Varela, N. Ranjbar Sahraie, J. Steinberg, W. Ju, H.S. Oh, P. Strasser, Metal-doped nitrogenated carbon as an efficient catalyst for direct CO_2 electroreduction to CO and hydrocarbons, Angew. Chem. - Int. Ed. 54 (2015) 10758–10762, https://doi.org/10.1002/anie.201502099.
[358] Y. Hou, X.J. Hu, H.Y. Tong, Y.B. Huang, R. Cao, Unraveling the relationship of the pore structures between the metal-organic frameworks and their derived carbon materials, Inorg. Chem. Commun. 114 (2020), https://doi.org/10.1016/j.inoche.2020.107825.
[359] W. Ju, A. Bagger, X. Wang, Y. Tsai, F. Luo, T. Möller, H. Wang, J. Rossmeisl, A. S. Varela, P. Strasser, Unraveling mechanistic reaction pathways of the electrochemical CO_2 reduction on Fe-N-C single-site catalysts, ACS Energy Lett. 4 (2019) 1663–1671, https://doi.org/10.1021/acsenergylett.9b01049.
[360] A. Roy, D. Hursán, K. Artyushkova, P. Atanassov, C. Janáky, A. Serov, Nanostructured metal-N-C electrocatalysts for CO_2 reduction and hydrogen evolution reactions, Appl. Catal. B Environ. 232 (2018) 512–520, https://doi.org/10.1016/j.apcatb.2018.03.093.
[361] G.R. Bhadu, B. Parmar, P. Patel, A. Paul, J.C. Chaudhari, D.N. Srivastava, E. Suresh, Co@N-doped carbon nanomaterial derived by simple pyrolysis of mixed-ligand MOF as an active and stable oxygen evolution electrocatalyst, Appl. Surf. Sci. 529 (2020), https://doi.org/10.1016/j.apsusc.2020.147081.
[362] Y. Chen, L. Zou, H. Liu, C. Chen, Q. Wang, M. Gu, B. Yang, Z. Zou, J. Fang, H. Yang, Fe and N Co-Doped Porous Carbon Nanospheres with High Density of Active Sites for Efficient CO_2 Electroreduction, J. Phys. Chem. C. 123 (2019) 16651–16659, https://doi.org/10.1021/acs.jpcc.9b02195.
[363] C. Kim, Y.K. Choe, D.H. Won, U. Lee, H.S. Oh, D.K. Lee, C.H. Choi, S. Yoon, W. Kim, Y.J. Hwang, B.K. Min, Turning harmful deposition of metal impurities into activation of nitrogen-doped carbon catalyst toward durable electrochemical CO_2 reduction, ACS Energy Lett. 4 (2019) 2343–2350, https://doi.org/10.1021/acsenergylett.9b01581.
[364] L. Takele Menisa, P. Cheng, C. Long, X. Qiu, Y. Zheng, J. Han, Y. Zhang, Y. Gao, Z. Tang, Insight into atomically dispersed porous M-N-C single-site catalysts for electrochemical CO_2 reduction, Nanoscale 12 (2020) 16617–16626, https://doi.org/10.1039/d0nr03044a.
[365] F. Pan, W. Deng, C. Justiniano, Y. Li, Identification of champion transition metals centers in metal and nitrogen-codoped carbon catalysts for CO_2 reduction, Appl. Catal. B Environ. 226 (2018) 463–472, https://doi.org/10.1016/j.apcatb.2018.01.001.
[366] L. Chen, Z. Guo, X.G. Wei, C. Gallenkamp, J. Bonin, E. Anxolabéhère-Mallart, K. C. Lau, T.C. Lau, M. Robert, Molecular catalysis of the electrochemical and photochemical reduction of CO_2 with earth-abundant metal complexes. Selective production of CO vs HCOOH by switching of the metal center, J. Am. Chem. Soc. 137 (2015) 10918–10921, https://doi.org/10.1021/jacs.5b06535.
[367] T.N. Huan, N. Ranjbar, G. Rousse, M. Sougrati, A. Zitolo, V. Mougel, F. Jaouen, M. Fontecave, Electrochemical Reduction of CO_2 Catalyzed by Fe-N-C Materials: A Structure-Selectivity Study, ACS Catal. 7 (2017) 1520–1525, https://doi.org/10.1021/acscatal.6b03353.
[368] I. Masood ul Hasan, L. Peng, J. Mao, R. He, Y. Wang, J. Fu, N. Xu, J. Qiao, Carbon-based metal-free catalysts for electrochemical CO_2 reduction: Activity, selectivity, and stability, Carbon Energy 3 (2021) 24–49, https://doi.org/10.1002/cey2.87.
[369] Z. Qin, X. Wang, L. Dong, T. Su, B. Li, Y. Zhou, Y. Jiang, X. Luo, H. Ji, CO_2 methanation on Co/TiO_2 catalyst: Effects of Y on the support, Chem. Eng. Sci. 210 (2019), https://doi.org/10.1016/j.ces.2019.115245.
[370] A.S. Varela, M. Kroschel, T. Reier, P. Strasser, Controlling the selectivity of CO_2 electroreduction on copper: The effect of the electrolyte concentration and the importance of the local pH, Catal. Today 260 (2016) 8–13, https://doi.org/10.1016/j.cattod.2015.06.009.
[371] A.S. Varela, M. Kroschel, N.D. Leonard, W. Ju, J. Steinberg, A. Bagger, J. Rossmeisl, P. Strasser, PH Effects on the Selectivity of the Electrocatalytic CO_2 Reduction on Graphene-Embedded Fe-N-C Motifs: Bridging Concepts between Molecular Homogeneous and Solid-State Heterogeneous Catalysis, ACS Energy Lett. 3 (2018) 812–817, https://doi.org/10.1021/acsenergylett.8b00273.
[372] E. González-Cervantes, A.A. Crisóstomo, A. Gutiérrez-Alejandre, A.S. Varela, Optimizing FeNC Materials as Electrocatalysts for the CO_2 Reduction Reaction: Heat-Treatment Temperature, Structure and Performance Correlations, ChemCatChem 11 (2019) 4854–4861, https://doi.org/10.1002/cctc.201901196.
[373] N. Leonard, W. Ju, I. Sinev, J. Steinberg, F. Luo, A.S. Varela, B. Roldan Cuenya, P. Strasser, The chemical identity, state and structure of catalytically active centers during the electrochemical CO_2 reduction on porous Fe-nitrogen-carbon (Fe-N-C) materials, Chem. Sci. 9 (2018) 5064–5073, https://doi.org/10.1039/c8sc00491a.
[374] A. Serov, K. Artyushkova, P. Atanassov, Fe-N-C oxygen reduction fuel cell catalyst derived from carbendazim: Synthesis, structure, and reactivity, Adv. Energy Mater. 4 (2014) 1301735, https://doi.org/10.1002/aenm.201301735.
[375] I. Katsounaros, J.C. Meier, S.O. Klemm, A.A. Topalov, P.U. Biedermann, M. Auinger, K.J.J. Mayrhofer, The effective surface pH during reactions at the solid-liquid interface, Electrochem. Commun. 13 (2011) 634–637, https://doi.org/10.1016/j.elecom.2011.03.032.
[376] A. Bagger, L. Arnarson, M.H. Hansen, E. Spohr, J. Rossmeisl, Electrochemical CO reduction: a property of the electrochemical interface, J. Am. Chem. Soc. 141 (2019) 1506–1514, https://doi.org/10.1021/jacs.8b08839.
[377] N. Gupta, M. Gattrell, B. MacDougall, Calculation for the cathode surface concentrations in the electrochemical reduction of CO_2 in $KHCO_3$ solutions, J. Appl. Electrochem 36 (2006) 161–172, https://doi.org/10.1007/s10800-005-9058-y.
[378] A. Vasileff, Y. Zheng, S.Z. Qiao, Carbon solving carbon's problems: recent progress of nanostructured carbon-based catalysts for the electrochemical reduction of CO_2, Adv. Energy Mater. 7 (2017), https://doi.org/10.1002/aenm.201700759.
[379] L. Ning, S. Liao, H. Li, R. Tong, C. Dong, M. Zhang, W. Gu, X. Liu, Carbon-based materials with tunable morphology confined Ni (0) and Ni-Nx active sites: Highly efficient selective hydrogenation catalysts, Carbon N. Y 154 (2019) 48–57, https://doi.org/10.1016/j.carbon.2019.07.099.
[380] A. Hasani, M.A. Teklagne, H.H. Do, S.H. Hong, Q. Van Le, S.H. Ahn, S.Y. Kim, Graphene-based catalysts for electrochemical carbon dioxide reduction, Carbon Energy 2 (2020) 158–175, https://doi.org/10.1002/cey2.41.
[381] Y. Liu, J. Zhao, Q. Cai, Pyrrolic-nitrogen doped graphene: A metal-free electrocatalyst with high efficiency and selectivity for the reduction of carbon dioxide to formic acid: A computational study, Phys. Chem. Chem. Phys. 18 (2016) 5491–5498, https://doi.org/10.1039/c5cp07458d.
[382] G.L. Chai, Z.X. Guo, Highly effective sites and selectivity of nitrogen-doped graphene/CNT catalysts for CO_2 electrochemical reduction, Chem. Sci. 7 (2016) 1268–1275, https://doi.org/10.1039/c5sc03695j.
[383] H. Wang, T. Maiyalagan, X. Wang, Review on recent progress in nitrogen-doped graphene: Synthesis, characterization, and its potential applications, ACS Catal. 2 (2012) 781–794, https://doi.org/10.1021/cs200652y.
[384] D.G. Madden, R. Babu, C. Çamur, N. Rampal, J. Silvestre-Albero, T. Curtin, D. Fairen-Jimenez, Monolithic metal-organic frameworks for carbon dioxide separation, Faraday Discuss. 231 (2021) 51–65, https://doi.org/10.1039/d1fd00017a.
[385] M.S. Yao, K.I. Otake, Z.Q. Xue, S. Kitagawa, Concluding remarks: Current and next generation MOFs, Faraday Discuss. 231 (2021) 397–417, https://doi.org/10.1039/d1fd00058f.
[386] M.I. Severino, E. Gkaniatsou, F. Nouar, M.L. Pinto, C. Serre, MOFs industrialization: A complete assessment of production costs, Faraday Discuss. 231 (2021) 326–341, https://doi.org/10.1039/d1fd00018g.
[387] Z. Chen, M.C. Wasson, R.J. Drout, L. Robison, K.B. Idrees, J.G. Knapp, F.A. Son, X. Zhang, W. Hierse, C. Kühn, S. Marx, B. Hernandez, O.K. Farha, The state of the field: From inception to commercialization of metal-organic frameworks, Faraday Discuss. 225 (2021) 9–69, https://doi.org/10.1039/d0fd00103a.
[388] P.M. Stanley, M. Parkulab, B. Rieger, J. Warnan, R.A. Fischer, Understanding entrapped molecular photosystem and metal-organic framework synergy for

improved solar fuel production, Faraday Discuss. 231 (2021) 281–297, https://doi.org/10.1039/d1fd00009h.
[389] S. Kumar, S. Jain, M. Nehra, N. Dilbaghi, G. Marrazza, K.H. Kim (Eds.), Green. Synth. Met. Framew.: A state—art. Rev. potential Environ. Med. Appl., Coord. Chem. Rev. 420 (2020), 213407, https://doi.org/10.1016/j.ccr.2020.213407.
[390] M. Bonneau, C. Lavenn, P. Ginet, K.I. Otake, S. Kitagawa, Upscale synthesis of a binary pillared layered MOF for hydrocarbon gas storage and separation, Green. Chem. 22 (2020) 718–724, https://doi.org/10.1039/c9gc03561c.
[391] P.J. Celis-Salazar, M. Cai, C.A. Cucinell, S.R. Ahrenholtz, C.C. Epley, P.M. Usov, A. J. Morris, Independent quantification of electron and ion diffusion in metallocene-doped metal–organic frameworks thin films, J. Am. Chem. Soc. 141 (2019) 11947–11953, https://doi.org/10.1021/jacs.9b03609.
[392] M. Cai, Q. Loague, A.J. Morris, Design rules for efficient charge transfer in metal–organic framework films: the pore size effect, J. Phys. Chem. Lett. 11 (2020) 702–709, https://doi.org/10.1021/acs.jpclett.9b03285.